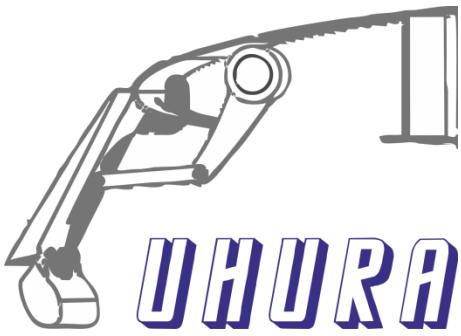

Deliverable D51-10

The work leading to this report has received funding from the European Union's Horizon 2020 Research and Innovation Programme under Grant Agreement No 769088.

Final Project Report

Document control data		
Deliverable No. :	UH-D*51-10*	Author(s): Task & WP leads, CO
Version:	final – v1.0	
Date of issue:	21-10-2022	Accepted by: J. Wild (CO)
Release status:	Confidential	Date: 21-10-2022

No	Partner	Short name	Country
1	Deutsches Zentrum für Luft und Raumfahrt e.V.	DLR	DE
2	Centro Italiano Ricerche Aerospaziali S.c.p.A.	CIRA	IT
3	Vyzkumny A Zkusebni Letecky Ustav A.S.	VZLU	CZ
4	Office National d'Etudes et de Recherches Aérospatiales	ONERA	FR
5	Instituto National de Tecnica Aerospacial	INTA	ES
6	Stichting Nationaal Lucht- en Ruimtevaartlaboratorium	NLR	NL
7	ASCO Industries N.V.	ASCO	BE
8	Kungliga Tekniska Hoegskolan	KTH	SE
9	IBK Innovation GmbH	IBK	DE
10	Airbus Operations GmbH	AID	DE
11	Dassault Aviation SA	DASSAV	F
12	Stichting Duits-Nederlandse Windtunnels	DNW	NL

Content

List of Tables

List of Figures

Abbreviations

A/C	aircraft
AoA	Angle of Attack
CAD	Computer Aided Design
CDR	Critical Design Review
CFD	Computational Fluid Dynamics
CM	Coordination Memorandum
COVID-19	Coronavirus Disease 2019
CPU	Computer Processing Unit
CS-25	Certification Specification – Large Aeroplanes
CSM	Computational Structure Mechanics
D##.#	Deliverable
DoA	Description of Action
DDES	Delayed Detached Eddy Simulation
DFEM	Dynamic FEM
DLR-F15	DLR research configuration #15
EASN	European Aeronautics Science Network
ECCOMAS	European Community on Computational Methods in Applied Sciences
FAA	Federal Aviation Adminitration
FE	Finite Elements
FEM	FE Method
FSI	Fluid-Structure Interaction
GBD	Ground Based Demonstrator
GFEM	Generalized FEM
IB	Immersed Boundary
IDDES	Improved DDES
LBM	Lattice Boltzmann Method
LES	Large Eddy Simulation
LLE	Laminar Leading Edge
LLF	Large Low-speed Facility
LS	Large and Swept
LST	Low Speed Wind Tunnel
MEMS	Micro-Electronical Mechanical Systems
MPI	Message Passing Interface
NWB	Niedergeschwindigkeits-Windkanal Braunschweig
M##	Project Month no. ##

PDR	Preliminary Design Review
PIV	Particle Image Velocimetry
PPM	Project Progress Meeting
PRM	Project Review Meeting
PS	Policy Statement
RANS	Reynolds-averaged Navier-Stokes
RBF	Radial Basis Function
RBM	Rigid Body Motion
RF	Reserve Factor
SA	Spalart-Allmaras turbulence model
SPIV	Stereo-PIV
SPR	Stereo Pattern Recognition
STS	Special Technology Session
TR-PIV	Time-Resolved PIV
URANS	Unsteady Reynolds-averaged Navier-Stokes
VLES	Very Large Eddy Simulation
WEB	internet
WMLES	Wall Modelled LES
WP	Work Package
WT	Wind Tunnel
ZDES	Zonal Detached Eddy Simulation

1 Executive summary

This is the final technical report of UHURA covering the second project runtime from 1 September 2018 to 31 August 2022.

The first reporting period has seen a smooth ramp-up of activity nearly as planned. The early distribution of background information allowed all partners to start their scheduled activities in time. The major design tasks in WP1 were finalize within the first reporting period, only the task on kinematics design is extended to include the outcome of verified wind tunnel loads into the assessment of kinematics weight on aircraft level at the end of the project. In WP2 the work on unsteady numerical simulation techniques was technically finalized. In WP3 the design of model modifications of the DLR-F15 model was completed, the corresponding parts are mostly manufactured. In WP5 the project management is running smoothly and first dissemination activities have been conducted at the EASN event in M25.

At the beginning of the second reporting period (M19), the project faced a minor time delay of about three months. The major reason has been a cyber-attack on ASCO, a key contributor to the model design. There was good hope to recover the delay within the next 12 months.

Due to COVID-19 crisis the work especially in WP3 was significantly delayed. Model manufacturing needed onsite activities, which were not possible during the period March to June 2020. Afterwards, due to different ramp-up of activity at different sites and subcontracted entities for manufacturing, the model modification of the DLR-F15 model was further delayed and completed with a further 5 months delay. Thus, wind tunnel testing in WP3 was delayed with a start of the first test entries in M26. Close monitoring of activities is in place to minimize the impact on the project.

Towards the end of the second reporting period, the project was significantly delayed in terms of schedule. This was mainly caused by the two reasons mentioned above out of influence of the project and its beneficiaries:

1. The beneficiary ASCO suffered a severe cyber-attack preventing progress in a critical phase of model design
2. The COVID-19 outbreak with its consequences (lock-down, travel restrictions, quarantines) slowed down the manufacturing and assembly progress of the wind tunnel model modifications. In addition, the further development of the pandemic resulted in a strict travel ban at the time of the test slot, making it impossible for the DLR PIV-group to be on-site at DNW-LLF for the test in M32. It was decided to perform the test and to arrange for a separate second entry in order to not cancel the running test preparation and to at least acquire the other measurement technique's data

In consequence of late finalization of models, wind tunnel tests had to be rescheduled. Now, also due to COVID-19, all other projects are delayed too and wind tunnel schedules get very squeezed with only minor flexibility on wind tunnel slots. As industrial tests are clearly prioritized at the suppliers, the guaranteed wind tunnel slots are quite limited.

In July 2021 the Amendment AMD-769088-17 and has been signed and activated, granting the project an extension of 12 months in order to complete the remaining wind tunnel tests and the comparison of experimental and numerical data.

Within the third reporting period covering the project extension, the wind tunnel tests were completed at the ONERA L1-tunnel in September/October 2021, and the final PIV wind tunnel campaign in DNW-LLF in April 2022, which were the earliest available dates according to current wind tunnel schedules. Time resolved wind tunnel data was processed, which took some effort to fully synchronize and time/phase average the transient data of multiple measurement techniques. The CFD simulations of the wind tunnel setups were fully conducted by all the partners with all the different methods. Finally, the comparison between numerical results and experimental data was done.

At the end the project achieved its two major objectives: First, to validate the numerical simulation approaches for these kinds of flows; and second, to gain knowledge about the unsteady flow behaviour and its consequences on aircraft level.

The project was concluded by a Workshop and Final Review Meeting at Airbus Premises, Bremen, Germany, on Sept 5th/6th, 2022. In the workshop the project results were presented to a wider audience, especially towards industrial entities not directly involved. For a wider communication to the public research community, special sessions have been arranged within the ECCOMAS 2022 Congress, June 6th – 9th, 2022, Oslo, Norway, and the 12th EASN International Conference, Oct. 18th-21st, 2022, Barcelona, Spain.

1.1 Project objectives

The major objectives for the second reporting period M19-M36 of UHURA are listed below, sorted by the project's reporting periods and subdivided in portions of 6 months .

work package	M1-M6	M7-M12	M13-M18
WP1	design a deployable Krueger leading edge device, based on laminar leading edge shape for the DLR-F15 wind tunnel model.	finalization of design of the Krueger shape and kinematics	none, Tasks 1.1 an d 1.3 are completed. Task 1.2 is planned to be concluded in M28
WP2	start to work on numerical tools assessments / improvements on both, grid strategy and unsteady simulation.	progress on numerical methods	completion of numerical tools adaptations for their use in UHURA
WP3	none	design of the wind tunnel model modifications	complete design and manufacturing of the modifications for the DLR-F15 wind tunnel model
WP4	none	initial document on expectations on wind tunnel data to be used for comparison with numerical data	start preparation activities for Krueger deployment simulations at WT conditions
WP5	installation of database for communication and data exchange; continuous management and progress monitoring of the project including preparations of major meetings	monitoring of project progress	monitoring of project progress

work package	M19-M24	M25-M30	M31-M36
WP1	none, Tasks 1.1 and 1.3 are completed. Task 1.2 is planned to be concluded in M28	Task 1.2 is planned to be concluded in M28	Task 1.2 is shifted to conclude in M36
WP2	completion of WP2 activities.	finalization of last deliverables	Activity closed
WP3	finalize modifications for the DLR-F15 model and design of the F15 LS model modifications	finalize modifications for the F15 LS model, perform wind tunnel tests in ONERA L1 and DNW-NWB wind tunnels	Perform wind tunnel test at DNW-LLF. Prepare F15 model for second Onera-L1 test
WP4	computational analyses of the planned experimental test cases	computational analyses of the planned experimental test cases	computational analyses of the planned experimental test cases
WP5	monitoring of project progress, first dissemination activity	monitoring of project progress, dissemination activity	monitoring of project progress

work package	M37-M42	M43-M48
WP1	Complete weight assessment of full A/C scale kinematics	Activity closed
WP2	Activity closed	Activity closed
WP3	Perform second wind tunnel test campaign in ONERA L1	Perform second wind tunnel test campaign with PIV at DNW-LLF
WP4	computational analyses of the planned experimental test cases	Validation and assessment of experimental and numerical results
WP5	monitoring of project progress	monitoring of project progress, final dissemination activity

1.2 Project achievements at a glance

A Krueger flap and corresponding kinematics has been designed for the DLR-F15-LLE airfoil. To achieve a realistic design, requirements from aircraft level have been specified and considered. The designs of the aerodynamic shape and the kinematics have been performed in a loop where side constraints on kinematics feasibility have been developed and included in the aerodynamic design iteration. The geometry of the Krueger flap configuration and the kinematics has been provided to wind tunnel model design. The designed Krueger flap configuration has been analyzed and loads for sizing model components have been provided. Further on, from an aircraft view, recommendations for the speed of deployment and retraction of the Krueger device have been established. These numbers reflect the manufacturer knowledge on handling quality and certification criteria for Krueger devices.

Using initial design iterations, the simulation methods have been setup and sharpened for designated simulation type. On grid generation side, a robust implementation of local reconnection algorithm for unstructured meshes was obtained. Further, a demonstration of local-grid refinement

in conjunction with Chimera capability on structured meshes has been established. Beside this, Immersed Boundary Methods and full re-meshing has been successfully applied. With regard to flow solver technologies, most of the partners have demonstrated their capabilities of simulating the deployment of the Krueger device. Methods in use range from URANS methods via different turbulence-resolving methods at the length and time scales of relevance up to particle-based Lattice Boltzmann Methods (LBM). The methods are therefore ready to be used to simulate the experimental setup.

The modifications for both wind tunnel models have fully been designed and manufactured. Finite Element Analysis has been used to complete corresponding stress reports justifying the model to be entered into the wind tunnel tests. The models are be equipped with a significant number of unsteady pressure sensors, both on MEMS and by using conventional pressure transducer for dynamic measurements in the envisaged frequency. The PIV methodology to be used to monitor the dynamic flow field has been selected and the implementation in terms of measurement window as well as hardware setup in the tunnel has been achieved. As there are a number of different measurement systems, a synchronisation approach has been established, including trigger, automation and communication approaches.

A series of five wind tunnel tests have been conducted in all designated wind tunnel test facilities. A first exploratory test entry in ONERA-L1 provided experience on the model behaviour, revealed critical areas in routing sensor connections and proved at first the baseline conditions in first glance comparison of CFD and PIV data based on steady flow conditions. The lessons learned from model handling were further incorporated in both model setups. The wind tunnel test in DNW-NWB with the straight and swept cantilever wing arrangements were fully completed. A first entry has been conducted in DNW-LLF for the pressure and deformation measurements – as PIV was unable to be performed due to COVID-19 travel restrictions of the staff. Nevertheless, the full test matrix has been accomplished for the available measurement techniques. The tests were completed by second entries in ONERA-L1 and DNW-LLF, both concentrating on PIV for the dynamic deployments. Phase averaged PIV was achieved for 300-1000 samples per deflection position with a temporal resolution of about 20Hz.

In order to prepare the comparison of numerical and experimental data, guidelines for validation have been compiled. By specifying common formats and templates and by collecting the expected list of measured values, a common ground for comparison is established. Specific simulations of the different wind tunnel setups were performed, both in free air and within the wind tunnel environment. Especially using real-time recorded data of the drive system allowed to closely match the real deflection process. In general, the validation revealed an appropriate simulation by URANS methods. Hybrid RANS-LES methods provide some more detailed information in the high frequency range, but the low frequency behaviour is similar. Other emerging methods show potential for future applications.

The combination of both, experimental and simulation data, reveal the most important flow features during the Kruger flap deflection. A significant lift drop is observed that is caused by the lower side separation at partially deflected Krueger flap hitting the trailing edge flap. The deployment speed of the Kruger mainly affects the phase delay of the lift drop but only minor the amplitude. Further, the effect is verified by simulation and experiment to be less prominent with part-span Krueger flap arrangement and at swept wings. This further allowed to assess the Krueger flap motion impact on aircraft level regarding some requirements on system architecture and on handling qualities.

On management side, a timely conduction of regular Progress Project Meetings as well as the in-time compilation of Quarterly Status Reports & Project Progress Reports serve a smooth progressing of the project. All remaining deliverables (48) have been submitted in the reporting period. Contributions to scientific conferences have been made, the most recent ones at the ECCOMAS 2022 congress and the 12th EASN International Conference. A public WEB-site has been

created and is online for communicating the project to the general audience. Several partners have communicated the project via their company WEB-site. Further, a project entry has been created on ResearchGate and some progress (especially on the wind tunnel tests) have been announced via LinkedIn personnel channels. For the data exchange between partners the UHURA databank is in service. Technical support is constantly provided.

2 Work progress and achievements

2.1 WP 1: Aero Design and Definition

Task	*Title*	*Starting at*	*Completion*	*Status*
1.1	**Shape**	**M1**	**M6**	**completed**
1.2	**Kinematics**	**M1**	**M41**	**completed**
1.3	**Definition of deployment cases**	**M1**	**M6**	**completed**

Lead: AID

The objective of WP1 until M18 was to design a deployable Krueger leading edge device, based on laminar leading edge shape for the DLR-F15 wind tunnel model.

The shape of the Krueger device (device length, nose shape) as well as the deployed position in front of the wing were optimised to achieve an aerodynamic lift optimum. At the same time constraints & requirements from aircraft level had to be respected (e.g. insect shielding requirement), as well as for kinematic design and sizing.

In Task 1.1, CIRA and DLR established a parametric description of the Krueger shape, incorporating requirements and constraints from kinematic design (Task 1.2) and overall aircraft level (Task 1.3). Embedded in a seamless end to end CFD process, numerical optimisation was applied to define the Krueger shape and its deployed position, maximising a lift objective. As two completely different methods were applied by CIRA and DLR, the achieved optimum can be judged as robust. A cross comparison of the partners final results was performed by DLR and CIRA.

Aerodynamic component loads were derived from the CFD calculations and from semi empirical approaches for the Krueger flap in intermediate and fully deployed positions. These loads were fed to Task 1.2 to size the kinematic and structure components.

ASCO designed and sized a realistic kinematic mechanism within Task 1.2 to deploy the Krueger flap from its retracted position on the wing lower side into deployed in front of the wing. Several iterations were performed with Task 1.1 to achieve a feasible and aerodynamically well performing integrated solution.

Task 1.3 provided constraints and requirements from aircraft level into the design process of Task 1.1 and Task 1.2 to ensure a realistic and relevant configuration.

Deliverables regarding the designed shape (D11-1), the kinematics design (D12-1) and the aircraft related requirements (D13-1, D13-2) have been completed and submitted. Only D12-2 will be delivered in M30 instead M5 according to the agreed shift, but all data needed for further progressing by WP3 and WP4 has been made available by a Coordination Memorandum. The activities linked to D12-2 will be initiated in M28 after the wind tunnel tests in WP3 are complete. ASCO completed the deliverable D12-2 (Weight report of full-scale Krüger panel kinematics) in M41. It was shifted to the end of this reporting phase to take benefit on loads measured during wind tunnel test 3 in DNW, which allowed a more accurate sizing and weight prediction.

Additionally, few activities were done in supporting the kinematics design and stress analysis for the wind tunnel models. These activities are summarized in more detail within the description of Task 3.1

2.1.1 Task 1.1 – Shape

Lead: DLR

Task 1.1 objectives

- performing the aerodynamic design of the Krueger flap, providing the final shape for WP3 and WP4

Progress achieved/results

Within the first reporting period of the project, the design of a Krueger device suitable for the targets of the project has been finalized. Baseline geometries from former studies have been collected and provided to partners in Task 1.1 and covering an initial Krueger device and a classical three-element airfoil for WP2. Two concurrent design optimizations have been performed by the partners in Task 1.1. From these results after a cross-check of the shapes, a synthesis of the design has been achieved by combining favourable aspects of both designs. In a last step, requirements from the kinematics design have been incorporated (Figure 1). This last design has been evaluated also regarding loads, which have been provided to Task 1.2 for a final sizing loop of the kinematics.

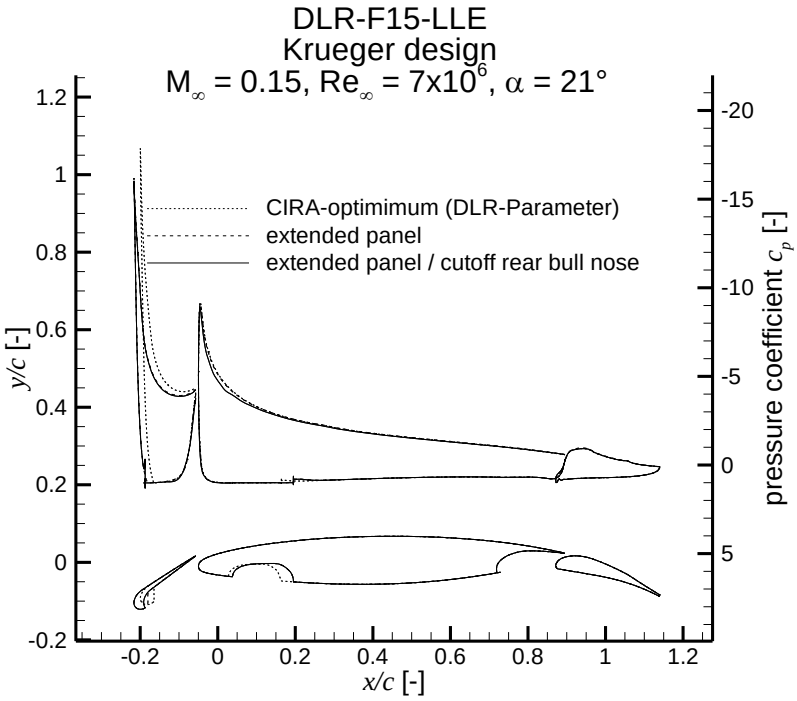

Figure 1: pressure distributions of the finally refined Krueger device with respect to kinematics requirements

Contribution of Partner 1 – DLR

Background information on airfoil geometry has been collected and provided for the targeted DLR-F15-LLE airfoil and a reference baseline DLR-F15 3-element airfoil.

To provide initial datasets for Task 1.2 and WP2, an initial Krueger device has been implemented based on results of the DeSiReH project. As an alternative, a movement law for the 3-element airfoil has been provided based on former studies. An initial set of loads data has been provided for Task 1.2 to start an initial sizing loop for the kinematics.

A numerical optimization loop has been performed to propose a meaningful Krueger device for the DLR-F15-LLE airfoil as the initial Krueger device shows premature separation. After comparison with data obtained by the partner CIRA and considering preliminary design constraints from the

kinematics (Task 1.2), a synthesis of DLR and CIRA designs has been performed leading to a suitable final shape of the Krueger device.

The design synthesis has been completed for the folding bull-nose Krueger device. The geometry has been provided to the partners of WP2, WP3, and WP4. The corresponding deliverable D11-1 has been provided and submitted.

Contribution of Partner 3 - CIRA

CIRA set up an optimization procedure to perform the geometry design of the Krueger element. A specific, kinematic constraints-driven parameterization has been conceived to generate feasible shapes. An improved Krueger shape has been obtained as a result of a series of CFD-based optimizations aimed at increasing the maximum lift performance. The design has been cross-checked and validated by DLR.

A series of iterative refinements have been performed side by side with DLR for aerodynamic shape design. Cross-check analysis with DLR mesh and flow solver have been carried out together with turbulence model sensitivity analysis. Finally, CIRA contributed to detail the whole aerodynamic design process in the deliverable D11-1.

The task was completed within the 1st reporting period.

2.1.2 Task 1.2 – Kinematics

Lead: ASCO

Task 1.2 objectives

- Define kinematics constraints linked to Krueger panel, actuation and deployment mechanisms for Task 1.1 and determine corresponding structural weights
- Define a Krueger kinematics design to be used as baseline for the DLR-F15 and DLR-F15*LS* model modification in WP3.
- Assess kinematics weight on aircraft level

Progress achieved/results

The initial Krueger shape from Task 1.1 was analysed regarding space allocation constraints. D12-1 ('Kinematic constraints linked to Krueger panel, actuation and deployment mechanisms') was compiled and delivered according to planning in M3.

A preliminary kinematics design (and preliminary sizing) was completed for the initial Krueger shape. This preliminary sizing was required to perform the space allocation and kinematics integration analysis that delivered the integration constraints captured in D12-1 (Figure 2).

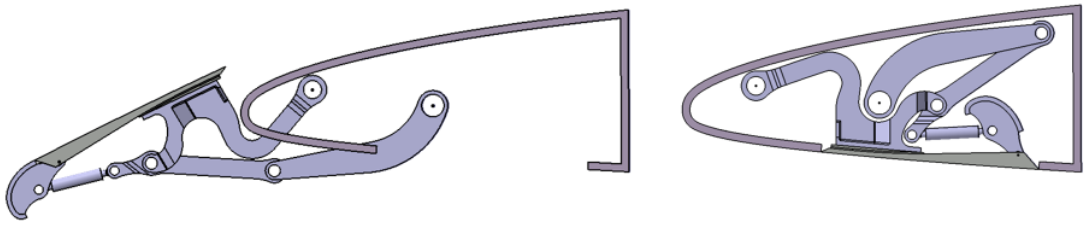

Figure 2: preliminary kinematics design A01 as provided in M3 together with D12-1

All the activities related to deliverable D12-1 and required to provide the necessary inputs for Task 3.1 should have been completed by M5. D12-1 was provided in time and a first design was delivered by M5. The remainder of this task (D12-2) has been shifted until completion of the wind tunnel campaigns in WP4 (M30).

The activities within Task 3.1 (which ASCO is supporting as well) identified some space allocation issues in the kinematical design provided in D12-1. Therefore, the kinematics design activity in Task 1.2 has been reopened and the design was updated in order to solve the integration issues (such as finding a good position to accommodate the drive shaft) identified during the DLR-F15 model modification activities (Figure 3).

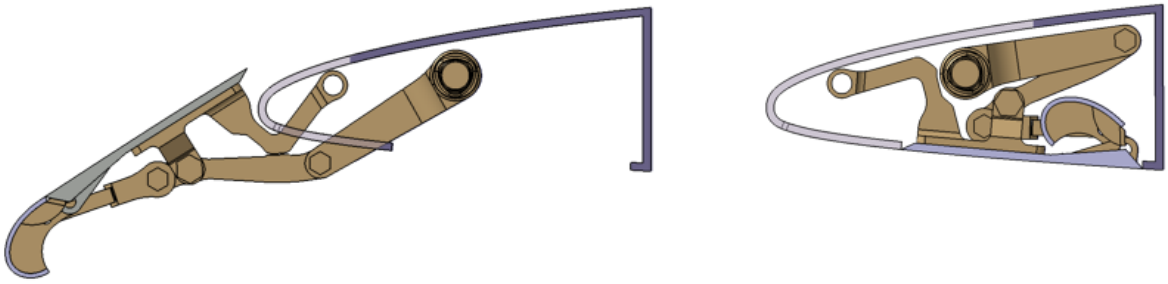

Figure 3: final designed Krueger kinematics H01 in (left) deflected and (right) retracted position

This design was fully sized within Task 3.1. Moreover, specific features where included in the kinematics design to alleviate the very large torques on the drive shaft that would appear during the static Krueger-extended AoA-sweeps during wind tunnel testing (refer to Task 3.1 section). This updated kinematical geometry was fully accepted during the CDR of the DLR-F15 model modification within Task 3.1 in M16.

The ASCO contribution to the DLR-F15 Stress Report (D31-3) was released in M18.

A secondary (not-formal) deliverable of this Task was the relationship between the 3 different deployment angles (Krueger extension angle around its rotation point, drive lever rotation angle around the drive shaft & bull nose rotation angle around its rotation point on the upper Krueger panel). These relations are directly resulting from the geometrical configuration of the kinematical system. They serve, for example, also as an input in WP4 for the CFD computations of the dynamic flow conditions around the deploying Krueger flap.

During the second reporting period, Task 1.2 was mainly supporting Task 3.1 in terms of kinematical design and sizing in order to reach DLR-F15LS PDR-status on 1-July-2020 (M23) & CDR-status on 3-Sept-2020 (M25). No changes have been made to the baseline kinematical design provided in D12-1. All rotation points were kept in the same position since no specific space allocation problems were identified for on DLR-F15LS.

The final kinematics design (following a resizing accounting for the higher load levels) for DLR-F15LS was accepted and frozen during the CDR-meeting within Task 3.1 in M25.

The ASCO contribution to DLR-F15LS Stress Report (D31-5) was released in M30. Mainly due to the COVID-19 pandemic, the schedules of the wind tunnel test campaigns were delayed

In order to assess the weight of the Krueger panel actuation and deployment mechanisms on a real aircraft scale, ASCO defined a new theoretical kinematics design at this scale while implementing some common aircraft design principles and practices that were omitted on both wind tunnel designs due to scaling issues. For the material selection for this aircraft design, only approved and commonly used aero-grade materials were considered.

The aerodynamic load case data were derived from the experimentally obtained LLF wind tunnel data and, hence, contained, next to the static (stationary Krueger Panel) load cases, also the dynamic load cases (moving Krueger Panel). Including the latter in the assessment was the reason to postpone deliverable D12-2 towards the end of the project.

The aircraft kinematics design was sized with respect to those load cases. Typical failure cases that can occur on an aircraft were also identified by ASCO and considered in the sizing and fail-safety

assessment in order to meet the CS-25 requirements for systems and structures (that are applicable to the state-of-the-art commercial aircraft models).

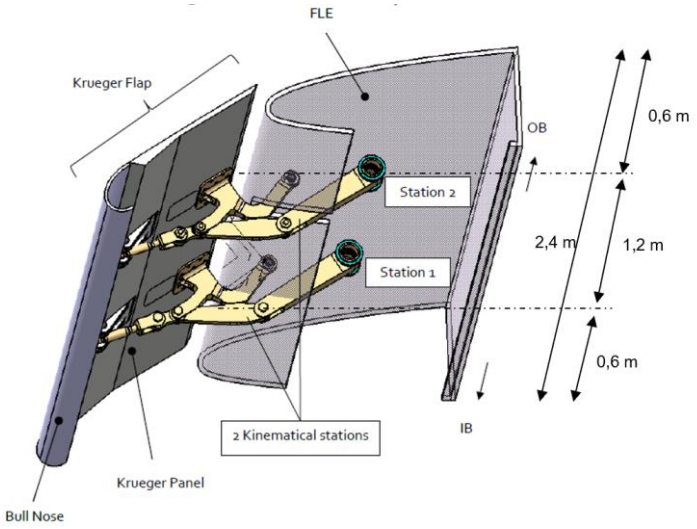

Figure 4: Aircraft-scale Krueger kinematics architecture considered for UHURA

ASCO calculated a weight of approximately 26kg for one UHURA Krueger kinematics station scaled to a real aircraft scale and application.

As a side study, ASCO investigated the impact of the new system fail-safe regulation (published in FAA amendment PS-ANM-25-12) on the kinematical architecture and weight. Since every individual single actuation station failure must be considered, an architecture comprising only 2 stations per panel is not an option on a next aircraft platform (minimum 3 are required to guarantee the structural integrity of the system). ASCO calculated that to reach the same level of loading in the kinematics (and hence the same size and weight per station), the number of stations shall be doubled for the same Krueger panel span.

All the results and findings were summarized in D12-2, which was released in M41.

Contribution of Partner 7 – ASCO

ASCO is the only partner in Task 1.2 and the above activities have been solely contributed by ASCO.

2.1.3 Task 1.3 – Definition of deployment cases

Lead: AID

Task 1.3 objectives

- Specification of A/C related requirements for the design of Krueger flap devices
- Specification of the selected cases to represent most aerodynamic-critical intermediate Krueger positions during deployment phase

Progress achieved/results

The goal of WP1 was to design a Krueger system in a limited amount of time, which is fit for UHURA purpose and well represents a potential aircraft solution. Based on A/C manufacturers design experience, aircraft-level Krueger design requirements & constraints were introduced into the Krueger design process (Figure 5). During regular WP1 phone calls, requirements like relaxed shielding criteria, range of target deployment angle and aircraft-based clearances have been discussed and applied to the aerodynamic shape and kinematic design process in Task 1.1 and Task 1.2. The applied recommendations have finally been summarized in D13-1. Finally Task 1.1 & Task 1.2 have achieved an integrated Krueger design, which is well balanced between shape and

kinematic design space. It perfectly fits the need of UHURA's wind tunnel models and numerical objectives.

Task 1.3 also provided recommendations for the speed of deployment and retraction of the Krueger device. These numbers reflect the manufacturer knowledge on handling quality and certification criteria for Krueger devices, which finally allows the UHURA project to deal in a realistic and challenging scenario of deployment and retraction sequence. Performance critical deployment angles have been provided in order to allow for critical failure case analysis. The recommendations on deployment speed and critical deployment angle have been summarized in D13-2.

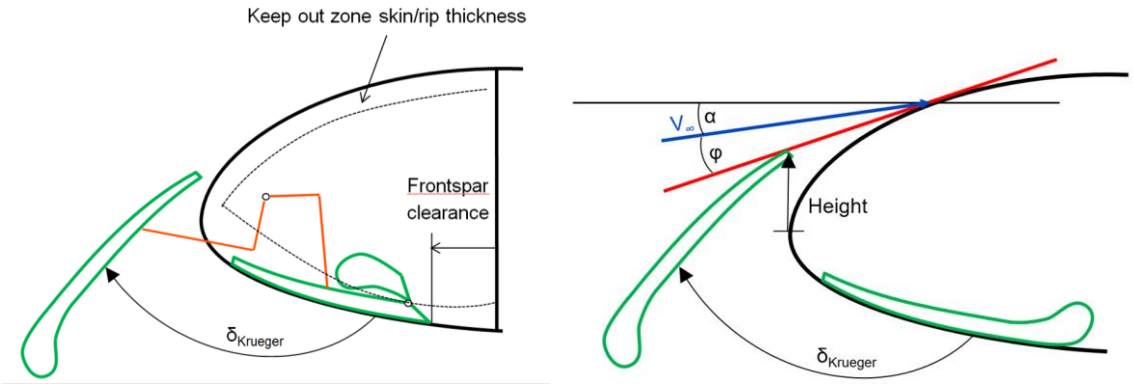

Figure 5: Illustration of design requirements provided within D13.1

Contribution of Partner 10 – AID

AID is the only partner in Task 1.3 and the above activity has been solely contributed by AID

2.2 WP 2: Numerical Simulation

Task	*Title*	*Starting at*	*Completion*	*Status*
2.1	**Improvement of meshing**	**M1**	**M23**	**completed**
2.2	**Improvement of CFD solution methods**	**M1**	**M31**	**completed**

Lead: ONERA

The objectives of WP 2 were to work on numerical tools assessments / improvements on both, grid strategy and unsteady simulation. The baseline configuration to be considered is the background information provided from WP 1, but partners can work on academic cases, too.

For Task 2.1, works on grid adaptation tools has been performed, for block structured grids (NLR) and unstructured grids (DLR) . It combined grid deformation, sliding grid, re-gridding and local grid refinements on blocks.

For Task 2.2, most of the partners have initial steady RANS simulations on preliminary Krueger shape. For some results (DLR, VZLU or KTH), a critical situation is observed when the Krueger is deployed perpendicular to the incident flow. A large separated flow is observed on the lower surface and a transient separation appears at main wing leading-edge that leads to a significant loss in performance (to be verified with unsteady simulations). Some works start on Krueger deployment simulations using chimera technique, mesh deformation, Immersed Boundary Methods. Preliminary results obtained using LBM methods have been presented by INTA. Concerning the acceleration of unsteady methods, NLR presented some results for a line-implicit scheme for both steady RANS and URANS (oscillating plate). Finally, IBK (in cooperation with CIRA) have developed an interface tool for fluid-structure interaction.

A large portion of work was dedicated to the use of the chimera method to manage the Krueger movement (DLR, ONERA, VZLU, NLR) with some differences linked to the solver used. Some partners consider a mix between grid generation using scripts for discrete Krueger position, and mesh deformation method for intermediate settings (VZLU, KTH). Works on the acceleration of URANS methods have been presented, as well as the progress of CFD/CSM interface tool for FSI simulations. DLR has presented a parametric study of the rotation speed for the complete cycle deployment/retraction on a preliminary Krueger shape.

Finally, the finalisation of the different tools to be used for UHURA purpose (i.e. two parts of a (possible) deformable Krueger flap deployed with independent kinematics under unsteady flow conditions) has been completed. The last activities were dedicated to the delivery of the modified/enhanced numerical tools for their use in WP4. In addition, the dissemination of the work through contributions to the EASN virtual conference, held in Sept. 2020, and to ECCOMAS 2020, held in Jan. 2021, was conducted. The pending deliverables have been processed and delivered. The Work package is completed.

Table 1 WP2 Milestones, deliverables, time schedule & spending

Deliverables in WP2		***Partner(s)***	***Month due***	***Month completed***
D21-1	Development of a multi-block local grid refinement method for a moving Krueger device	NLR	M13⇨M18	M23
D21-2	Effect of local reconnection during mesh deformation on the simulation accuracy	DLR	M13⇨M18	M18

	of a deploying Krueger device			
D22-1	Flow simulation developments for high-lift applications featuring rigid body motion and unsteady flows	NLR	M18⇨M21	M22
D22-2	Technical report on assessment of LBM and "best practices" for the prediction of the unsteady aerodynamics during the deployment/retraction phases of high-lift systems	INTA	M18⇨M21	M21
D22-3	Technical report on the assessment of advanced turbulence models for DDES simulations	DASSAV	M18⇨M21	M31
D22-4	Technical report on "best practices" with DLR CFD solver technology for the prediction of the unsteady aerodynamics during the deployment/retraction phases of a Krueger device using the chimera technique	DLR	M18⇨M21	M25
D22-5	Technical report on "best practices" with VZLU CFD solver technology for the prediction of the unsteady aerodynamics during the deployment/retraction phases of a Krueger device using the chimera technique	VZLU	M18⇨M21	M24
D22-6	Report describing the methodology and the implementation of the FSI to couple the CFD solver by CIRA (Immersed Boundary Method based) and the structural solver	IBK	M18⇨M21	M22
D22-7	Report on extension of in-house Immersed Boundary method SIMBA to treat moving bodies and FSI coupling	CIRA	M18⇨M21	M23
D22-8	Report on best practice on applying elsA chimera capabilities for Krueger flaps	ONERA	M18⇨M21	M24
D22-9	Report on efficient hybrid RANS/LES techniques for slowly moving geometries	KTH	M18⇨M21	M21

Milestones in WP2		***Partner***	***Month due***	***Month achieved***

2.2.1 Task 2.1 – Improvement of meshing

Lead: NLR

Task 2.1 objectives

- Explore feasibility and potential of mesh quality improvements by local reconnection during mesh deformation of unstructured meshes.
- Development of a block-structured local grid refinement method and combination with the Chimera approach.

Progress achieved/results

Contribution of Partner 1 - DLR

Local reconnection offers a suitable way to implement a re-meshing strategy based on the Chimera approach that eliminates the need for non-conservative interpolation. The strategy is based by replacing overlapping mesh regions by a conformal triangulation. An initial multi-block structured grid and a Chimera grid are used for the development and assessment of the local reconnection approach. The full sequence of a Krueger flap deflection has been obtained on meshes that differ significantly in mesh resolution (1:4). Figure 6 (left) shows the reconnected mesh region around the Krueger panel on the fine grid level. The mesh quality of the interfacing meshes has been assessed

based on established mesh quality criterions. It shows that the local reconnection retains the anisotropy of the baseline mesh over the full deflection range of the UHURA Krueger flap. Due to the triangulation, a slightly higher size variation is observed than in the baseline mesh. The method has been shown to be robustly implemented.

Contribution of Partner 6 - NLR

A baseline algorithm for block-structured local grid refinement has been revisited in view of high-lift applications including rigid body movements. The algorithm aims for a uniform mesh width by first refining the block topology and subsequently refining the grid per block. The local grid refinement capability will be combined with the Chimera approach to perform unsteady simulations of Krueger device deployment. The Chimera approach will facilitate the motion of the Krueger device, while local grid refinement will be used to inject grid points efficiently where needed for accuracy.

The local grid refinement algorithm has been improved on two accounts: First, when a block is locally refined, the smoothness of the grid is maintained by an appropriate smooth interpolation of the original grid-point distribution. Second, if a block is refined that is attached to a solid surface, the refined grid is mapped onto the original geometry definition in order to preserve the correct aerodynamic shape.

The validity of the method is demonstrated by a refined Chimera grid which has been generated around the DLR-F15 with a Krueger device consisting of two separate elements (bull nose and base, Figure 6 right). The grid around the main wing has been locally refined in order to accurately capture the flow characteristics of the separated flow region introduced by the moving Krueger device.

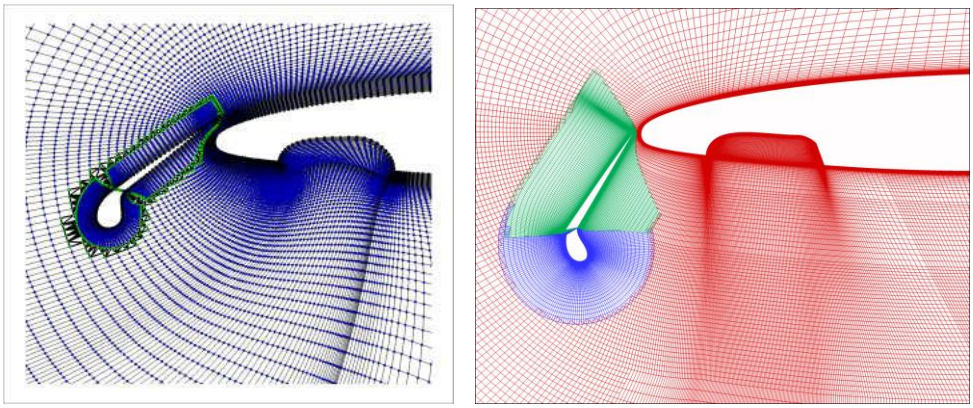

Figure 6: Improvement of meshing strategies for large deflections: (left) local mesh reconnection done by DLR; (right) local mesh refinement done by NLR

The task was completed within the 1st reporting period.

2.2.2 Task 2.2 – Improvement of CFD solution methods

Lead: KTH

Task 2.2 objectives

The objective with Task 2.2 is different improvement of CFD solution methods for deployment and retraction of a Krueger device. In specific:

- to assess the capabilities in simulating moving frames in the present computational frameworks,
- to develop and implement selected improvements for accelerating of unsteady CFD,
- to improve on flap movement algorithms, and
- to study alternative methods for capturing unsteady CFD with mowing Krueger flap.

Progress achieved/results

The work is divided into three subtasks with the following progress achieved:

(1) Acceleration of unsteady CFD. Numerical algorithms (NLR, KTH), quasi-steady approach (KTH) and efficient hybrid RANS/LES (KTH).
(2) Improvements of flap movement algorithms. Chimera (DLR, VZLU, ONERA, NLR) and Immersed boundary (CIRA).
(3) Alternative methods. Lattice-Boltzmann method (INTA) and advanced RANS for hybrid methods (Dassault).

Moreover, most of the partners have demonstrated their capabilities of simulating the deployment of the Krueger device.

The work within this task has been disseminated at the EASN 2020 virtual conference in September 2020.

- Capizzano, F. (CIRA) and Sucipto, T. (IBK), A dynamic Immersed Boundary method for moving bodies and FSI applications.
- Prachar, A. (VZLU), Heinrich, R. (DLR), Raichle, A. (DLR), Kok, J.C. (NLR), Moëns, F. (Onera), Renaud, T. (Onera), Progress towards numerical simulation of the dynamic Krueger motion with Chimera methods.
- Chen, S. (KTH), Bagheri, F. (neptech), Eliasson, P. (KTH) and Wallin, S. (KTH), Hybrid RANS-LES simulation of a deflecting Krüger device.

Moreover, at the ECCOMAS 2020 virtual congress in January 2021 within STS 07 High-Lift Aerodynamics

- Wallin, S. (KTH), Chen, S. (KTH), Capizzano, F. (CIRA), Prachař, A. (VZLU) and Ponsin, J. (INTA), Unsteady CFD results for deflecting high-lift systems.

Contribution of Partner 1-DLR

To model the deployment and retraction phase of a Krueger device the chimera technique with automatic hole-cutting has been selected. An unstructured 3 block 2D mesh has been created with the CENTAUR mesh generating system.

Successful steady simulation without deployment has been performed. The results look reasonable. The convergence was sufficient (more than 6 orders of magnitude in terms of the density residual).

Unsteady (URANS) simulations of the complete deployment and retraction phase of the Krueger device have been made and the influence of different deflection speeds have been investigated (Figure 7). It was found that the drop of lift coefficient for the critical position can be much reduced by a more rapid deployment. To model the deployment and retraction phase of a Krueger device the chimera technique with automatic hole-cutting has been selected.

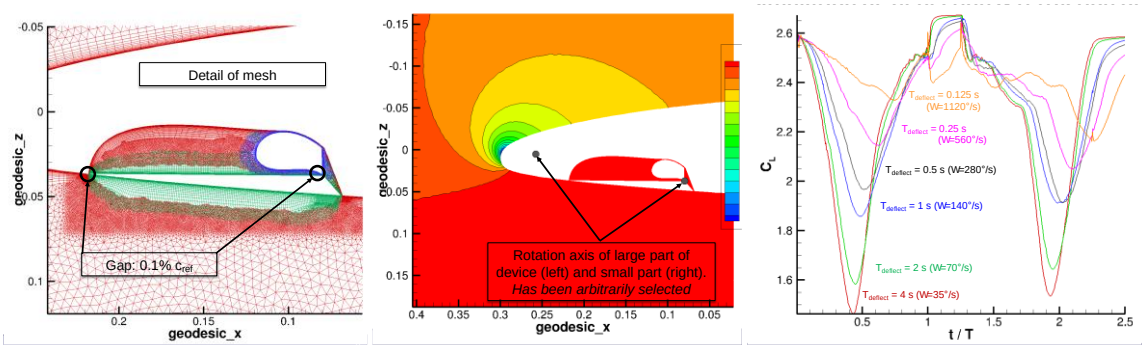

Figure 7: Chimera mesh and solution; lift coefficient during a complete cycle for different angular velocities, DLR TAU simulations.

Based on the 2D mesh a 3D mesh has been created (staggering of 2D meshes). So far, no 3D simulations have been performed.

A first 2D block-structured mesh for the wing with the Krueger device has been generated to save number of mesh nodes by using the DLR tool MEGACADS for mesh generation. This is due to the fact, that very high numbers of nodes are required by using CENTAUR. 1st unsteady simulations for the deflection and retraction of the device are promising.

A concept is evolved to couple an alternative approach for the meshing of the movement of the Krueger device to the solver of the DLR TAU code. The alternative approach is using the local reconnection approach done in Task 2.1. Within the remaining activity of Task 2.2 the handling of changing grids in solution process will be implemented on solver side.

Contribution of Partner 2-CIRA

SIMBA method: the main activities planned for months M1-M18 are devoted to developing and validating a dynamic immersed boundary (IB) method for simulating compressible and viscous flows around moving/deforming objects. Besides, part of the developments deals with a CIRA-IBK interface for coupling the in-house SIMBA code with a structural solver in the framework of a CFD/CSM partitioned approach. A brief summary is listed below.

1. The CIRA Cartesian method has a new data management that allows automatic mesh adaptation during time-accurate computations. A proper Lagrangian-Eulerian model considers the effects of rigid movements and structural deformations in the surrounding flow field.
2. The SIMBA validation campaign covers some test-cases from the literature dealing with imposed rigid body motions (RBM). The dynamic IB-method is used to compute the transient turbulent flow around the "DLR-F15-3eRef" slat-main-flap and "DLR-F15-LLE+Krueger" Krueger-main-flap airfoils during their rigid deployment laws (Figure 8).
3. CIRA and IBK have developed an FSI interface to allow the loads' mapping and communications between CFD and CSM meshes. The research effort aims at exploring different coupling strategies.
4. A "Static two-way FSI-coupling" allows a loose interaction between CFD and CSM. Time-accurate aerodynamic loads are used to compute structural deformations at each time-step or every N time-steps. The structural solver applies linear and static assumption and delivers the modified shapes to CFD. An implicit loop drives the codes to loads-convergence. The deformation velocities are not accounted for. This FSI strategy has been applied to compute the 2D aeroelastic loads during the "DLR-F15-3eRef" deployment (Figure 8 left).
5. The development of a "Dynamic two-way FSI-coupling" is ongoing. This allows a tight interaction between CFD and CSM. The instantaneous CFD loads are feed into the CSM non-linear solver, which gives back the deformation and its velocities in a seamless way. An implicit loop drives the codes to loads-convergence. If successful, the dynamic coupling will be used to compute the 2D aeroelastic loads during the "DLR-F15-LLE+Krueger" deployment (Figure 8 right).

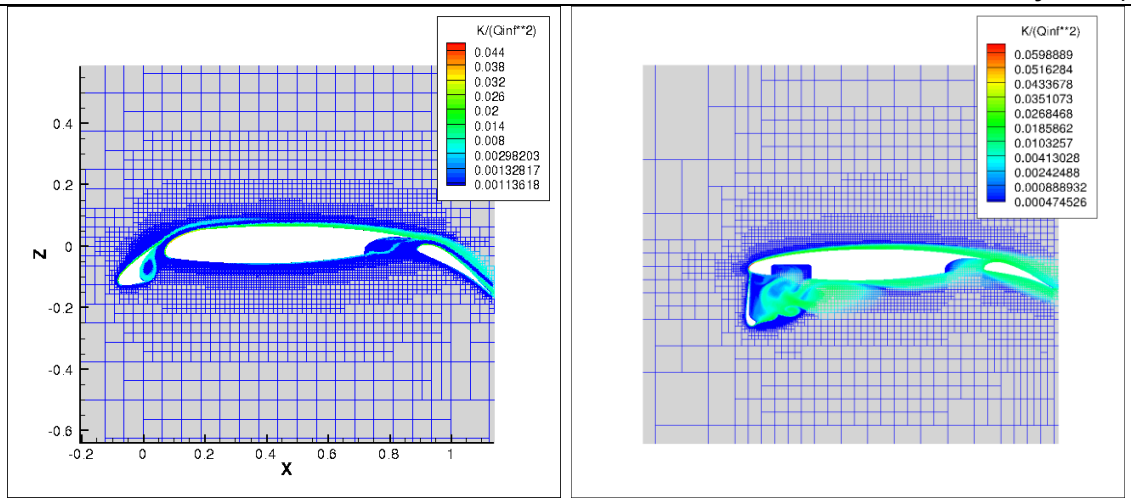

Figure 8: Snapshots of transient DLR-F15 slat and DLR-F15-LLE Krueger deployments, SIMBA solutions

UZEN method: a procedure for parametric re-meshing has been developed, in order to update the multi-block mesh during the Krueger motion at every time step, following the assigned trajectory. In principle the procedure should handle a new Krueger shape and motion with minor development effort. The procedure is going to be tested for the DLR-F15-LLE test case delivered by DLR at the beginning of the project.

Contribution of Partner 3-VZLU

Work has been started by sorting incoming geometries, grid generation of test geometries. The limits of the available mesh deformation strategy for CFD simulation have been tested. The sequence of grids was prepared by a script and grid deformation with solution remapping was used, which serves as a reference case. For further use and higher flexibility, the interface boundary conditions between independent regions were tested and improved, too.

The Chimera technique has been implemented in sequential steps in order to evaluate the possibilities and compatibility with the CFD solver. In the first step the implementation was done to test the interface data management inside the solver, so test case grids were prepared and tested on 2D and 3D in 1CPU as well as with parallelization via MPI library. The solver relies on grids prepared with overlap by ad hoc tools. In the second stage the grid hole cutting algorithm with adjustable overlap has been implemented outside of the solver. Special care has been taken to maintain functionality of the solver acceleration techniques, like multigrid, and also of the functionalities as aero-elasticity.

In the third stage the chimera technique was implemented with the possibility to deactivate parts of the domain directly inside the solver (Figure 9), which brings the possibility of the Krueger device movement while lowering the pre-processing demands.

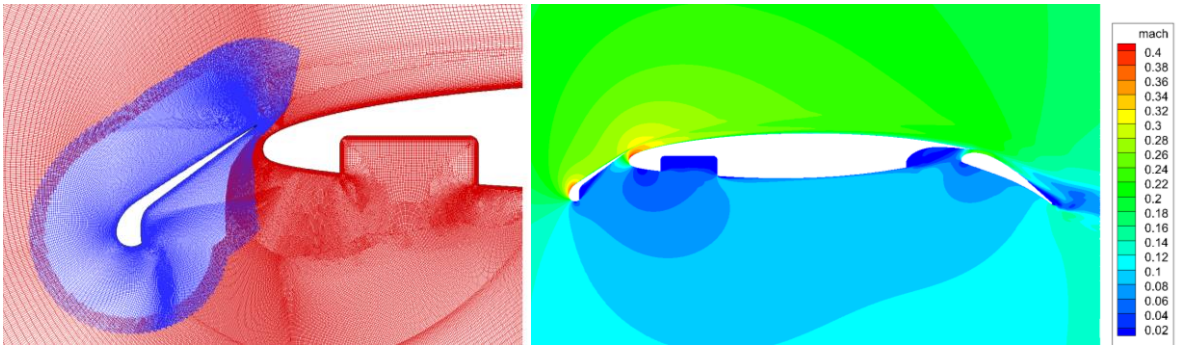

Figure 9: Chimera grid illustration, VZLU implementation

Contribution of Partner 4-ONERA

Preliminary automatic pre-processing procedure with Cassiopee tools of chimera grids around the different elements at two fixed positions has been implemented in the elsA environment. The two different positions considered are fully deployed and partially deployed (~90°, Figure 10).

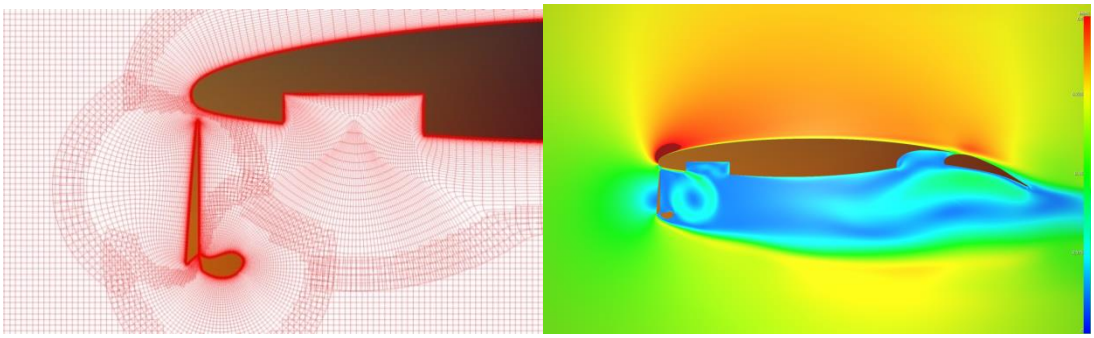

Figure 10: Chimera grid and solution – ONERA implementation

Then, kinematics of the Krueger elements (main part and bull nose) are controlled independently and first URANS computations of a complete cycle of deployment / retraction has been done.

This first methodology is ready for use for UHURA test cases to be investigated. A second methodology for the blanked cells management is under evaluation in term of computational efficiency.

Contribution of Partner 5-INTA

An assessment of a Lattice Boltzmann Method (LBM) based on a stress wall-modeled LES (WMLES) has been carried out. Studies regarding grid resolution and numerical settings for LBM WMLES have been performed with the aim of establishing best-practices guidelines for the validation phase to be carried out in WP4. First, a set of 3D (2.5D) static simulations (with fixed geometry position) have been conducted on the DLR-F15-LLE initial design at four selected representative positions of the Krueger device deployment/retraction: retracted, ~90°, leading-edge passage and fully deployed (Figure 11). Results have been compared with reference 2D RANS calculations for two configurations (retracted and deployed). Preliminary results showed that tripping turbulence was necessary to obtain resolved turbulence in the boundary layer of the upper surface. Hence, the strategy of turbulence tripping by means of roughness elements has been examined in the context of WMLES. A parametric study of the size and geometrical distribution of the roughness elements has been conducted for the retracted Krueger device position. The results show an improvement in the simulation in comparison with reference RANS solution even though the flow is inevitably perturbed.

Finally, a set of dynamic computations have been carried out using the numerical settings obtained from the analysis of the static cases. Complete 3D deployment and retraction simulations of the Krueger device have been performed using an immersed boundary method to deal with moving geometries (Figure 11). The results look reasonable overall in spite of the aforementioned difficulties related to turbulence generation. The necessary computational resources in terms of CPU-hours have been assessed, showing the potential of this alternative method to tackle scale-resolving simulations for complete Krueger device retraction/deployment phases. The experience gained in the assessment study will be used in the validation stage within WP4.

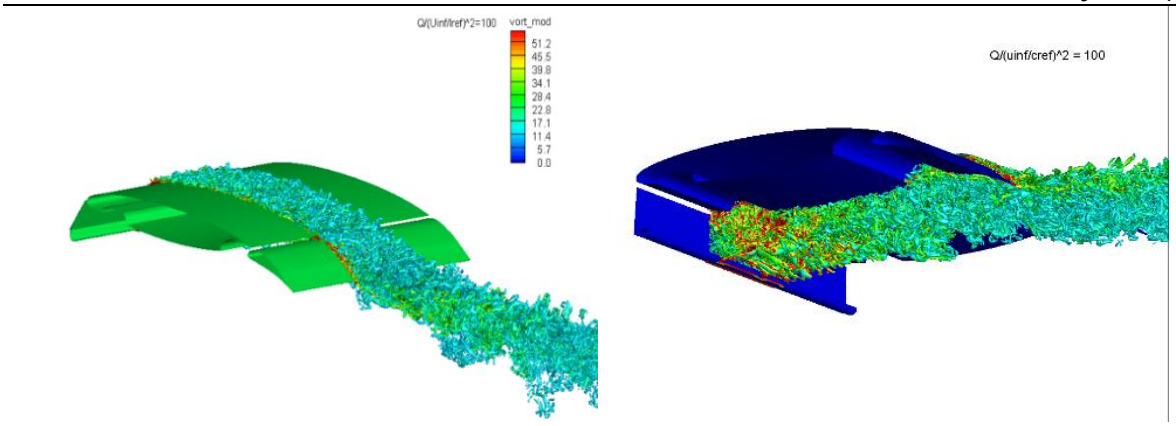

Figure 11: Iso-surface of dimensionless Q criterion for two positions of the Krueger device, LBM simulations by INTA.

Contribution of Partner 6-NLR

The flow solver development activities concern:

- Development of a line-implicit time integration approach for high-lift applications.
- Improvement of the interpolation process for large disparities in cell size in the interface region of discontinuous grids.

A line-implicit scheme has been implemented that accelerates the convergence per time step for the dual time-stepping approach. Its efficiency has been verified for building block applications that represent steady and unsteady flow cases such as an oscillating boundary layer. Test computations using this scheme are performed on the Chimera grid for the moving Krueger device generated in Task 2.1 to compute the time-dependent flow.

In order to improve the treatment of discontinuous interfaces, the in-house developed flow solver has been generalized to the full Chimera approach. Thus, full 3D interpolation is used instead of 2D interpolation along discontinuous interfaces, so that any disparity in cell size is automatically considered. The Chimera approach has been tested for the simulation of the unsteady flow field around a deploying Krueger device, consisting of a double-hinge motion for the bull-nose and base elements (Figure 12). Verification of the time-dependent flow solutions shows that the developed flow modelling capability is ready to be employed within UHURA.

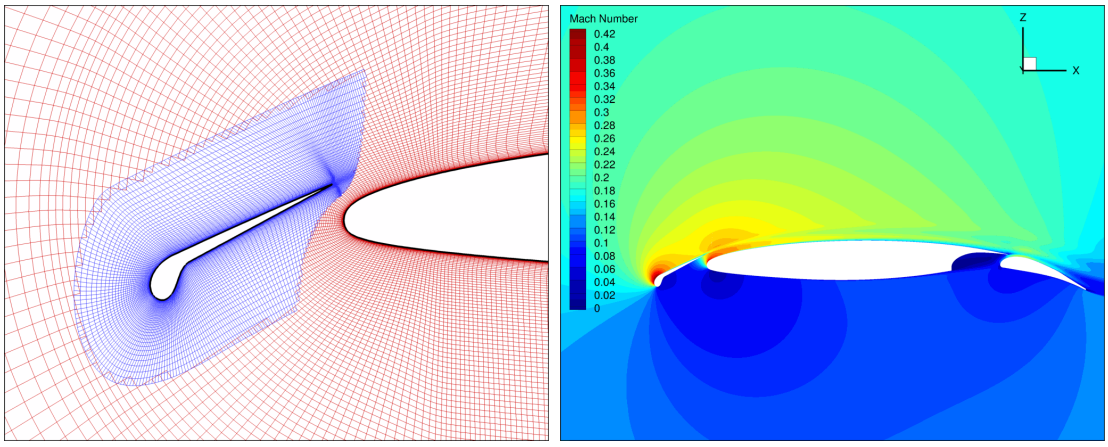

Figure 12: Chimera grid and solution for fully deployed Krueger flap, NLR implementation

Contribution of Partner 8-KTH

Automatic parametric meshing using Pointwise for different flap setting has been made (subcontracted as planned) for the initial and final test geometries containing a structured block in the wake region behind the Krueger flap suitable for LES resolution.

U-RANS of the moving two-hinged Krueger flap have been made by use of mesh deformation and remeshing using the automatic meshing tool for a full deployment and retraction cycle with different deployment velocities.

Refinements of numerical schemes for accurate and efficient hybrid RANS-LES computations have been made. Numerous hybrid RANS-LES studies of a fixed position around 90 deg are done for studying the effects of mesh refinement, time step and numerical schemes for best accuracy and efficiency. Different hybrid RANS-LES methods are tested and analysed concerning resolution and spectral content. The conclusion is that simulations of the full cycle will be affordable for the experimental setup, and that the Spalart-Allmaras DDES (SA-DDES) gives the most accurate and reliable results.

The quasi-steady approach has been implemented and tested for a pitching airfoil. The unsteady computation at a specific time can be well reproduced by a steady-state computation with forcing computed based on the unsteady RANS.

Hybrid RANS-LES (SA-DDES) computations of a full deployment cycle of 1.2s has been made for the two-hinged flap (Figure 13).

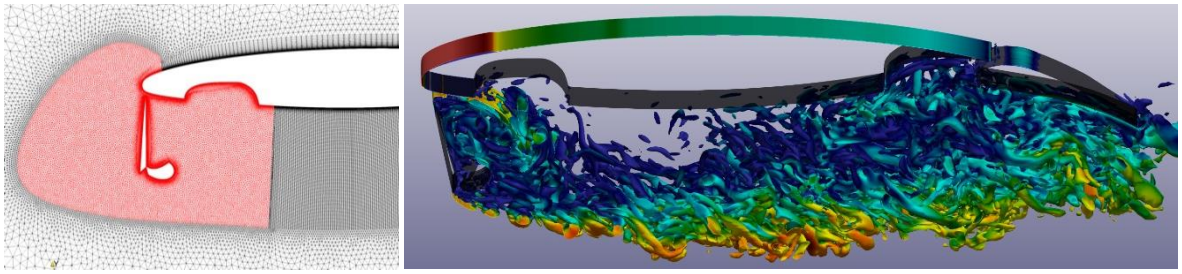

Figure 13: Mesh and snapshots of Q criterion at T = 0.5 s (71.5°) during the deployment, DDES simulations by KTH.

Contribution of Partner 9-IBK

IBK is developing an FSI-Interface tool in cooperation with CIRA. This tool should enable FSI-simulations employing existing CFD and CSM tools. The UZEN/SIMBA of CIRA and NASTRAN are used as CFD and CSM tools, respectively. The data exchange format will be adaptable to the used tools. In the current work, the CFD data exchange format is TECPLOT-format while the CSM uses the NASTRAN bdf-format. The main task of the FSI-interface tool is to provide a means of transferring aerodynamic loads from CFD to CSM and transferring mesh deformations and deformation velocities from CSM to CFD. With a proper tool chain, FSI-simulations involving CFD-tool, FSI-interface and CSM-tool should be realized. Therefore, the method development concerns primarily with the interpolation procedure, data processing and process control. The interpolation procedure is based on the radial basis function (RBF). The method enables accurate aerodynamic load data transfer from CFD-mesh to CSM-mesh and then to transfer the deformation data from CSM-mesh back to CFD-mesh. Prior to the application of the FSI-interface tool, CFD and CSM models have to be prepared and they should be compatible each other. IBK is responsible for preparing the CSM model.

The initial version of the FSI interface tool concerns a "static two-way coupling" in the way that the CSM applies the linear static solver. It allows a loose interaction between CFD and CSM where deformation velocities are not considered. This FSI-method has been successfully tested on the conventional 3 element airfoil (DLR-F15-3eRef) where slat and flap are simultaneously deployed.

The FSI interface tool is then further developed to deal also with a "dynamic two-way coupling", where the dynamic behavior of the structure is accounted for. Both structural deformations and deformation velocities will be then exchanged between CFD and CSM. The method is now exercised on the DLR-F15-LLE Krueger configuration (Figure 14). Due to current aerodynamic limitations the Krueger panel and Bullnose are merged into a single Krueger element. The Krueger kinematics is

accordingly adapted. Setups and computations are on-going. Small delay in delivering the results and deliverables is expected.

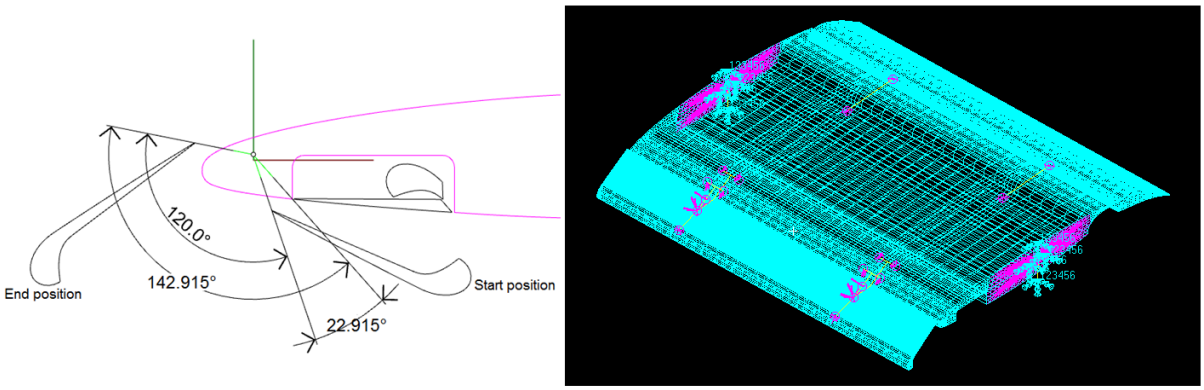

Figure 14: The FSI interface tool applied on the DLR-F15 LLR Krueger configuration

Contribution of Partner 11-Dassault

Different hybrid RANS-LES methods (VLES, IDDES and ZDES) as well as different subgrid length scale models have been implemented and tested. In particular advanced RANS models are considered. Implementation and validation is still ongoing.

DES computations have been performed on the fully extended Krueger slat configuration.

2.3 WP 3: Validation Experiments

Task	Title	Starting at	Completion	Status
3.1	**Model Modification**	**M7**	**M22**	**completed**
3.2	**Adaptations of Measurements**	**M5**	**M38**	**completed**
3.3	**Experiments**	**M15**	**M48**	**completed**

Lead: DNW

The objective of WP3 were the preparation, execution and analysis of a series of wind tunnel tests for obtaining high-quality validation data. For this, the DLR-F15 and DLR-F15LS model needed to be modified, measurement techniques had to be matured and synchronized, and wind tunnel tests had to be conducted.

The design of the wind tunnel model modifications for the DLR-F15 model has been finalised (CDR at M16). The model stress analysis has been finalised and reporting is scheduled to be delivered within this reporting period. Model manufacture of the new LE and Krueger parts is finished and assembly successfully completed in M26.

The design modification for the F15-LS model are finished. The stress analysis for the model modifications has been performed. All modifications have been discussed and agreed in a preliminary and a critical design review meeting. New model parts have been manufactured and assembly of the new parts on the F15-LS model was finished in M31.

The evaluation of the unsteady capability of standard pressure measurement equipment has been completed and reported in M12.The consortium has agreed on an approach to synchronise the different measurements. To achieve this, the drive system for the Krueger device has been reprogrammed to accept hardware triggering. Also, for the MEMS acquisition software a hardware triggering has been implemented. The setup of measurement techniques is completed. Approach and setup design of optical measurement techniques has been defined and was reported in M37 and M38.

After completion of the DLR-F15 model modifications, a first wind tunnel test in the ONERA L1 wind tunnel has been conducted in M27. Due to technical challenges and wind tunnel occupation, it was not possible to complete the full test program. Therefore, a second wind tunnel test at ONERA L1 was scheduled. After model improvements, the wind tunnel test in DNW-NWB on the DLR F15 model in cantilever configuration was prepared. The test program of the DNW-NWB was successfully finished in M31. Data of the DNW-NWB test was delivered to the consortium in M37.Wind tunnel testing on the large scale DLR-F15LS model in DNW-LLF was finalised in M33. Due to the COVID-19 crisis the partner DLR was unable to perform PIV testing. It was agreed to plan a second wind tunnel test to perform PIV on the F15 LS test. A partial data delivery (pressure data) of the DNW-LLF test to the consortium was performed in M35.

The second wind tunnel test campaign in the ONERA-L1 wind tunnel facility was conducted in M37/M38. The experimental data including PIV das delivered to the consortium as deliverable D33-2. In addition, the test report of the ONERA L1 test was submitted (D33-3).

The second DNW-LLF wind tunnel test was successfully completed with PIV performed by DLR in M44. Wind tunnel data of the second DNW-LLF test was delivered to the consortium. The SPR data model deformation data of the first DNW-LLF test was provided. PIV processing of the DNW-LLF was ongoing up to the end of the project. The test report of the DNW-LLF test campaigns was finalised and submitted (D33-9)

Table 2 WP3 Milestones, deliverables, time schedule & spending

Deliverables in WP3		*Partner(s)*	*Month due*	*Month completed*
D32-1	Pressure measurement requirements for the models	DNW	M7⇨M9	M12
D31-1	Description of model modification for the DLR-F15 model	DLR	M12⇨M14	M18
D31-2	Description of model modifications for the DLR-F15LS model	DLR	M16⇨M25	M31
D31-3	Stress report for the modified DLR-F15 model	IBK	M16⇨M18	M19
D31-4	Modified DLR-F15 model ready for testing	DLR	M16⇨M24	M26
D33-1	Test Matrix for ONERA L1 wind tunnel test	ONERA	M17⇨M19	M25
D33-2	Wind tunnel test report ONERA L1	ONERA	M18⇨M40	M42
D33-3	Post-processed PIV data and preanalysis of ONERA L1 tests	ONERA	M20⇨M40	M46
D33-4	Test Matrix for DNW-NWB wind tunnel test	DNW	M20⇨M27	M31
D31-5	Stress report for the modified DLR-F15LS model	IBK	M21⇨M25	M30
D31-6	Modified DLRF15LS model ready for testing	DLR	M22⇨M30	M31
D33-5	Wind tunnel test report DNW-NWB	DNW	M22⇨M33	M37
D33-6	Final Data of DNW-NWB wind tunnel test	DNW	M22⇨M35	M37
D32-2	Set-up design for the stereo pattern recognition test technique in DNW-LLF	DNW	M23⇨M33	M37
D32-3	Flow field measurement requirements and techniques for ONERA L1 and DNW-LLF	DLR	M23⇨M33	M38
D33-7	Test Matrix for LLF wind tunnel test	DNW	M23⇨M33	M34
D33-8	Wind tunnel test report DNW-LLF	DNW	M26⇨M44	M47
D33-9	Final Data of DNW-LLF wind tunnel test	DNW	M26⇨M46	M47

Milestones in WP3		*Partner*	*Month due*	*Month achieved*
M32-1	Time resolved pressure measurement technique ready	DNW	M7⇨M9	M12
M31-1	Model DLR-F15 modification completed	DLR	M16⇨M24	M26
M32-2	Time resolved stereo pattern recognition technique ready	DNW	M16	M23
M33-1	DLR-F15 model ready for testing at ONERA L1	ONERA	M17⇨M24	M26
M33-2	Finalization of test program L1	ONERA	M18⇨M38	M38
M33-3	DLR-F15 model ready for testing at DNW-NWB	DLR	M19⇨M31	M31
M33-4	Finalization of test program DNW-NWB	DNW	M21⇨M31	M31
M31-2	Model DLRF15 LS modification completed	DLR	M22⇨M32	M30
M33-5	DLR-F15 LS model ready for testing in the wind tunnel DNW-LLF	DNW	M23⇨M32	M31
M33-6	Finalization of test program LLF	DNW	M24⇨M44	M44

2.3.1 Task 3.1 – Model modification

Lead: DLR

Task 3.1 objectives

- design model modifications for DLR-F15 model to incorporate the Krueger device and leading edge designed in WP1
- perform FEM analysis for stress report on wind tunnel model
- manufacture and assemble DLR-F15 model modifications and instrumentation
- perform modifications of model mounting mechanism for DNW-NWB experiment
- manufacture and assemble model modifications of DLR-F15LS model

Progress achieved/results

The DLR-F15 model has been delivered to DNW-NWB for testing beginning of M31; the DLR-F15LS model was finalized and delivered to DNW-LLF for testing end of M31. The task is completed

Contribution of Partner 1 - DLR

After receipt of the wing geometry and the designed Krueger device from WP1, model design has been performed for the modification of the DLR-F15 wind tunnel model. The CAD data has been verified and the Krueger device has been implemented (Figure 15). The design comprises a full-span and a part-span version of the Krueger flap (Figure 16). First load assessments in wind tunnel conditions showed a high overload for the Krueger drive shaft. Load mitigations have resulted in a reduction of the angle of attack for the dynamic movement. This reduced angle of attack is in line with flight conditions for the operating Krueger device. The detailed design phase was initiated by issuing a design check list, which has been discussed and consolidated by a Preliminary Design Review (PDR) in conjunction with the 2nd Progress Meeting (PPM2). The design of the model has been finalized by a CDR held in M16. A corresponding design report (D31-1) has been provided. Manufacturing has been started right after and the process is in good progress. First parts – mainly parts of the kinematics – are ready and available (Figure 17). The remaining parts are expected for early M19 (March 2020) for final assembly. The shipping of the model to ONERA L1 wind tunnel is expected for late M19.

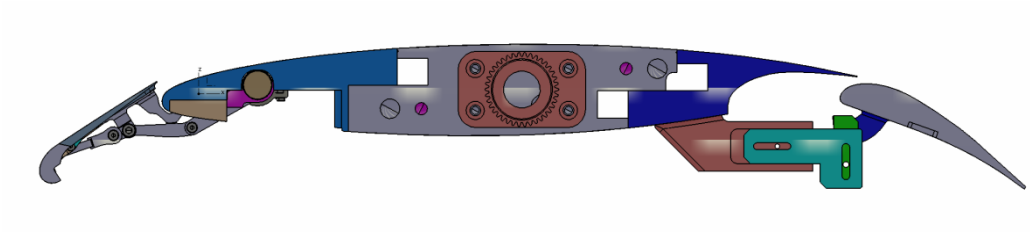

Figure 15: DLR-F15-LLE wind tunnel model with Krueger flap

Manufacturing of model modifications of DLR-F15 model is almost complete. Only few, but important parts (Krueger panels and bull noses) are still in delivery from subcontractor. The kinematics has been completed and assembled in the model. The mechanics has been produced at a very high accuracy, runs smoothly (as it can be actuated by hand force only) with only minor angular free play, giving confidence on a smooth actuation at the tunnel. The motor control has been adopted for the needs of the project implementing a cycling motion functionality and introducing handshake trigger signals for communication with the wind tunnel control. The circuit boards with the MEMS pressure sensors have been produced and tested. The setup provides a stable measurement of pressures at a sampling rate of 100Hz.

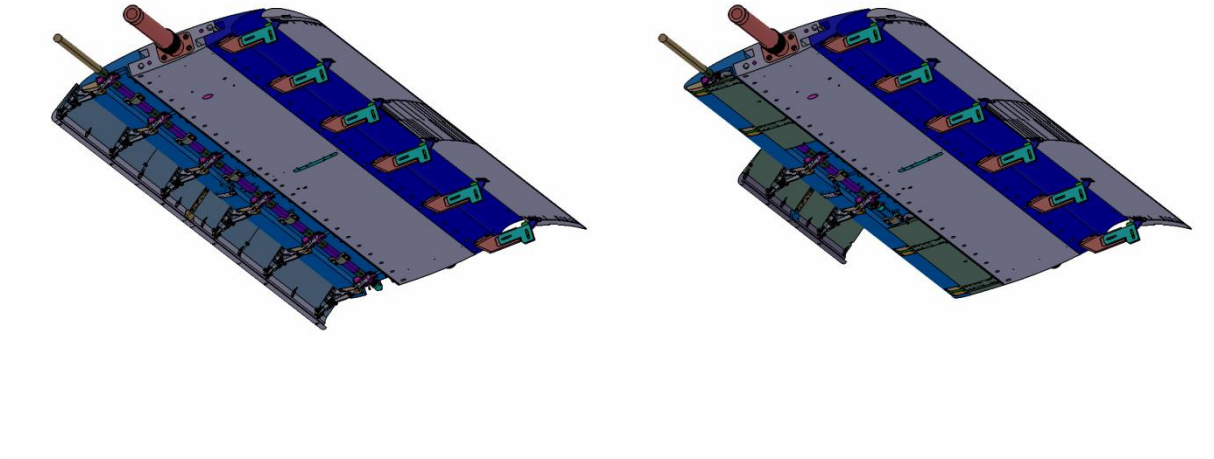

Figure 16: setup of wind tunnel model with (left) full span and (right) part span Krueger flap

Figure 17: manufactured Krueger kinematics for the DLR-F15 model

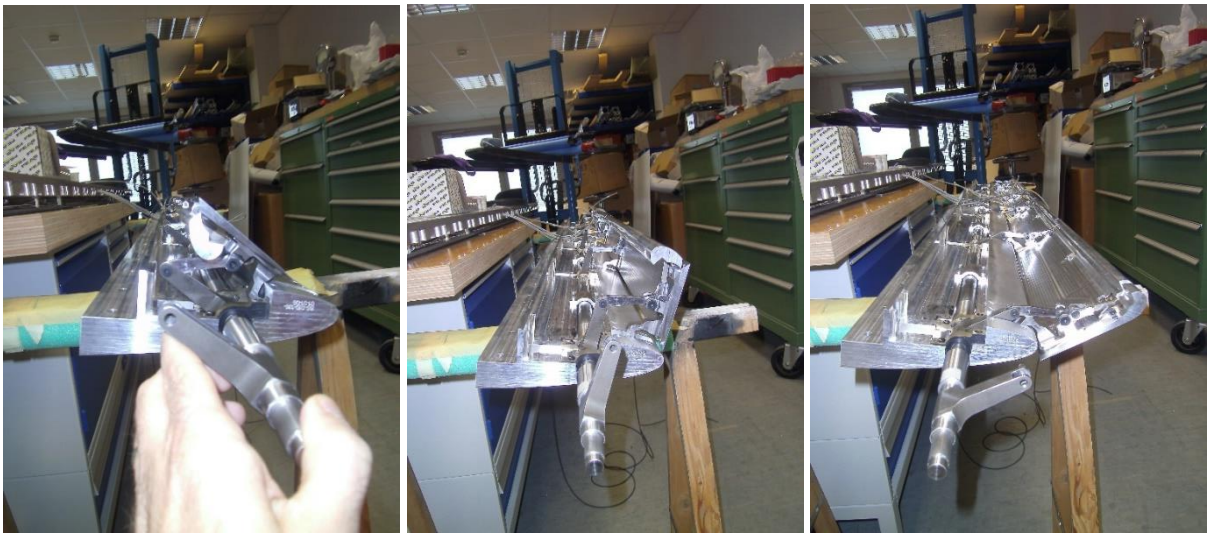

Figure 18: assembled leading edge for the DLR-F15 model. From left to right: motion of the Krueger from retracted to deflected by hand force only.

DLR completed the final assembly of the DLR-F15 model. Figure 18 shows impressions of the assembled leading edge before mounting to the main model. The precision of manufacturing is exceptionally high. As such, the Krueger on the full span can be driven by hand force in the full span configuration. Within the kinematics no significant free play or excess friction has been detected. Only the polygonal connections at the entry of the drive shaft shows slight free play.

The most difficult part in the final assembly has been the routing and connection of the different measurement techniques. Especially the installation of the strain gauges showed up to be very complicated and the count and space allocation of cables has been completely underestimated. This lesson learnt has been directly fed into the large model modification. Nevertheless, the line-up of all wires for strain gauges and MEMS was all but easy, but succeeded in the end. But the survivability of those connections during test has still to be proven as the wiring along moving parts seems critical in terms of disconnecting/cut-off cables.

The model assembly was finalized at beginning of M26 and sent directly to ONERA for testing in L1 (see Task 3.3). The model was received back from testing in Mid M27. Afterwards the preparation started for the test in DNW-NWB scheduled for M31. For this the model had to be refurbished and the Krueger flap configuration had to be changed from full-span to part-span. During refurbishment it was observed that all cables running to the strain gauges have been cut and the cable running to the MEMS have been severely damaged leading to a loss of connection to the circuit board in the bull nose. For the test in DNW-NWB, the routing has been reworked to mitigate any risks from getting the cables caught inside the kinematics. The cabling of the strain gauges has completely been removed and this technology is no longer foresee for the coming tests as it is highly risky in terms of survivability but a high effort to install. Anyhow, a limited set of data is available from the first tests to be used for calibration.

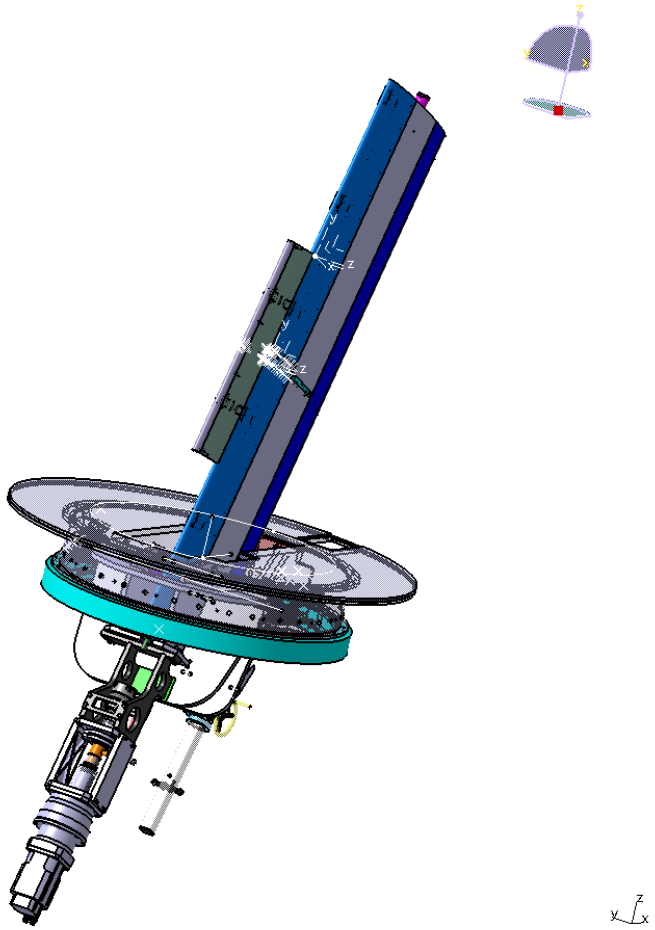

Figure 19: CAD of the DLR-F15 model in the DNW-NWB mounting mechanism for wing sweep

In addition, the mounting mechanism in DNW-NWB (Figure 19) providing the wing sweep has been modified to enable attachment of the Krueger drive motor. These adoptions have all been made and the model refurbishment has been completed in time for the DNW-NWB test entry.

In parallel, the manufacturing of the modifications of the large model DLR-F15LS has been initiated. The design has been approved by a Critical Design Review (CDR) in M25. Figure 20 shows the CAD of the final model assembly. Based on this the stress report was compiled by the partners ASCO and IBK and approved by DNW (see below).

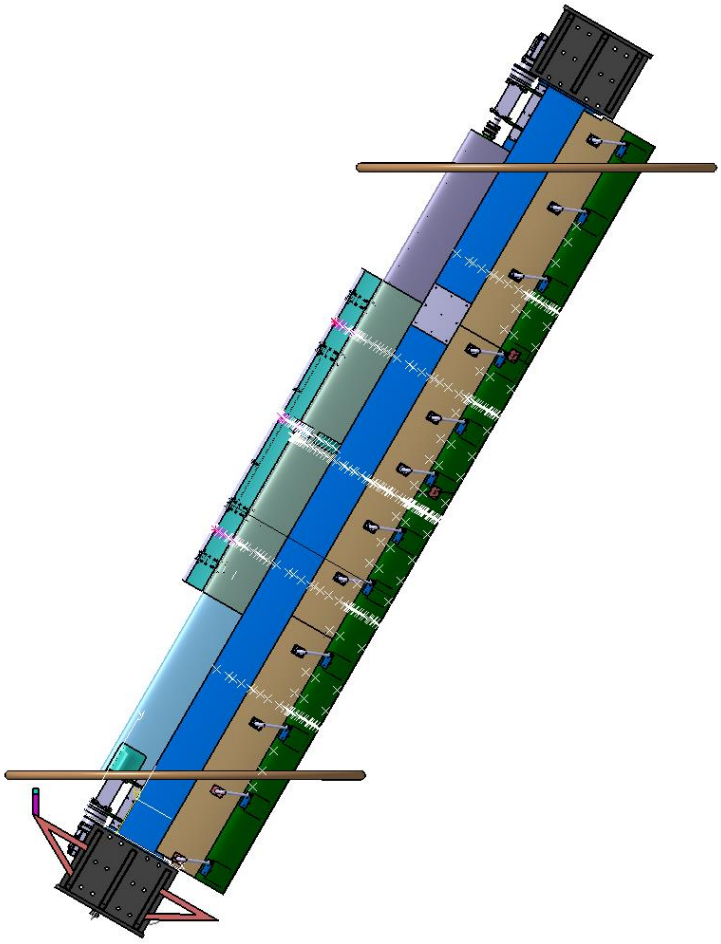

Figure 20: CAD of the DLR-F15LS model for the DNW-LLF wind tunnel with deflected Krueger flap in the center part and mounted drive engines

The design of the DLR-F15LS model modifications has been completed. A PDR has been held on July 2nd, 2020. A closing CDR scheduled for early September 3rd, 2020. A call for tender for manufacturing the big model parts has been launched.

An external manufacturer has been selected (call for tender had already been launched in M23) and subcontracted for manufacturing the leading edge and the Krueger panel and bull nose. In contrast to initial planning, the manufacturing of kinematics parts has not been subcontracted but kept inhouse. This was a conclusion based on the high precision observed on the small model. All parts of the external manufacturer were received within M29, the parts produced inhouse were received beginning of M30. Pre-assembly of the kinematics and drive train has started as well as instrumentation of the leading edge and the Krueger flap (Figure 21).

Figure 21: impressions of pre-assembly and instrumentation of the DLR-F15LS model parts: (left) drive train & kinematics; (middle) cabling and pressure tube installation in leading edge; (right) pre-assembly of Krueger flap and pressure tube installation

It was planned to start assembly just after, but a new winter weather prevented the movement of the model from storage to the workshop. Thus, the model assembly has to be postponed by three weeks due to weather conditions – squeezing the time for assembly down to three weeks. A tight time planning was made and nearly kept including the routing and installation of measurement instrumentation. Figure 22 shows an impression past assembly during installation of the instrumentation.

Figure 22: assembled DLR-F15LS model with Kreger mounted during instrumentation installation

The model was finalized in M31 and delivered to DNW-LLF. Figure 23 shows the loading of the model on March 25th, 2021. With this action the activity of model manufacturing is completed.

Figure 23: loading the assembled DLR-F15LS model into the truck for transport to DNW-LLF

Contribution of Partner 7 - ASCO

After participating to the Task 3.1 Kick-Off Meeting in M9, ASCO assisted in the definition of the design/sizing ownership split of the model. ASCO was identified as responsible for the final sizing of the kinematical (moving) components, excluding the Krueger panel and bull nose.

Based on the aerodynamic loads obtained from DLR in WP1, ASCO set up a full-span GFEM to compute all interface loads appearing within the kinematical system (Figure 24 & Figure 25). A selection of the critical load cases for component sizing was made. Three loading conditions were considered: static fully extended Krueger, dynamic (operating) Krueger & Krueger in 'barn-door' position (90° to flow field). Following interface loads and moments were computed for the 3 loading condition for all AoA.

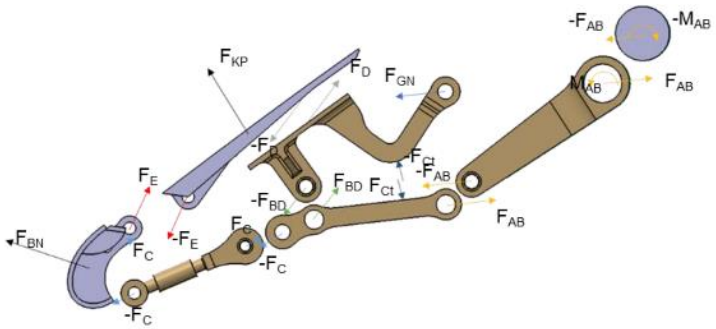

Figure 24: disassembly of kinematics into parts and corresponding interface loads to be respected

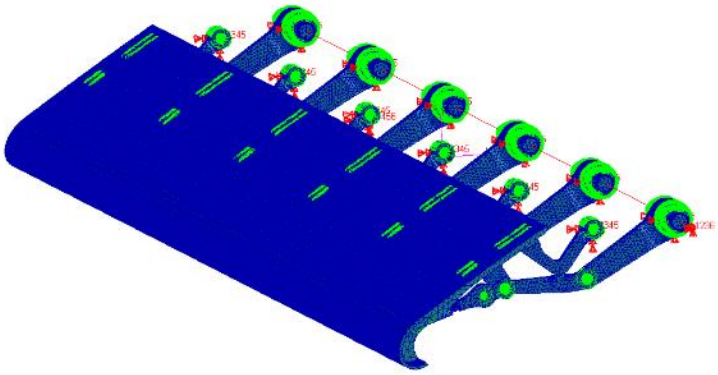

Figure 25: Illustration of the full-scale GFEM to compute all interface loads and moments

Following the results of the drive lever reaction torque computations, an issue was identified: the accumulated torque along the different support stations would require a drive shaft diameter that could not be integrated into the confined wing leading edge opening; moreover, the induced angular deformation of the drive shaft would be excessive. Hence, Task 1.2 (kinematics design) was reopened to investigate design changes that could solve this issue.

In order to reduce the reaction torque on the drive shaft in the most critical condition (i.e. statically fully extended Krueger at AoA = 21°) a contact feature between the Gooseneck and Drive Link components was introduced (Figure 26). Through this contact, reaction load is diverted to another load path and the drive shaft torque is drastically reduced. This leads to a drive shaft diameter that could be integrated into the wind tunnel model.

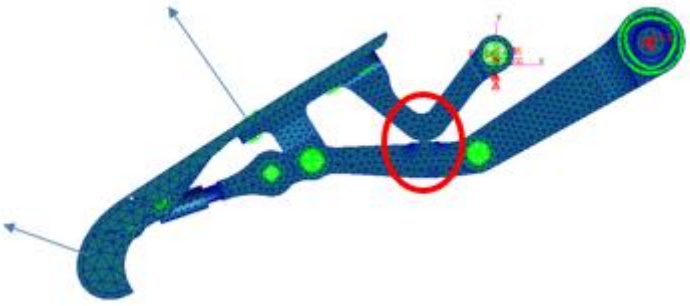

Figure 26: contact feature between Gooseneck and Drive Link to alleviate drive shaft reaction torques

All kinematical components in the ASCO-scope were sized to avoid failure of a kinematical component and protect the wind tunnel. Sizing was done by means of hand-calculation methods, DFEM or GFEM. An overview of the critical RFs is given in Figure 27 (RF > 1 proves sufficient strength; these values include the Safety Factors required by the wind tunnel institutions).

The final kinematics design and sizing was presented and accepted by the WP3 partners during PDR in M13 and CDR in M16. ASCO compiled a summary Stress Report of the sizing activities on the DLR-F15 model kinematics as Part 2 of the IBK deliverable D31-3.

The stress report for the kinematics of the small DLR-F15 model has been finalized and delivered as part 2 of deliverable D31-3. The sizing of the kinematics of the large model has been completed up to a CDR maturity with support of Task 1.2. The stress report as part of deliverable D31-5 is progressing and assumed to be completed in M25.

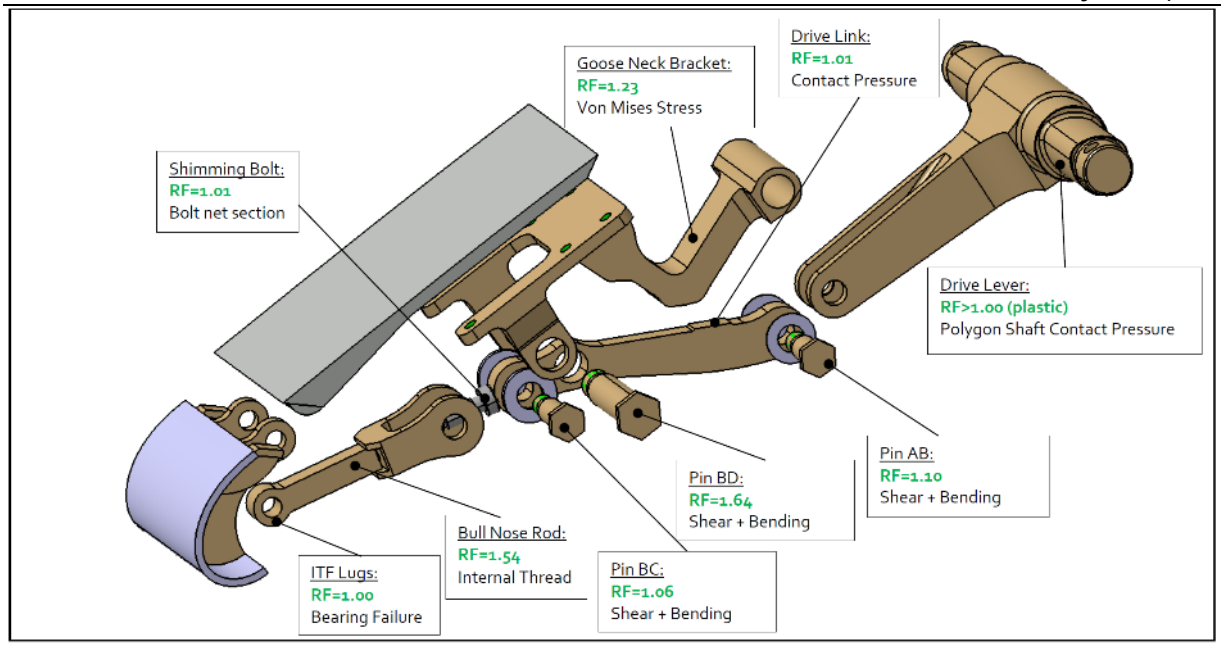

Figure 27: reserve factors obtained for the different parts of the kinematics

The sizing of the kinematics of the large model has been completed up to a CDR maturity (M25) with support of Task 1.2. The stress report for the kinematics as part of deliverable D31-5 has been completed and provided to IBK for delivery.

Contribution of Partner 9 - IBK

IBK is mainly responsible for Bullnose and Krueger panel structural design and their interface to the kinematics. Common criteria regarding max. combined stress, shear stress and max. dynamic loads have been derived for both wind tunnel entities ONERA and DNW. The distributed Krueger loads on the Bullnose and Krueger panel for the critical case have been mapped to the FE model. The FE-analyses for the Krueger configuration of the DLR-F15 model has been carried out. IBK and ASCO shared the work in the way that ASCO does the design and FE-analyses for the kinematics and IBK does the FE-analysis for the whole model. The stress report for the model is in progress.

The definition of a concept for strain-gauge measurement as a provision for Krueger-force measurement has been started. An FE-analysis to determine the proper location of strain gauges for load monitoring is ongoing.

The stress report for the DLR F-15 Small WT-model in part 1 of the deliverable D31-3 has been completed and delivered. For the larger DLR-F15LS model, a preliminary stress analysis was provided for CDR.

The stress report for the structural parts (leading edge and Krueger panel) has been completed. Together with the part of ASCO this has been compiled into the deliverable D31-5, which has been submitted in M30.

Contribution of Partner 12 - DNW

DNW participated in the PDR and CDR meetings to evaluate instrumentation and stress analysis approaches. DNW has evaluated integration of the pressure modules in the model LE. Design modifications have been proposed and implemented. The modules can be place in the model close to the pressure taps in the Krueger device.

DNW reviewed the stress report for the DLR-F15LS model to be in line with the requirements for the tunnel operation.

2.3.2 Task 3.2 – Adaptation of measurements.

Lead: DLR

Task 3.2 objectives

- Identify and prepare suitable optical measurement techniques (SPR, PIV)
- Mature dynamic pressure measurements by MEMS and pressure scanners
- Establish synchronization strategies for simultaneous time resolved measurements
- Adaptation of measurement techniques for time resolved recording of Krueger device deployment/retraction

Progress achieved/results

For the subtask 3.2.1 (DNW) (Unsteady pressure measurements / time resolved static pressure measurements) the aim is to establish if the standard pressure measurement system can be used for time resolved static pressure measurements. Within this reporting period, the effect of tube length has been assessed with a theoretical model. The results of the theoretical model were verified with a wind tunnel experiment in the DNW Low Speed Wind Tunnel (LST). The results include a definition of maximum tubing length and a data acquisition approach to synchronise the reading from conventional electronic scanning pressure modules with other measurement systems.

For Task 3.2 common progress of all involved partners (DLR, DNW and ONERA) has been made regarding discussion and definition of synchronization techniques and interchange of protocols between wind tunnel and measurement system units. The wind tunnel tests at ONERA L1, DNW-NWB and DNW-LLF will include a large variety of measurement systems and instrumentation. For a meaningful validation of unsteady CFD synchronicity between the sub-systems of different partners will is of high importance. The list below highlights the complexity of the wind tunnel experiment. The different sub systems have a multitude of sampling frequencies and data protocols:

List Data Acquisition Systems: (provider, description, WT test)

1. ONERA /DNW, Wind tunnel Flow Reference system (L1, NWB, LLF)
2. ONERA /DNW, Pressure modules (L1, NWB, LLF)
3. DLR, MEMS Unsteady pressure sensors (L1, NWB, LLF)
4. DLR, Angular Encoder of Krueger Shaft (L1, NWB, LLF)
5. DLR, Krueger Drive system, (L1, NWB, LLF)
6. DNW, SPR position Measurement system (LLF, possibly NWB)
7. DLR, Strain Gauges ion kinematic (L1, NWB, LLF)
8. DLR/ ONERA,PIV (L1, LLF)

The consortium is converging on a measurement approach to fulfil the requirement of synchronicity and to handle acquisition of all sub systems in an efficient manner. This approach will rely on:

- Hardware TTL level triggering to synchronise all sub-systems
- A Handshaking protocol to handle acquisition efficiently and to guarantee sound wind tunnel bookkeeping of data.

Contribution of Partner 1 – DLR

The available PIV related measurement methodologies have been assessed by all involved groups depending on the optical access and different sizes of the PIV field-of-view for the flow around the Krueger equipped F15 model at ONERA L1 and the respective larger F15LS model at DNW-LLF. Decisions regarding the particle image acquisition strategy and synchronization with SPR and dynamic pressure transducer probes have been made accordingly. For both wind tunnel tests phase-locked Stereo 3C2D- and 2C2D-PIV measurement techniques are foreseen allowing for unsteady phase resolved flow field measurements and mean and Reynolds stress statistics at many stages of the deployment and retraction phases of the Krueger device. Additionally, at ONERA L1 a time-

resolved PIV system will complement the overall measuring systems allowing for a transient flow field characterization in a sub-volume downstream of the moving Krueger device. In DNW-LLF a synchronized SPR system will be applied in order to receive the exact Krueger device shapes and deformations during the individual deployment processes and phase positions of the SPIV measurements. Furthermore, both models will be equipped with many dynamic (MEMS at ~150 Hz, few Kulites ~kHz) and static pressure transducers (see Task 3.1), which will acquire data in synchronization with the PIV and SPR techniques.

A second activity of DLR is concerned with the setup of dynamic MEMS pressure sensors for unsteady measurements of local pressures. For the DLR-F15 model the design of the circuit board for mounting the Bosch BMP388 sensors has been completed. The first circuit boards for the Krueger bull nose have been equipped (Figure 28) and are currently tested and calibrated. The programming for data acquisition is in progress.

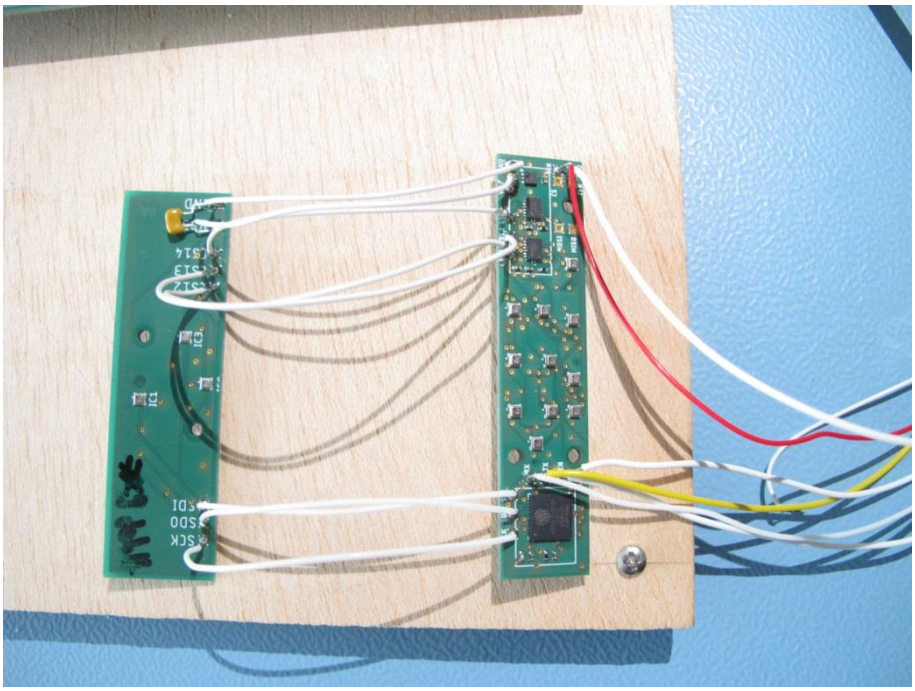

Figure 28: circuit boards with a total of 14 Bosch BMP388 MEMS pressure sensors for the Krueger bull nose of the DLR-F15 model

The target installation of SPIV in the DNW-LLF test has been further prepared (Figure 31). The final window position, laser sheet orientation and camera positions have been defined. A preparation mock-up with four cameras and dummy wing has been set-up in the DLR laboratory for the designated 2 x SPIV systems at DNW-LLF. With this setup, the orientation and optical details have been verified. The system is by this defined and ready for setup in the test facility. The system is by this finally defined and ready for setup in the test facility. A SPIV related timing scheme has been established with a hand-shake to the wind tunnel and for synchronization to the other measurement systems (Figure 30).

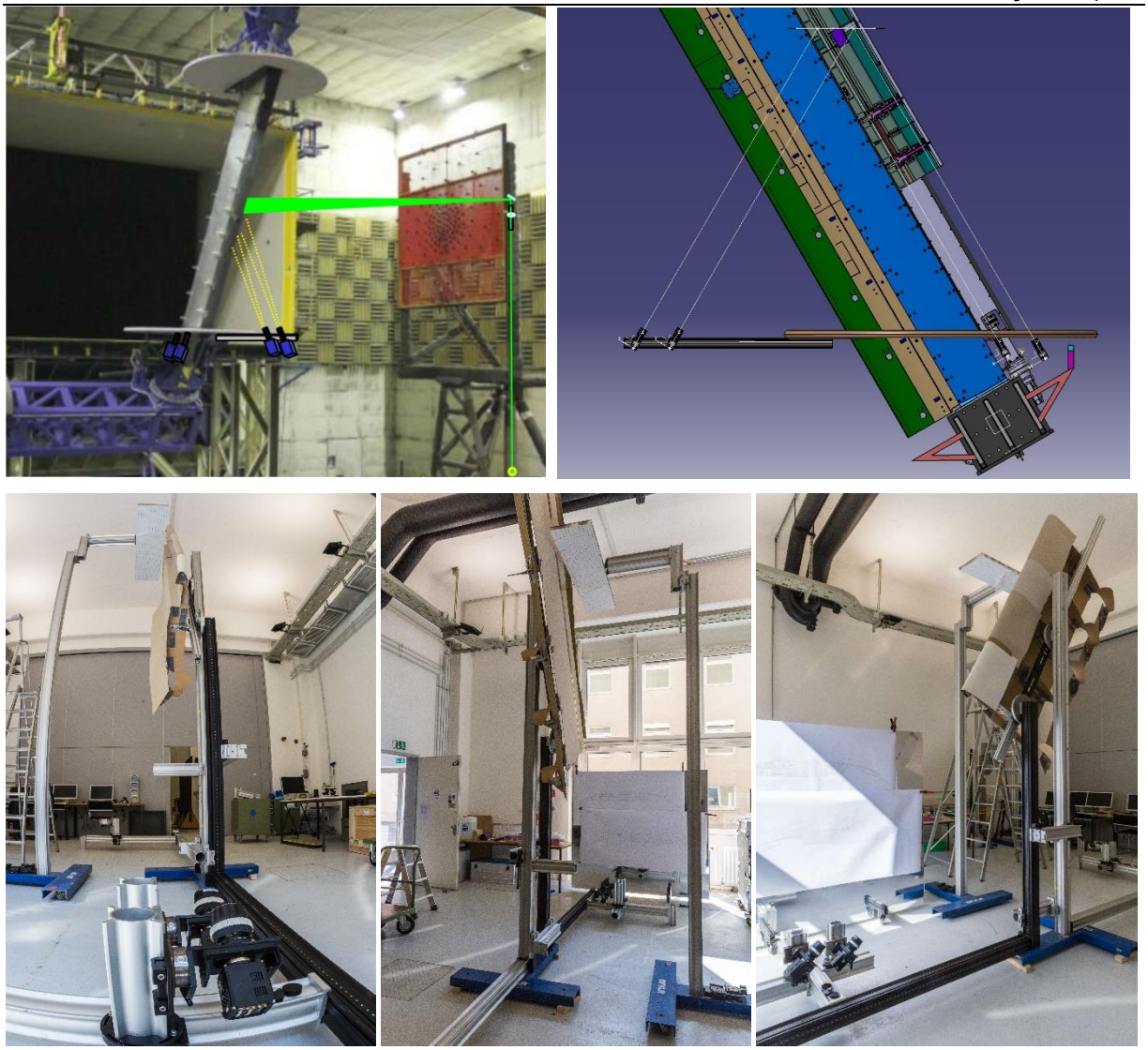

Figure 29: planned PIV installation in DNW-LLF and digital mock-up (DMU) (top-row) and corresponding laboratory mock-up (bottom-row) to check visibility, camera angles and optics.

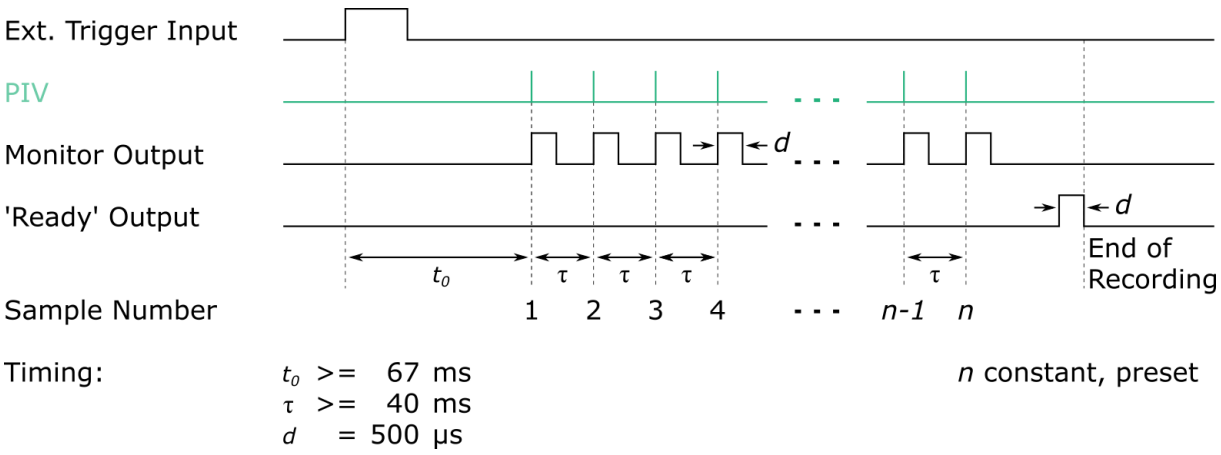

Figure 30: Timing diagram for synchronization of SPIV measurement system in DNW-LLF

The compilation of the deliverable D32-3 on "Flow field measurement requirements and techniques for ONERA L1 and DNW-LLF" is still ongoing, because of the COVID-19 related postponement of the LLF SPIV campaign to spring 2022.

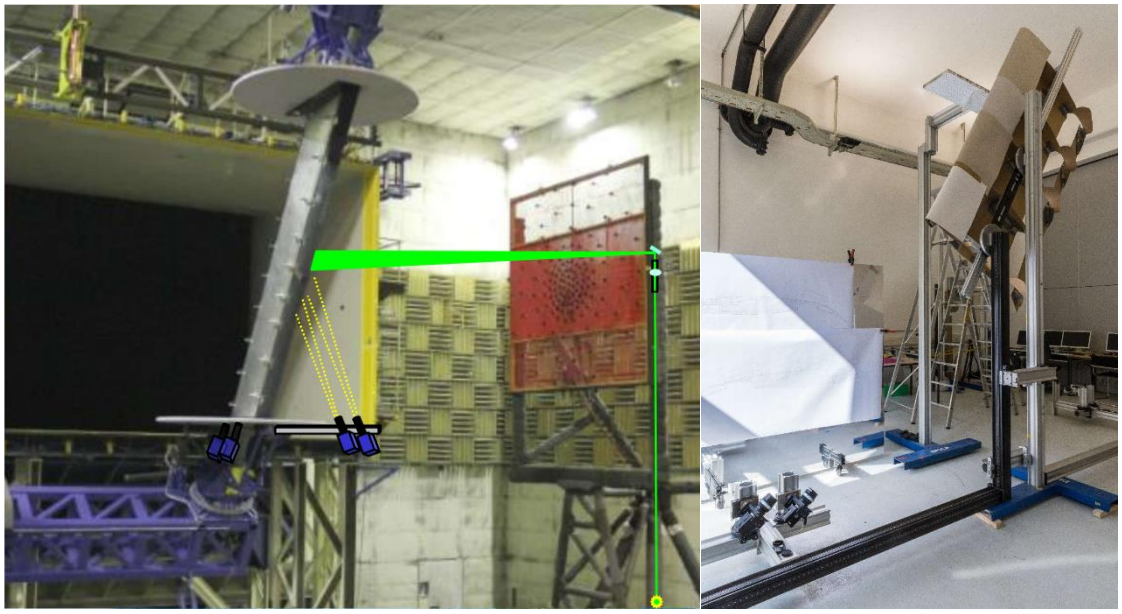

Figure 31: planned PIV installation in DNW-LLF (left) and corresponding laboratory mock-up (right) to check visibility, camera angles and optics.

The compilation of the deliverable D32-3 on "Flow field measurement requirements and techniques for ONERA L1 and DNW-LLF" is still ongoing, because of the COVID-19 related postponement of the LLF SPIV campaign to spring 2022.

Contribution of Partner 12 – DNW

The experiments to verify the measurements of unsteady pressures using conventional pressure modules have been performed in the DNW-LST. A moving wind tunnel model was manufactured consisting of a rotating cylinder (Figure 33). Model actuation rate was similar and above to the UHURA requirements (up to 180⁰/s was achieved). The pressure signal from conventional pressure tap-tubing -module configuration was compared to surface mount device (Kulite) results

Analysis of the results has been finalised and reporting was performed in order to complete deliverable D32-1. The results have shown that unsteady pressures at the acquisition frequencies required by UHURA can be measured using conventional pressure modules, provided that the tubing length is shorter than 0.7 m. Furthermore, DNW has developed a programmable sequencer and acquisition software modules within the wind tunnel data acquisition system to allow for synchronous time resolved measurement of both pressure signals and other measurement techniques. These experiences are a vital preparation for the final wind tunnel experiments in the DNW-LLF.

Within the consortium an approach to synchronise and harmonize the different measurement systems has been finally defined. DNW, DLR and ONERA have participated in these discussions. All systems will use TTL level triggering for synchronisation. The drive system can be phase shifted to perform PIV and SPR throughout all desired phase locked angles. Due to a very low identified time jitter of only less than 1 ms during repeated operations of the Krueger drive system and the used fast reacting hard- and software control devices for all individual measuring techniques the consortium is quite confident that many phase-locked- and partly time-resolved measurements of the desired transient and dynamical flow field, surface pressure and structure deformation quantities can be determined during the three wind-tunnel campaigns. The gained spatial and temporal resolution of

the used probe and field measurement techniques will be communicated to WP4 shortly after finalization of each of the three wind tunnel campaigns.

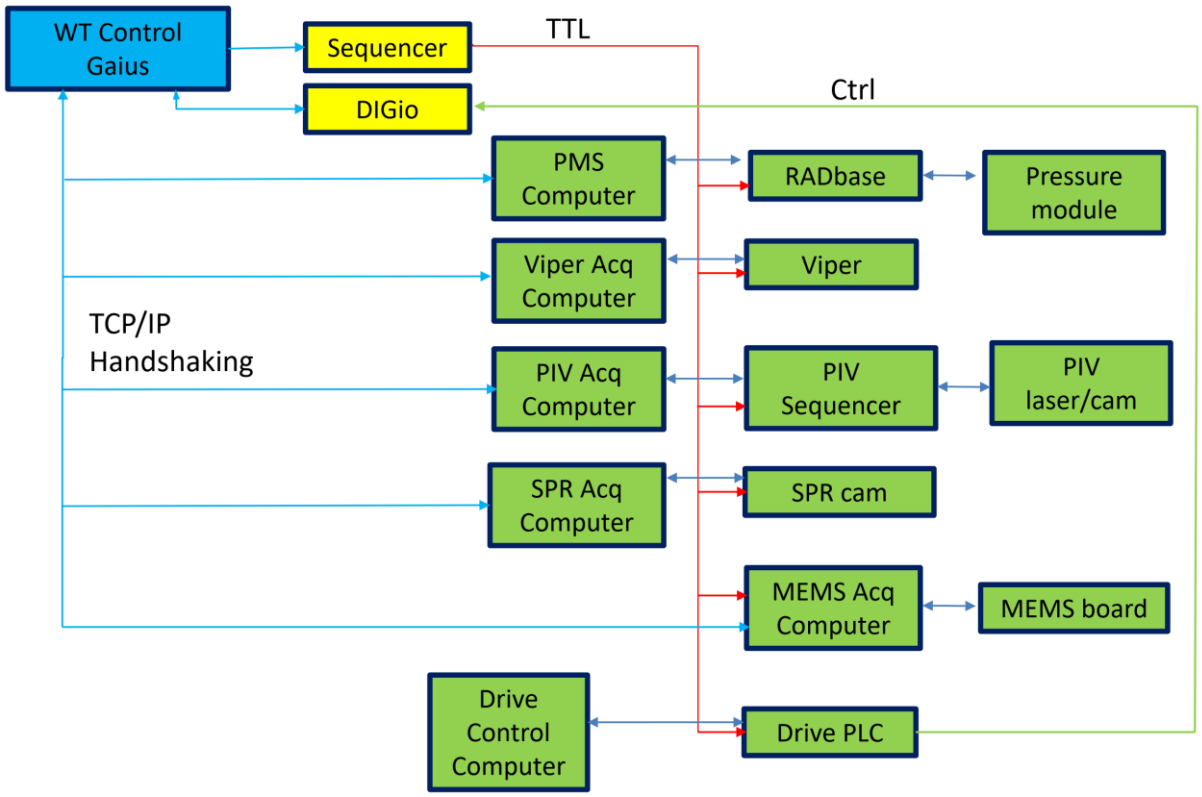

Figure 32: Synchronization and handshaking scheme with transient recording of all TTL trigger signal chains via multi-channel Viper for UHURA measurement campaign at DNW-LLF

The lessons learned from the L1 wind tunnel test at the F15 model (October/ November 2020) will round up and finalize the concept for the more complex large-scale measurements at the F15LS model at the DNW-LLF. According to the manufacturing schedule and the availability of the wind tunnel a measurement campaign in spring 2021 is very realistic.

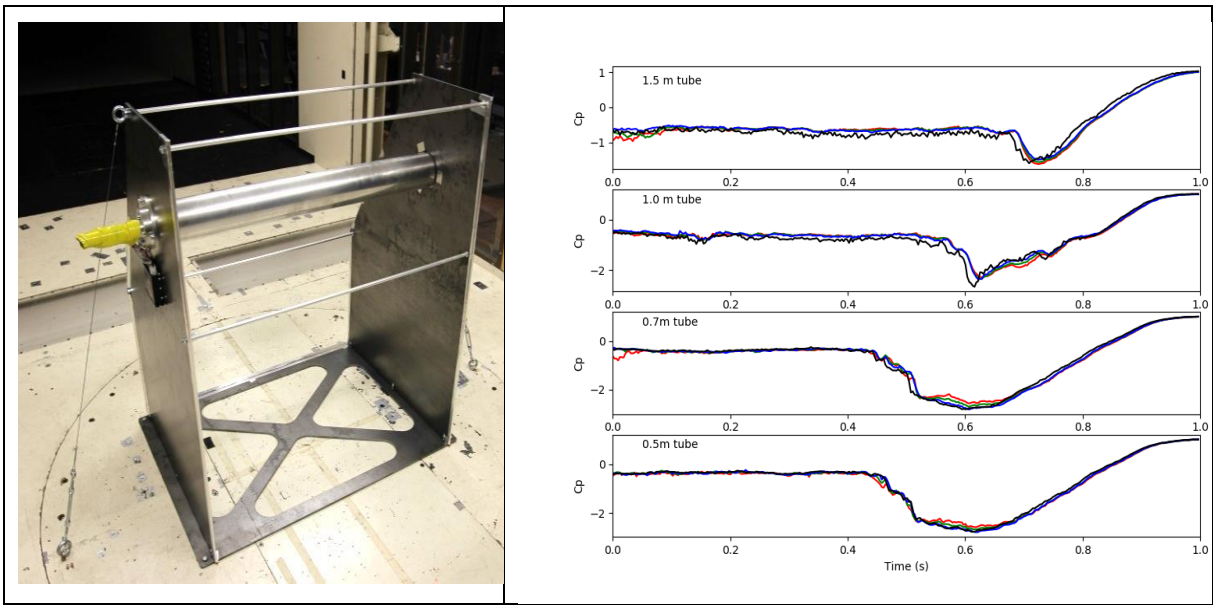

Figure 33: (left) Rotating wind tunnel model in the DNW-LST. (right) Pressure signal from a high bandwidth Kulite (black line) compared to a pressure tap-tube-transducer system (colored lines) for different tube lengths.

The SPR approach for the model deformation measurements has been defined. A 4-camera system will be used to capture the complete extraction cycle. Fluorescent markers will be placed on the model and UV illumination will be used. Furthermore, it has been explored that the vibration levels on the wind tunnel contraction are low enough to be used as camera support. The hardware integration of the DLR dual SPIV system has been defined together with DNW. Based on experiences of a similar LLF campaign in the past (FTEG 2011) optical access for laser and cameras will be provided and structure elements for supporting the PIV cameras will be mounted at the C-rig close to the lower splitting plate. A digital mock-up will be created before the CDR meeting of the LLF campaign.

DNW finalized the setup of SPR for the test with the large DLR-F15LS model in DNW-LLF. A four camera SPR setup was designed. A last step has been the distribution of the optical markers for motion and deformation tracking (Figure 34). The marker placement and post-processing strategy was established. Post processing outputs were discussed and agreed with WP4 partners. The final deliverables D32-2 (Set-up design for the stereo pattern recognition test technique in DNW-LLF) and D32-3 (Flow field measurement requirements and techniques for ONERA L1 and DNW-LLF) have been compiled and submitted in M37 and M38, respectively.

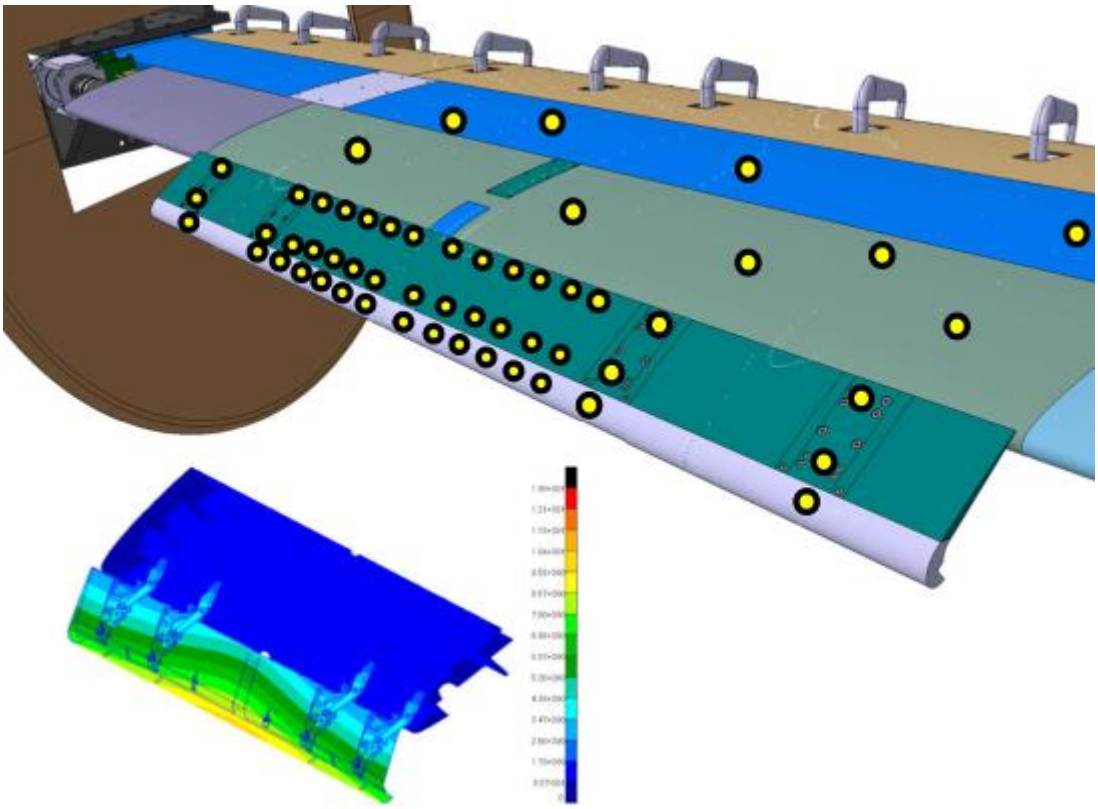

Figure 34: arrangement of surface markers on large DLR-F15LS model to capture Krueger flap deformation by SPR

2.3.3 Task 3.3 – Experiments

Lead: DNW

Task 3.3 objectives

- Design and preparation of the wind tunnel experiments.
- Ensure experimental design compatibility with model design and validation activities
- Conduct wind tunnel tests at ONERA L1
- Conduct wind tunnel test at DNW NWB
- Conduct wind tunnel tests at DNW LLF

- Process ONERA L1 wind tunnel and PIV data
- Process DNW-LLF wind tunnel, SPR and PIV data

Progress achieved/results

Discussions on the design of the wind tunnel experiments have been progressed. This includes discussions on synchronisation of different measurement sub-systems and the measurement sequence and automation.

The test setup of the wind tunnel test in ONERA L1 and DNW-NWB have been designed (Figure 35). This included design of the PIV setup and mounting of the Krueger device drive system.

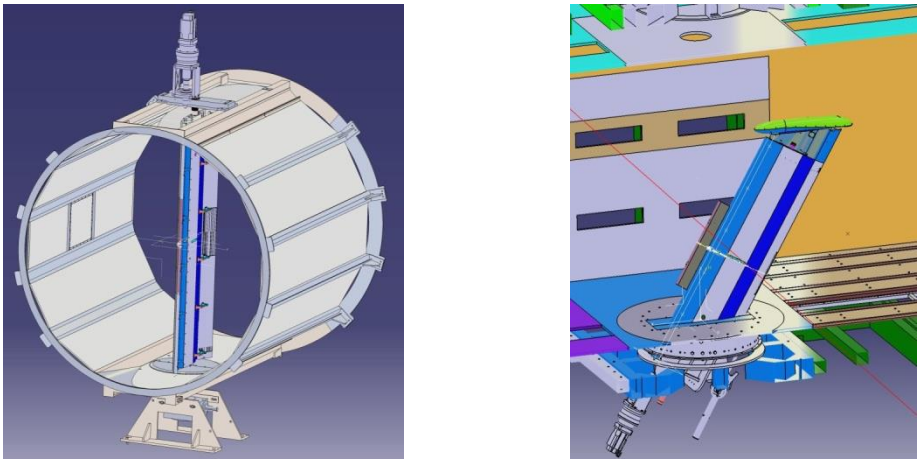

Figure 35: installation of DLR-F15 wind tunnel model in (left) ONERA L1 and (right) DNW-NWB wind tunnels

Key achievement of Task 3.3 within the reporting period was the successful conduction of a series of wind tunnel test despite all challenges posed by the current COVID-19 pandemic situation. A first test entry in ONERA-L1 tunnel has been performed in October/November 2020 (M26-M27) and model is just received and prepared in August 2021 (M36) for the second entry is just about to start in September (M37). The wind tunnel test in DNW-NWB has been fully accomplished in March 2021 (M31) and a first entry with the large model in DNW-LLF has been performed in April/May 2021 (M32-M33).

Contribution of Partner 1 – DLR

The contribution of DLR to the measurement campaigns was planned for the following topics:

a) Operate MEMS pressure measurement system
b) Operate Krueger drive motor control
c) In DNW-LLF, setup & operate PIV system
d) Synchronize and prepare MEMS and drive data

Due to COVID 19 pandemic travel restrictions applied preventing DLR staff to be present at remote tunnel sites. Only the on-site operation at the DNW-NWB entry was enabled. In the external locations at ONERA Lille and DNW-LLF the MEMS system was operated by the tunnel crew, enabled by a self-contained measurement system. The drive system was also operated by the local staff with remote support from DLR in case of difficulties. The PIV operation was postponed into the planned second entry in March 2022.

Past the performed campaigns, the data analysis of the MEMS and the drive systems have been processed. In conjunction with the tunnel condition data, the pressure and position data has been time-averaged for quasi-steady conditions and phase-averaged from multiple runs of dynamic Krueger operations. The data has been made available via the database to Task 4.2 for inspection. Figure 36 shows an example of time snapshots of one time series measured in DNW-LLF as provided to the partners.

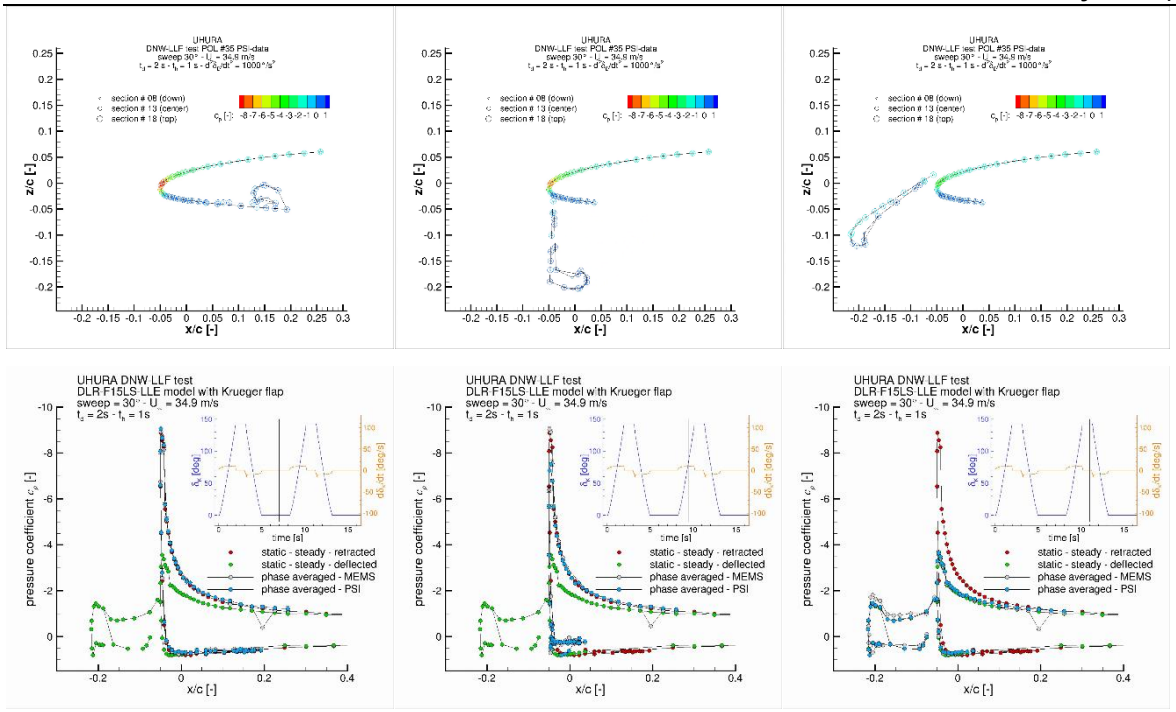

Figure 36: synchronized phase-averaged time sequence of pressure data measured at DNW-LLF

The PIV setup for the F15-LS model test in DNW-LLF was extensively prepared using a mock-up at DLR. Calibration plate, camera supports and camera geometry were all down selected in advance to reduce setup time in the wind tunnel. Installation of all PIV hardware in the DNW-LLF was performed by DLR. A stereoscopic camera system was attached using a truss to the model support frame. A 4-camera system was employed to enlarge the field of view on the pressure side of the wing. A complex high-power laser system was installed on an elevator platform next to the open test section. PIV acquisition on both static Krueger angles and dynamic Krueger deployment were performed. PIV synchronisation using TTL triggering was successfully implemented. Afterwards DLR iteratively refined the evaluation process for the large amount of SPIV image data achieved during the campaign in March/April 2022. Data from static and dynamic cases at two wind tunnel - and two Krueger speeds are available. Problems with model and camera vibrations, laser-reflections and trigger-loss are solved by image pre-processing, masking and correction schemes for the vast majority of the image data. Preliminary results with 2D2C velocity vector fields are available. Delivery of final results is foreseen for September 2022 and reporting is under preparation. On some Krueger angles stereo PIV data is not of sufficient quality. Trigger issues (EM noise) for one camera during recording of some dynamic cases and overexposure by laser light reflections at specific Krueger angles limit partly the useable SPIV data.

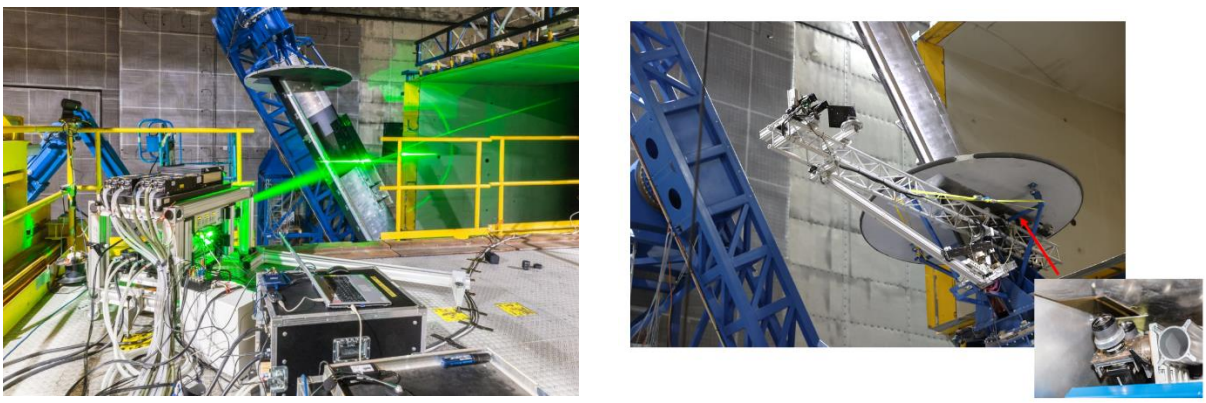

Figure 37 PIV setup at DNW LLF

In addition, DLR analysed the transient data recordings of all test entries. By a phase-averaging procedure, the real motion profiles and the corresponding dynamic pressure signals were statistically evaluated and provided to the data pack for the consortium partners.

Contribution of partner 4 - ONERA

The preparations for the wind tunnel test have been finalised. New end plates for the F15 model including provisions for optical access have been designed and manufactured. The design of the PIV setup has been finalised. Furthermore, the wind tunnel test matrix has been discussed amongst partners and a final version has been delivered. Due to the delay in model manufacture and wind tunnel accessibility, the test matrix is split into two parts (one entry in 2020 and another in 2021) with clear priorities identified.

ONERA conducted the first set of tests in M26-M27. Focus has laid on de-risking experiments. First, angle of attack sweeps have been performed at two flow speeds in steady flow with Krueger flap fully retracted and fully retracted to ensure the establishment of the baseline flow patterns by comparison with simulation data (target pressure distribution). Figure 35 shows the model installation during model mounting and the comparison of target and measured pressure data, showing an acceptable agreement. Further on, the flow field at steady conditions at different Krueger flap deflections have been measured including PIV images to investigate the fluctuating flow field, especially at intermediate positions. Figure 39 shows some preliminary impressions of the PIV images obtained. Finally, few dynamic deflections have been measured to get an insight into the dynamic behaviour of all measurement techniques and their synchronisation. Several important information has been gathered that is fed into the coming test in the other tunnels. The test data is now in post-processing, especially extracting the PIV data information and synchronizing pressure and drive data.

The first test entry has been concluded beginning of M28. The experiments have resulted in valuable lessons in cable routing for the Krueger instrumentation. The model has been dismounted and was sent back to DLR for improvements, refurbishment and preparation for the upcoming test at DNW-NWB.

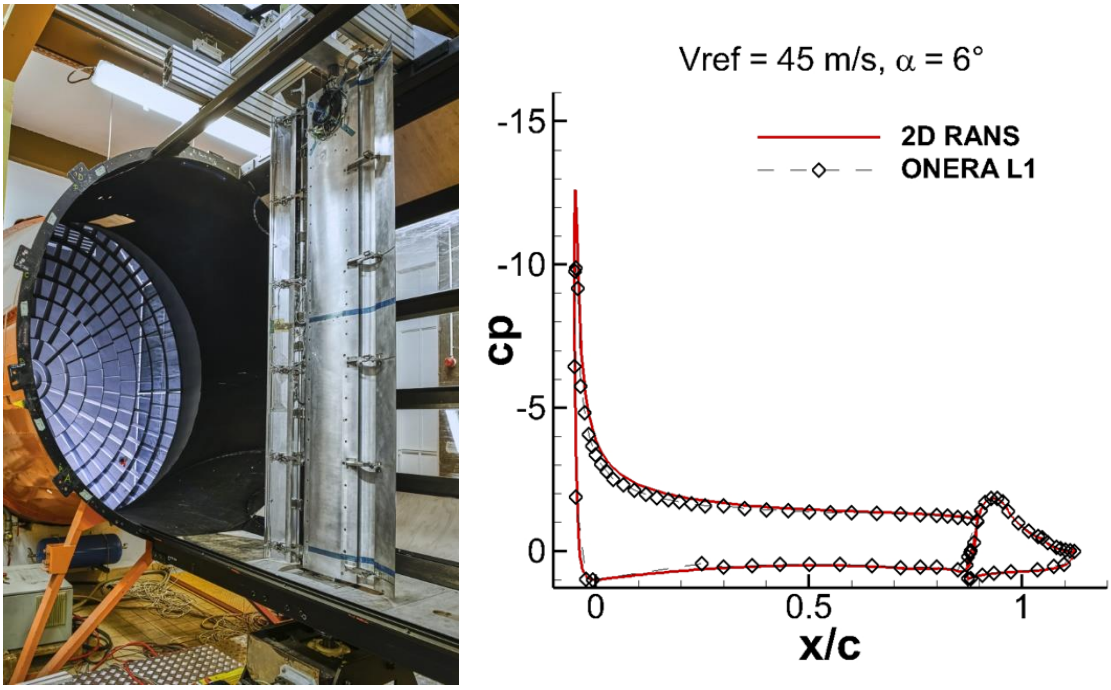

Figure 38: Installation of DLR-F15 model in ONERA L1 wind tunnel (left) and comparison of simulated target pressure distribution with measured data in first steady flow condition measurements

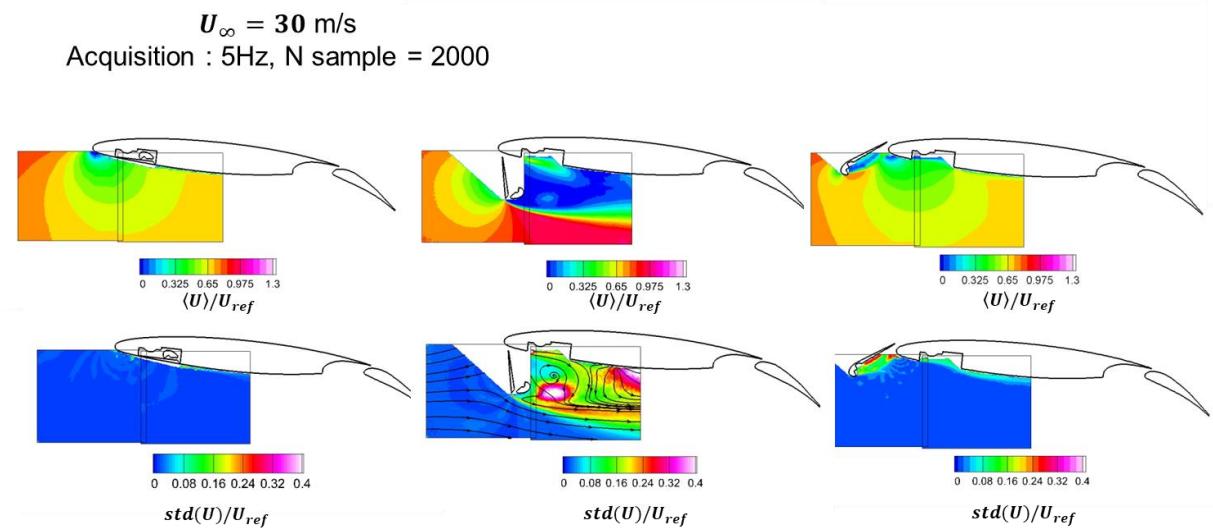

Figure 39: preliminary PIV results of the average flow field and fluctuation at static Krueger flap deployed positions: (left) retracted; (middle) half deflected; (right) fully deflected

The second wind tunnel test at ONERA L1 started at the beginning of September 2021 (M37) and finished as planned at the end of October 2021 (M38). The wing model was shipped back to DLR on January 2022 (M41).

The campaign included synchronized PIV measurements of on the lower surface of the wing to investigate the flow field during the deployment and retraction of the Krueger. Conventional static pressure measurements on the main surface of the wing and the flap were also performed. Finally, the transient static pressure on the Krueger was recorded with MEMS devices integrated within the model.

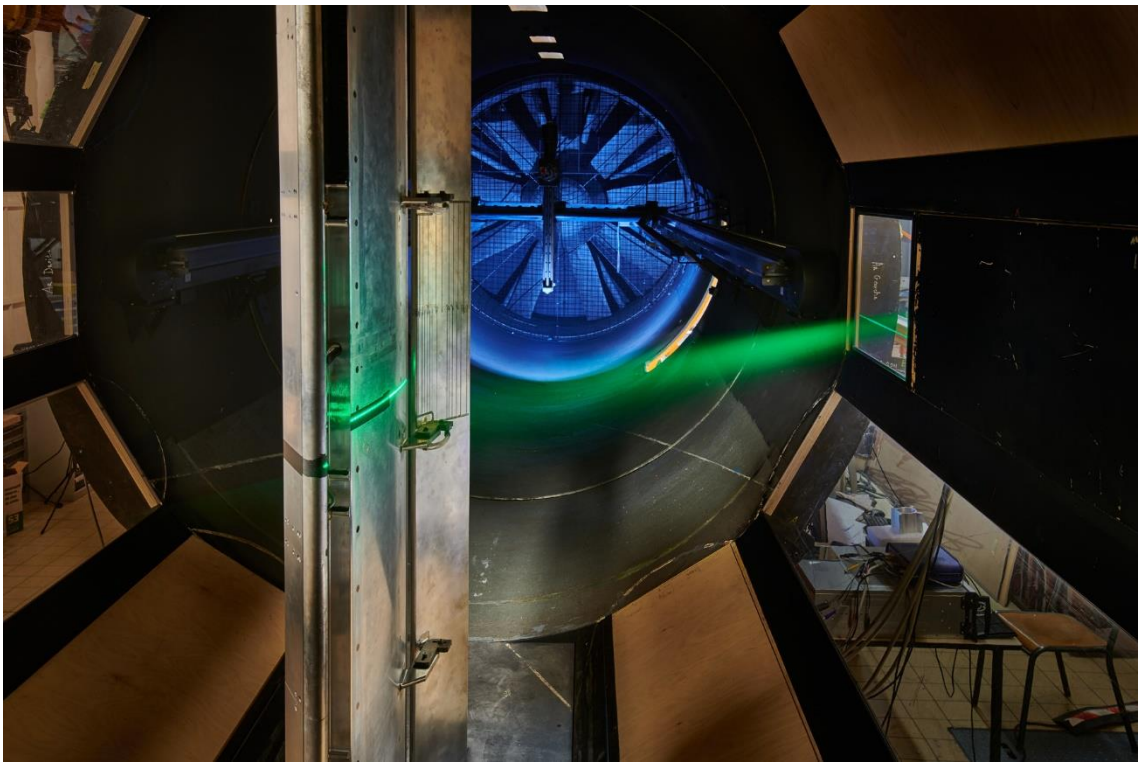

Figure 40: DLR-F15-LLE model with deflected Krueger mounted in ONERA-L1 test section with PIV laser sheet on middle section.

The synchronisation and the quality of the PIV data achieved during the experiment are sufficiently good to be used to validate the unsteady CFD simulations of WP4.

Two wind tunnel velocities of 30 m/s and 45 m/s were investigated. The deployment and retraction time of the Krueger were also investigated from 1s to 4s. Most of the initial test matrix was performed according to plan.

Within the initial test matrix, it was also planned to investigate the flow with only the centre Krueger panel deployed. Unfortunately, due to model modifications since the 1st experimental campaign, it was not possible to uncouple the two outboard panels with the model inside the test section. It was assessed that taking the model outside the working section was a risky operation that would take too much efforts and time considering the remaining time available for the test campaign. Instead, it was decided to investigate additional Krueger deployment configurations.

Due to the high number of deployment cycles performed during the PIV measurements, the MEMS located within the Krueger bull-nose and panel failed during the test campaign. As a result, the transient pressure on the surface of the Krueger may not be available for CFD comparison.

The PIV data from the wind tunnel test were processed to velocity fields. Both static and dynamic cases were processed. The in-plane velocity measurements highlighted the transient flow topology that constantly changes during the Krueger movement. The use of integrated MEMS pressure sensors captured the variation of static pressure on the Krueger surface during the deployment. The large database measured during the experimental campaign, which includes the effect of Krueger velocity deployment and wind tunnel velocity over the flow field will serve as reference data to validate URANS calculations within the WP4 of the project.

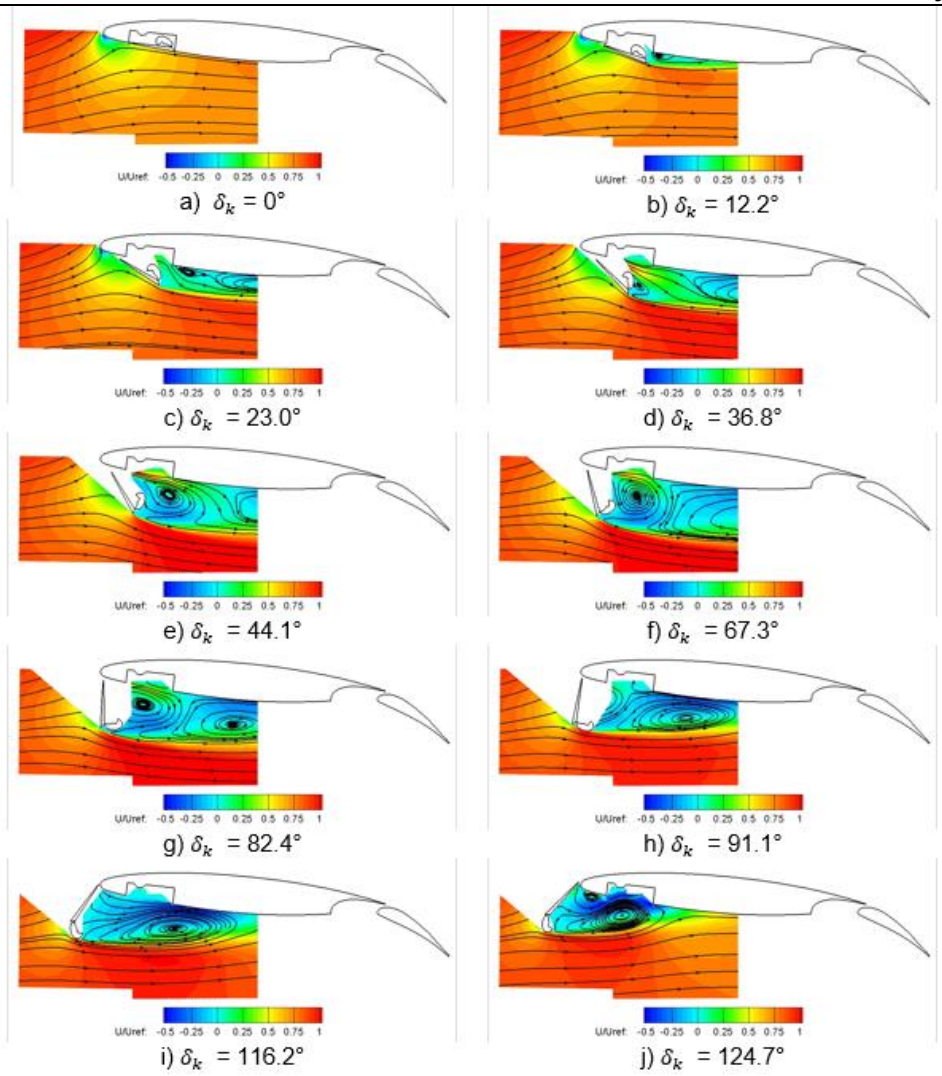

Figure 41 Phase averaged velocity magnitude during the Krueger deployment (4 s deployment time) from PIV measurements for 45 m/s

Contribution of partner 4 - DNW

DNW has prepared the wind tunnel tests for the test campaign at DNW-NWB and DNW-LLF. For use in the wind tunnel test at DNW-NWB a modified model mounting interface has been received from Task 3.1 and was installed in the tunnel's turn-table. The SPR system has been upgraded to a four-camera system. Deliverable D33-4 "Test Matrix for DNW-NWB wind tunnel test" has been submitted two weeks past M30. Figure 42 shows the installation of the model in the test section of DNW-NWB beginning of M31. The test matrix for both the unswept and swept configurations was concluded in M31. Dynamic extraction of the Krueger during testing was successful and the reproducibility of the extraction process was found to be very good. The time resolved measurements of the MEMS sensors and the upgrade SPR system were successful (Figure 43). Synchronisation of all measurement systems and the Krueger drive control was performed and worked as planned.

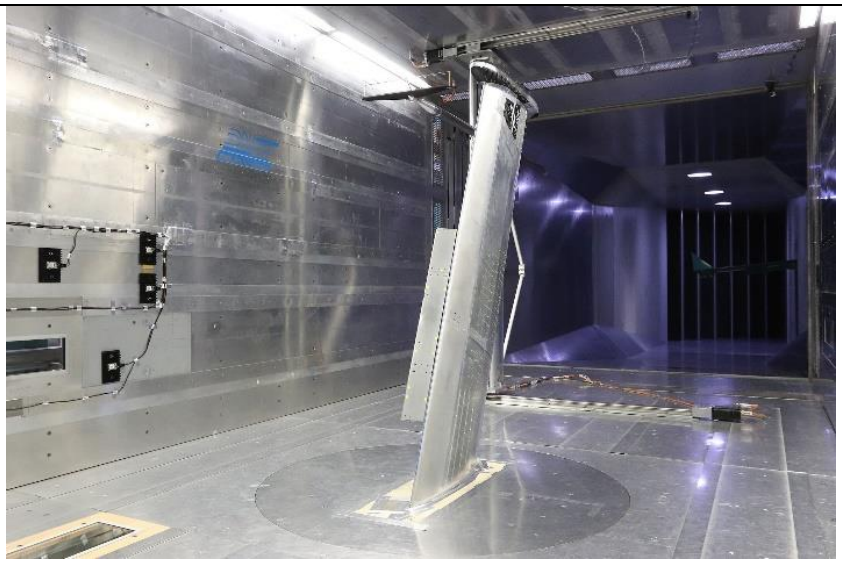

Figure 42: DLR-F15 model with Krueger flap mounted as swept wing in DNW-NWB wind tunnel

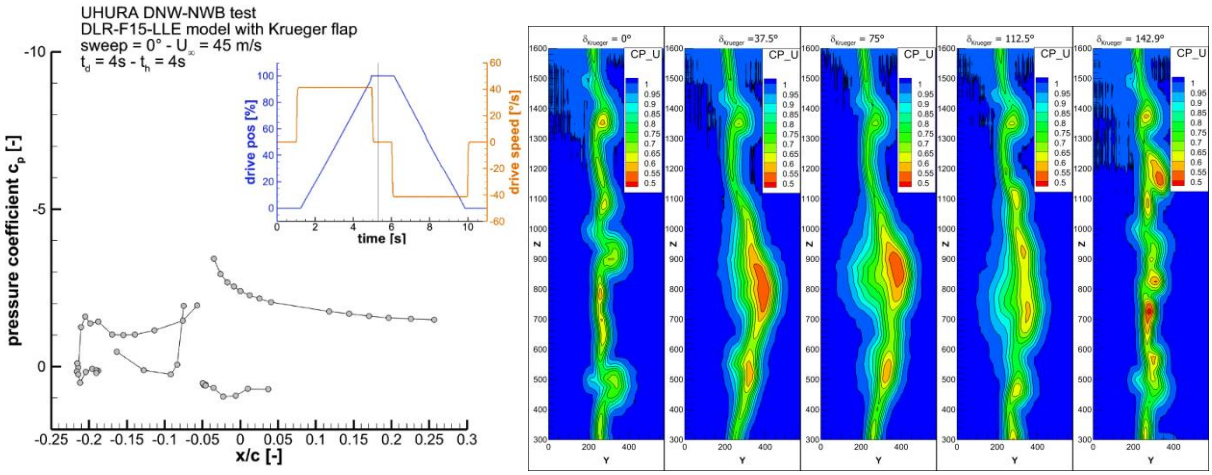

Figure 43 MEMS Unsteady Krueger pressure distribution (left) and the Krueger wake (right) of the F15 model at DNW-NWB

At DNW-LLF, test preparations were performed by DNW by assembly of the AMAS support frame. The test matrix was finalised and submitted a deliverable. The UHURA F15-LS model was delivered by task 3.1 at the end of M31 to the LLF. Model commissioning and integration of the model and drive was performed by DNW. A complete testing of all measurement and control systems was performed prior to installing the wind tunnel model into the test section. Due to COVID travel restriction the partner DLR was not able to provide PIV support during the wind tunnel testing. It was agreed within the consortium to proceed testing without PIV and include the PIV in a possible second wind tunnel test. The model was installed in the wind tunnel in M32 (Figure 44) and wind tunnel testing was finalised the first week of M33. Time resolved pressure measurements during Krueger deployment using both the MEMS sensors and pressure modules were successful (Figure 45). Krueger deformation was measured using SPR. The Krueger deployment process was found to be reproducible and synchronisation of the deployment with the measurement systems was achieved. Pressure data from the testing was delivered to the consortium partners in M35.

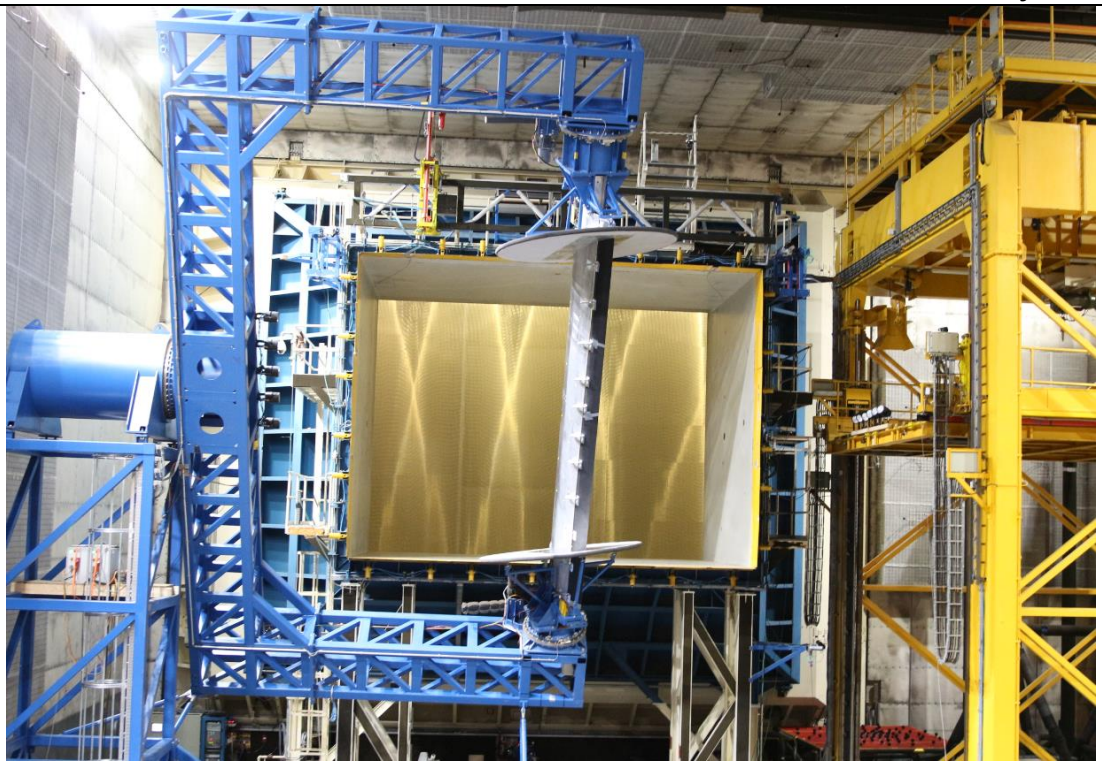

Figure 44 UHURA F15-LS model in the DNW-LLF

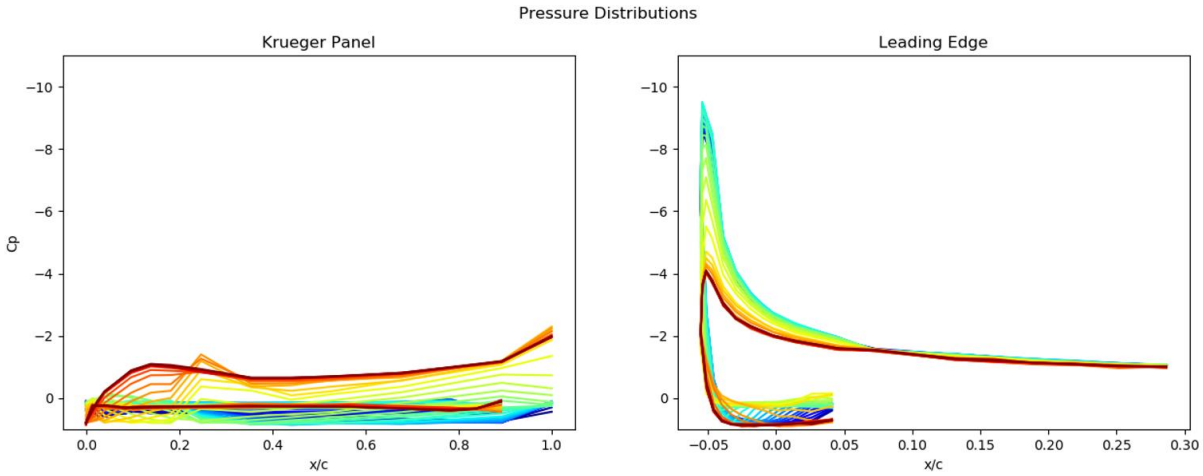

Figure 45 Time resolved pressure distributions from retracted (blue) to deployed (red)

For the second wind tunnel test including PIV the model support was again assembled and installed on site. The model was installed and broken pressure ports on the Krueger panel were refurbished. The Krueger drive system was again made operational and tested beforehand. Prior to installation in the test section all instrumentation systems including PIV triggering were tested outside the wind tunnel circuit. The wind tunnel test was concluded in M44. All primary test points in the test matrix were acquired.

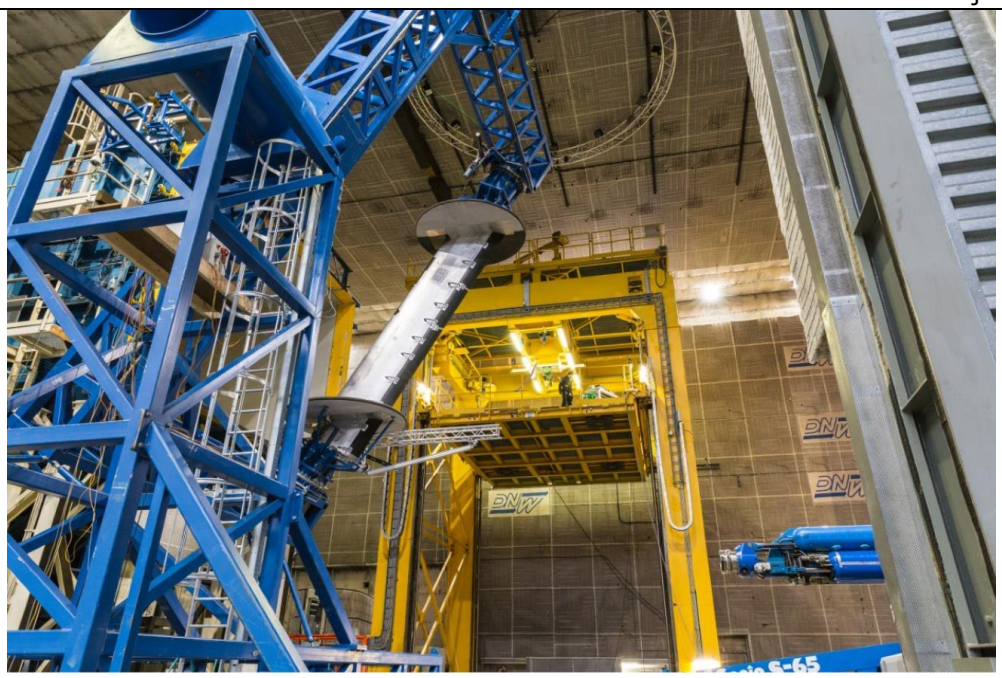

Figure 46 DLR F15-LS model in the DNW-LLF. The PIV laser platform is located on the starboard (pressure) side of the model

All wind tunnel data (pressures, transient recordings and conditions) of the second wind tunnel test were processed and provided to the consortium. The SPR model deformation data of the first wind tunnel test were processed. Deformation vectors compared to the undeformed model for individual markers were calculated for both static and dynamic deployment cases. Time resolved Krueger deployment was successfully captured using SPR.

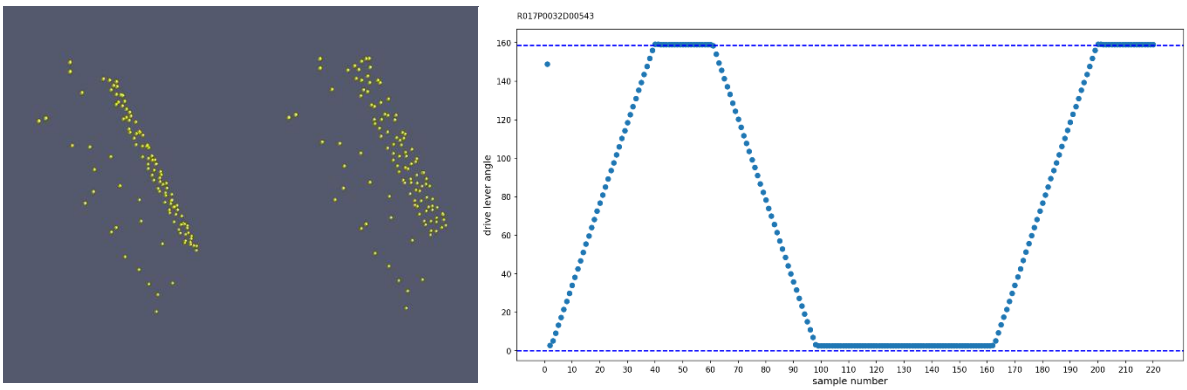

Figure 47 SPR marker positions (left) and reconstructed drive lever position from the SPR results

2.4 WP 4: Validation & Assessment

Task	Title	Starting at	Completion	Status
4.1	**Assessment of simulation methodologies**	**M14**	**M48**	**completed**
4.2	**Validation and assessment – data comparison of numerics and experiment**	**M7**	**M48**	**completed**
4.3	**Assessment and exploitation**	**M31⇨ M37**	**M48**	**completed**

Lead: NLR

Task 4.2 features an early start to facilitate a harmonisation activity on experimental and numerical data for validation purposes. Future comparisons are described in deliverable D42-1. Task 4.1 was planned to start in M14. However, several partners are in the finalisation of their CFD tool developments (Task 2.2) and the final geometry definition for the wind tunnel model was delivered late (M17). As a consequence, the activities for Task4.1 have been delayed. This might not necessarily affect the target date of most of the Task 4.1 deliverables since partners are well prepared for Krueger deployment simulations due to signification commonalities with the applications adopted in Task 2.2.

The progress relates to the single active Task 4.1 where preparatory and exploratory activities have been performed for multidisciplinary simulations involving aerodynamics and computational mechanics at anticipated wind tunnel conditions. Here, the ONERA L1 wind tunnel model configurations have been adopted to advance the CFD models and prepare the coupling to structural models. The progress concerns verification of the established simulation models and the task is still awaiting the initial experimental results for validation purposes. The projected planning for delivery of validation data is scheduled for the next reporting period. However, a continued increase in delay from 3 months to more than 6 months is now observed. This renders the finalisation of the task activities within the original runtime as questionable.

The first batch of the ONERA L1 test campaign has been completed and the data processing for delivery to WP4 is ongoing. An intermediate progress meeting for Task 4.1 shows a prudent but steady progress with respect to in-depth preparations for aerodynamic and fluid-structure coupling simulations. This includes kinematic approaches for arbitrary hinge-lines, wind tunnel wall effects on aerodynamics loads of a test article and initial model deformation assessments using static/dynamic approaches. Complementary activities on the evaluation of refined flow physics models show the initial results of Lattice Boltzmann and DDES applications. Furthermore, partners anticipate on the test results of the DNW-NWB and DNW-LLF wind tunnel campaigns which are expected in the next reporting period. Here, the experience obtained earlier in the project regarding the generation of computational grid is being exploited.

The measurement data of test campaigns conducted in the ONERA L1, DNW-NWB and DNW-LLF wind tunnels have been received along with the test reports. The test results cover the effect of wing sweep and deflection speed on the deployment characteristics of a two-component Krueger. The partners utilize the measured time histories of the motorized Krueger device in their final predictions for the dynamic deployment cases. Validation of the numerical results is being carried out in comparisons with experimental data using sectional pressure distributions on the moving Kruger components as well as the high-lift wing. For this purpose, the large set of experimental data has been analysed in order to select a suitable set of measurement data. Here, the individual partners concentrate on specific aspects leading to a broad utilisation of the comprehensive database.

The established deployment characteristics of the Krueger are exploited in various studies at aircraft level. The time-dependent loss of lift is incorporated in a flight simulator model for the A320 to

evaluate the impact of spanwise implementation concept of Krueger devices on the aircraft dynamic response. Furthermore, the critical loads case is identified from the time-dependent loads on the Krueger components and are being exploited for a conceptual structural design on full-scale with an emphasis on weight optimisation.

The partners involved in the exploitation studies are finalizing their technical activities as well as the related documentation of their achievements.

Table 3 WP4 Milestones, deliverables, time schedule & spending

Deliverables in WP4		*Partner(s)*	*Month due*	*Month completed*
D42-1	Roadmap for the comparison of wind tunnel test data and numerical results of CFD simulations	VZLU	M9⇨M13	M18
D41-1	Summary of results on aeroloads prediction by using UZEN with dynamic mesh and non-conformal mesh coupling	CIRA	M26⇨M42	M48
D42-2	Report on influence of wind tunnel setups on characteristic flow features for validation	DLR	M28⇨M42	M48
D41-2	Summary of results on aero-loads prediction and scaling effects on swept wing configurations	DLR	M30⇨M42	M48
D41-3	Summary of CIRA-IBK results on aero-loads prediction by using Immersed Boundaries method in an FSI environment	IBK	M30⇨M42	M48
D41-4	Assessment of critical loads estimation during the deployment phase	DASSAV	M30⇨M42	M48
D41-5	Summary of Lattice Boltzmann-LES technique results for aero-loads prediction	INTA	M30⇨M42	M48
D41-6	Report on temporal aspects of the flow dynamics and characterization of the aero-loads during Krueger deployment	NLR	M30⇨M42	M48
D41-7	Report on Chimera approach for flow simulations of Krueger deployment by using ONERA's inhouse solver elsA	ONERA	M30⇨M42	M48
D41-8	Summary of KTH results from Static-Unsteady URANS approach complemented by hybrid RANS-LES	KTH	M30⇨M42	M48
D41-9	Summary of VZLU results from Static-Unsteady and Dynamic-Unsteady URANS approaches complemented by hybrid RANS-LES	VZLU	M30⇨M42	M48
D42-3	Validation and assessment of the unsteady flow and load characteristics for a deploying Krueger device	VZLU	M34⇨M46	
D42-4	Analysis of the unsteady turbulent flow field characteristics at critical deployment stages	KTH	M34⇨M46	M49
D42-5	Validation of loads prediction and impact of static/dynamic structural deformations for a deploying Krueger device	NLR	M34⇨M46	M48
D42-6	Validation of LBM approach for a deploying Krueger device	INTA	M34⇨M46	M49
D42-7	Report on the comparison between calculated loads and deformations of the Krueger flap and WT Measurements	IBK	M34⇨M46	
D42-8	Analysis of flow field characteristics in the L1 test campaign. Comparison between experiments and numerical results	ONERA	M34⇨M46	M50

Deliverables in WP4		*Partner(s)*	*Month due*	*Month completed*
D43-1	Exploratory handling quality assessment of spanwise deployment concepts for a Krueger device	NLR	M36⇨M48	M49
D43-2	3D Krueger flap structural concept and preliminary weight estimation. Comparison with existing CS-25 slats	IBK	M36⇨M48	
D43-3	Impact of unsteady Krueger motion on overall aircraft level	AID	M36⇨M48	M50
D43-4	Feasibility analysis of transposing unsteady flow simulation technology	DASSAV	M36⇨M48	M48

Milestones in WP4		*Partner*	*Month due*	*Month achieved*
M41-1	ONERA L1 test case simulations completed	ONERA	M24⇨M42	M48
M41-2	DNW-NWB test case simulations completed	DLR	M27⇨M42	M48
M41-3	DNW-LLF test case simulations completed	NLR	M29⇨M42	M48

2.4.1 Task 4.1 – Assessment of simulation methodologies

Lead: CIRA

Task 4.1 objectives for the reporting period (M19-M36) of UHURA

- prepare CFD activities (mainly CAD/CSM preparation and meshing) for the subsequent computation of the modified DLR-F15-LLE and DLR-F15LS-LLE model.
- verify the sharing of WT tests among the partners in order to ensure a complete covering
- perform CFD simulations activities on final CAD geometries related to wind tunnel conditions
- preliminary assessment of the reliability and accuracy of numerical results.

Progress achieved/results

A first complete CAD of the DLR_F15-LLE model with Krueger (ONERA-L1 geometry) was delivered end of M17 from Task 3.1, while several partners are in the finalization of their CFD tools upgrading in Task 2.2. Accordingly, little activities were carried out in Task 4.1 so far. This is not seen as critical, as Task 4.1 activities are embedded between (and linked to) Task 2.2 and Task 3.1, and logically follow the timeline of such tasks.

On July 8th 2020 a Task 4.1 kick-off meeting was held, including all Task 4.1 partners and supported by main WP3.1 partners for updates about WT models developments and WT testing. The meeting was very useful to clarify both the input geometries and expected measurements coming from WP3, relevant to the several WT entries planned. Also, the workshare among the organizations involved has been clarified in terms of WT cases to be considered. A specific folder was created on the IBK-server containing, for each of the experimental test cases: *i)* input CAD and FEM models; *ii)* all relevant documentation from WP3 (e.g., test matrix, test report, useful deliverables, etc.; *iii)* the most relevant WT-data (when available). This centralized setup will avoid the spreading of different geometries between Task 41 partners (and consequently the results) and it will allow all contributors to have a fully documented experimental test case to be reproduced by CFD tools.

Due to delays in the WT model(s) design and manufacturing activities due to both Covid19 pandemic and cyber-attack at ASCO, occurred in WP3, the final CAD models for both ONERA-L1 and DNW-NWB wind tunnel installation setup were delivered to WP4 with some delays (between July-20 and Sept-20).

Nevertheless, most partners have started setting up their numerical procedures by using preliminary CAD models available, which allowed recovering of some delays mentioned above. Activities are in progress and first WT data for ONERA-L1 case is expected in Oct-Nov 2020, in order to provide final experimental setup info and data for codes assessment purposes.

On February 24th 2021 a Task 4.1 progress meeting was held in preparation of the incoming 4th project progress meeting. The final CAD models and the time history files for Kruger motion are available, and all the Task 4.1 partners started with CFD simulations using the last provided inputs. Those simulations cover almost all the cases from WP3. Some partners carried out preliminary computations sharing the obtained results. Comparisons between static and dynamic computations were performed, showing similar results except for some specific Kruger deflection angle. Preliminary comparisons between different numerical approaches, including the WT walls effects, were carried out as well. Some simulations, considering the model structure flexible, were completed, in static and dynamic mode, by coupling an IB-CFD solver with NASTRAN CSM tool. Other FSI simulations, with different numerical approaches, are on-going.

On June 24th 2021 a Task 4.1 progress meeting was organized to discuss about different possible project extension scenarios and their impact on milestones and deliverables. The project coordinator J. Wild (DLR) participates at the meeting to inform the partners about the possible project extension and it impact on budget and deadlines. A project extension of 12 month is confirmed and the official amendment was provided in July 2021. As a consequence, the end of the project is postponed to month 48 (01/09/2022). The project budget will not be incremented but will be possible a remaining budged sharing among the partners. The project extension will permit the re-entry in DNW-LLF facility for PIV tests during the 2022. All the deadlines for Task 4.1, milestones and deliverables, are postponed to month 42 (01/03/2022). On September 5th the UHURA final workshop was held, where all partners showed the last results and the final status of their activities.

Contribution of Partner 1 – DLR

With input from Task 3.3, the full CAD models for all test setups have been derived, cleaned for CFD simulations and provided to the partners. In total five different setups including the tunnel test section geometries have been created:

1) ONERA L1 test, 2D wall to wall, full-span Krueger
2) ONERA L1 test, 2D wall to wall, part span Krueger
3) DNW-NWB test, cantilever wing, part span Krueger, 0° sweep
4) DNW-NWB test, cantilever wing, part span Krueger, 23° sweep
5) DNW-LLF test, wing with end plates, part span Krueger, 30° sweep

CFD activities are progressing. Previously in Task 2.2 a first block structured 3D mesh has been generated, based on a 2D grid. At first the basic 2D grid has been tested. It has been found, that the grid has to be refined locally, to guarantee consistency of the Chimera method. First simulations on the new block structured grid have been run successfully. Based on the new 2D grid now a new 3D mesh has been created. Simulation tests will follow soon.

DLR worked on pre-processing of CAD models developed in WP3 for manufacturing purposes and made them suitable for CFD activities, by also including WT walls where applicable. At present, all CAD models related to the WT entries are made available to Task 4.1 partners, as well as time histories of Krueger deflection recorded from isolated drive tests. A functionality to allow a rotation of Krueger device around arbitrary hinge line was set up, and a second functionality to read in measured time histories of deflection angles and rotational speeds was coded. Furthermore, using TAU Python, a script for simulation activities in Task 4.1 (verified with "equivalent test cases") was generated.

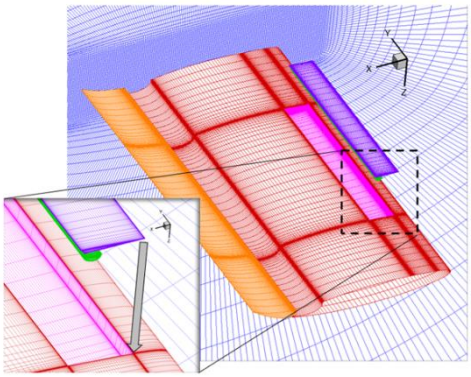

Figure 48: Chimera block-structured mesh particular

Mesh generation and CFD setups for ONERA-L1, DNW-NWB (0° and 23° sweep angles) and DNW-LLF were completed.

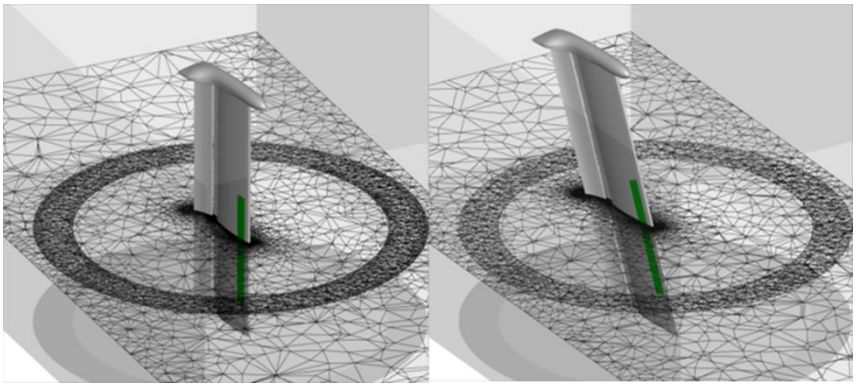

Figure 49: DNW-NWB setups (0° and 23° sweep)

Steady and unsteady simulations are currently performed with all CENTAUR meshes. As an example, **Fehler! Verweisquelle konnte nicht gefunden werden.** and **Fehler! Verweisquelle konnte nicht gefunden werden.** show time series of surface pressures and streamlines for the two DNW-NWB setups at 0° sweep and 23° sweep, respectively. The ongoing simulations will go through the different conditions of the test matrices of the different tunnel tests. At least different deflection speeds at both wind speeds are in the simulation matrix.

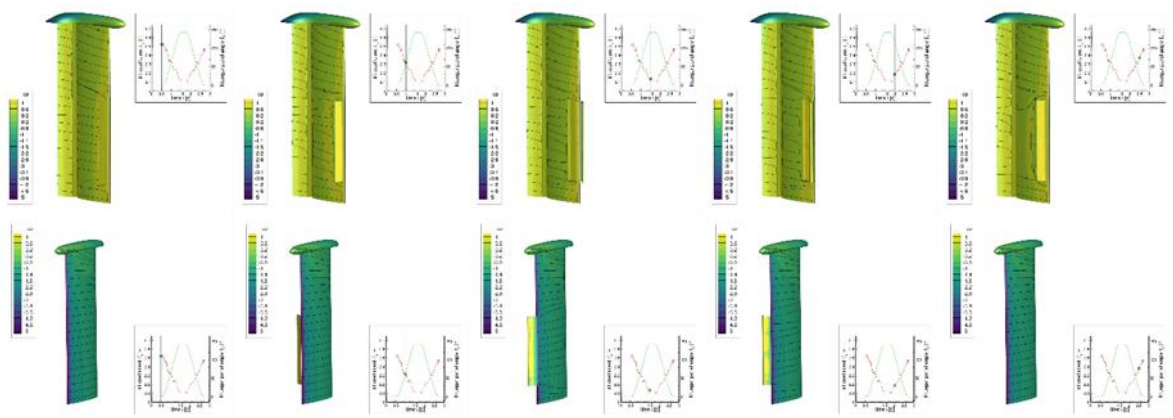

Figure 50: time sequence of DNW-NWB setup at 0° sweep, fast deflection (1s) at 45 m/s wind speed

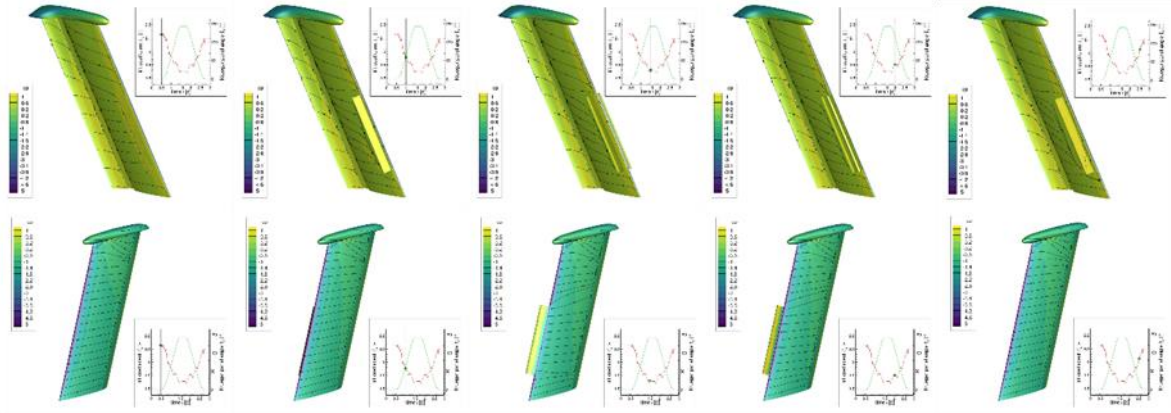

Figure 51: time sequence of DNW-NWB setup at 23° sweep, fast deflection (1s) at 45 m/s wind speed

In the period of interest from M37 to M48 ,the numerical simulations of the setups on DNW-NWB (straight and swept wing) has been performed for different wind speeds (V_N = {30 m/s, 45 m/s}), different deployment times (t_d = {1 s, 2 s, 3 s}), different hold times (t_h = {1 s, 2 s, 3 s}), and different accelerations ($d^2\delta/dt^2$ = {165°/s², 300°/s², 500°/s², 1000°/s²}).The simulations reveal a significant impact of the deployment speed and the sweep angle. Majorly the phase shift or time delay of the lift fluctuation is impacted. The magnitude of variation of lift coefficient is not significantly affected. At high deployment speeds a very significant oscillation of the drive load is observed in the retraction motion. The wing sweep affects the sensitivity of the flap flow distortion caused by the Krueger flap motion. For the swept wing, the variation of the lift coefficient at the flap is less affected than for the straight wing. The numerical simulations for the ONERA-L1 part span and full-span and for the DNW-LLF test setups are also completed. More details on performed activities are available in UH-D41-2 issued on 16/08/2022 and approved on 31/08/2022.

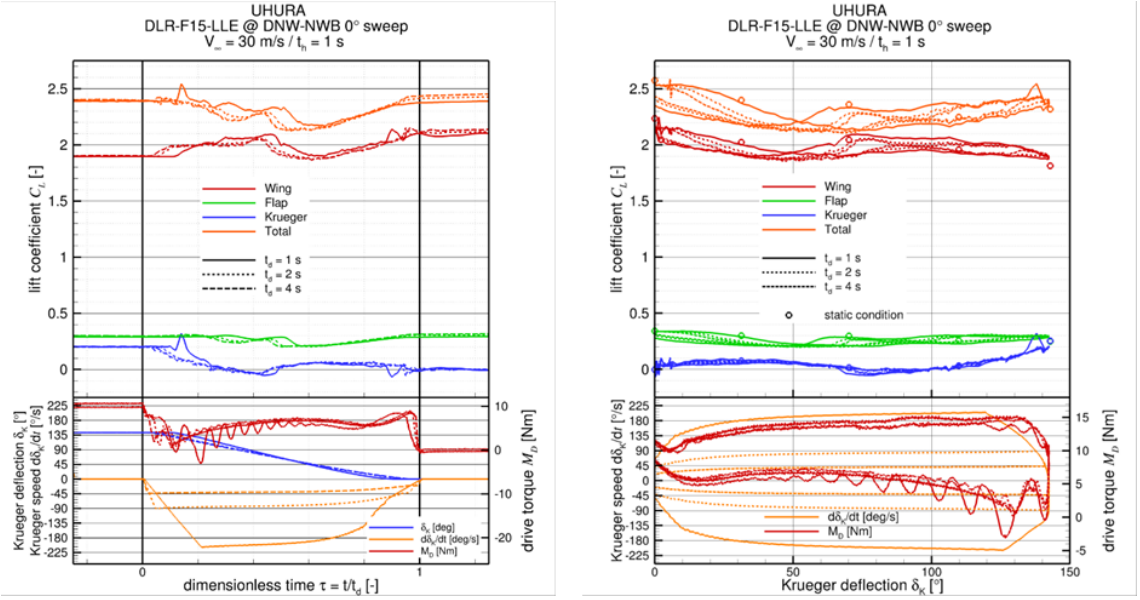

Figure 52: comparison of of aerodynamic lift coefficients of wing section integration for different deflection times during retraction (left) time histories (right) hysteresis. Wing sweep 0°, wind speed V_N = 30 m/s; hold time t_h = 1 s.

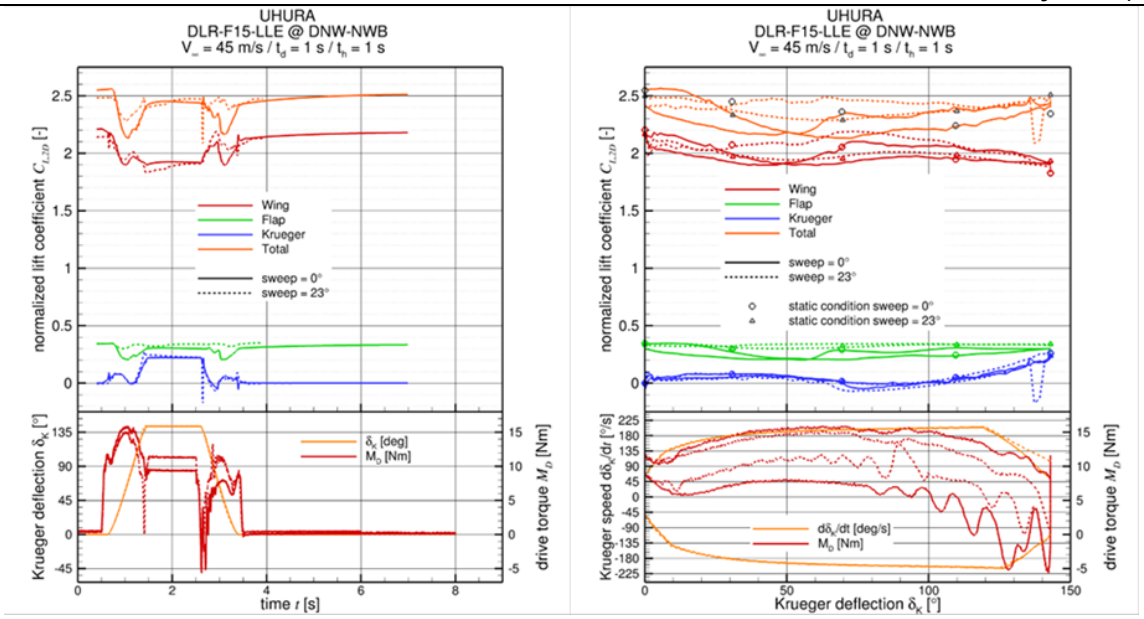

Figure 53: comparison of of aerodynamic lift coefficients of wing section integration for different sing sweeps (left) time histories (right) hysteresis. Wind speed V_N = 30 m/s; deflection time t_d = 1 s, hold time t_h = 1 s

Contribution of Partner 2 – CIRA

CIRA is leading Task 4.1. Planned activities is to launch the task activities, harmonize the task time schedule with respect to Task 2.2 and WP 3 timing and expected outputs, prepare and harmonize inputs coming from WP 3. A virtual Task 4.1 kick-off has been launched held on July 8th with participation of partners from Task 4.1 and WP 3. Harmonization of partner's activities has been established and inputs from WP3 (WTT data availability) have been clarified. A specific folder has been created on the IBK databank to control input data (geom, FEM models, etc.) related to the several test cases to be considered (ONERA-L1, DNW-NWB, DNW-LLF). This shall avoid the spreading of CAD models and inputs data to be considered by cooperating partners.

The SIMBA (immersed boundary) solver has been updated to deliver friction wall forces as well as static pressure to CSM. The new geometry with a more pronounced flap-deflection (due to the ONERA L1 test-section constraints) is built and triangulated for the SIMBA_MESH pre-processing. The CFD set-up phase is finished and a two-dimensional URANS computation at α = 6° and Krueger fixed deflection of θ = 23° is frozen as starting condition for the next FSI test. IBK has developed a FEM model for the fully 3D configuration for a 2.5D CFD-CSM coupling. The mid-plane section is considered for the loads exchange with CFD.

CIRA, in collaboration with IBK, carried out some FSI simulations for the ONERA-L1 case. At the present 2.5D static and dynamic-FSI simulations with 1s deployment, 1s fixed fully deployed and 1s retraction phase were performed by considering the Kruger panel connected with the bull-nose (no bull-nose rotation is simulated). The approach used for those simulations involves the home-built CIRA IB-CFD solver SIMBA and the NASTRAN CSM tool.

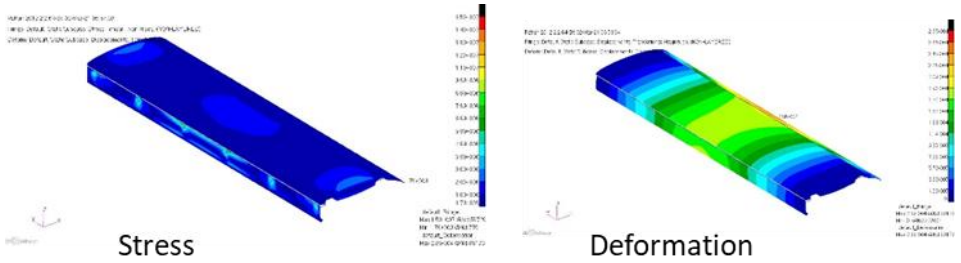

Figure 54: FSI static two-way coupling example (ONERA-L1)

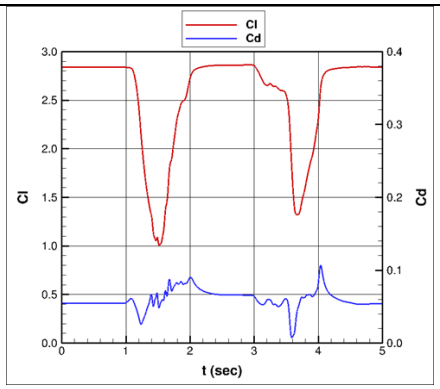

Figure 55: CL and CD behaviours in a full cycle dynamic simulation (ONERA-L1)

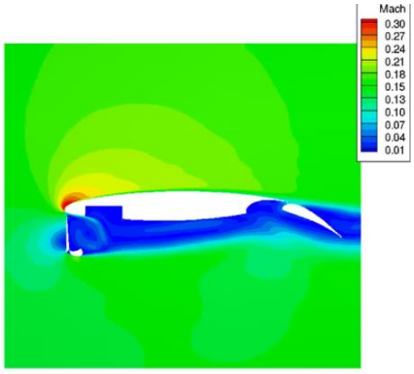

Figure 56: CFD deployment/retraction for separated Krueger-plate and bull-nose (Onera-L1 config.)

The interface driver is built and a dynamic FSI is has covered the entire Krueger deployment. Simulations related to the ONERA-L1 configuration for the "Separated" Krueger-plate and the bull-nose device in FF conditions for V = 45 m/s were performed using 2D and 3D approaches.

The 2D numerical analyses refer to:

- 2D RANS static, Krueger-flap fully retracted (0°),
- 2D URANS static, Krueger-flap 75° deployed,
- 2D RANS static, Krueger-flap fully deployed (149.2°),
- 2D RANS static, Krueger-flap fully deployed (149.2°), AOA sweep (0-20°),
- 2D URANS with Krueger-flap 1 s deployment-1 s hold-1 s retraction.

The 3D URANS analysis considers 1 s deployment followed by 1 s hold. The 3D hybrid RANS-LES analysis is very time-consuming and only the 1 s deployment is currently available. Thus, the 3D solutions for the dynamic Krueger-flap deployment are:

- 3D URANS with Krueger-flap 1s deployment and 1s hold,
- 3D hybrid RANS-LES with Krueger-flap 1s deployment.

As expected, the fast rotation velocity of 149.2°/s causes a delay between the "dynamic" and the "static" loads. Besides, this delay is more pronounced for the retraction phase for which the inertial effects are almost gathered from the deployment and hold phases. The maximum lift-load is obtained during the 1 s hold phase and not at the end of the deployment rotation. Besides, the deployment and retraction loads are not symmetric. For example, the minimum lift as well as the maximum pitching moment differ between the two rotation phases. These are further evidences of the inertial effects that play during the Krueger rigid motions.

Flow simulation of Krueger deployment by means of a structured home-built multiblock dynamic URANS solver were carried out as well. A parametric procedure was set up, capable to produce multi-block computational mesh on the configuration named DLR-F15-LLE-Krueger_WTflap (including

Krueger and bullet nose rotation) at any input driver lever setting, depending on deployment laws and time. The procedure can work for 2D and 3D swept wing (for given sweep angle) and supports automatic remeshing during unsteady deployment flow simulation. Two-dimensional test cases were carried out with free stream M =0.132, Re = 1.85 x 10^6 AOA=6 degrees (corresponding to ONERA L1 wind tunnel test conditions): flow simulations at several fixed deployments angles (from fully deployed to retracted), unsteady deployment and retraction with different deployment time from 1 s to 4 s. 30 degrees periodic swept wing test cases were carried out with free stream M = 0.153 and Re = 4.3 x 10^6 AoA = 5.2 degrees (corresponding to DNW-LLF test conditions): flow simulations at several fixed deployments angles, unsteady deployment and retraction with deployment time from 1 s, to 4 s. Details and results of flow simulations were summarized in deliverable D4.1-1.Post processing of the flow simulations to obtain output data files in TECPLOT format, delivered to support task 4.2.

Contribution of Partner 3 – VZLU

The aim of VZLU activities within Task 4.1, is to describe the results obtained during the project. In the work package WP2 (Numerical Simulation of the Krueger slat deployment) and namely in Task 2.2, VZLU contributed to the development of the chimera grid technique, evaluation of different grid strategies and improvement of CFD tools. VZLU focused its effort on the implementation and testing of the chimera grid approach, which is attractive for its flexibility. In contrast to the standard mesh deformation strategy, it does not suffer from grid quality issues. On the other hand, chimera grid technique required additional implementation of several functionalities into the existing CFD code. The results presented in this Task are partially based on the mentioned developments, which focused on the improvement of the CFD methods for dynamic movement in the unsteady flow simulations. The CFD results based on the methods developed and tested within Task 2.2 and applied in Task 4.1, will be used, together with the experimental data available from Task 3.3, in the final phase of the project. The validation and mutual comparison of various numerical approaches of diverse group of partners will be addressed in Task 4.2. In particular, VZLU was involved in CFD simulation of several configurations of the high-lift wing with Krueger flap. Namely the configuration of the ONERA-L1 experiment, which utilizes unswept wing with c_{ref} = 0.6m, and the DNW-LLF experimental setup with c_{ref} = 1.2m (orthogonal to the LE) and the sweep angle of the wing to 30 degrees. The wind tunnel setups differ in size and in general layout. The CFD simulations followed a certain level of simplification. In case of ONERA-L1 configuration a portion of the wing was considered with artificial periodic boundaries, equivalent to the simulation of infinite wing. The DNW-LLF case was considered in a detail that was close to the real environment: a swept wing with part span Krueger flap and side plates, where only cleaning of the outer structures was done to simplify the CFD simulation. The obtained results on ONERA-L1 and DNW-LLF test articles, from Static-Unsteady and Dynamic-Unsteady URANS approaches complemented by hybrid RANS-LES, are available in Deliverable D41-9. The outputs of VZLU activities are focused mainly on Cp distributions in order to make the comparisons with experimental data easier.

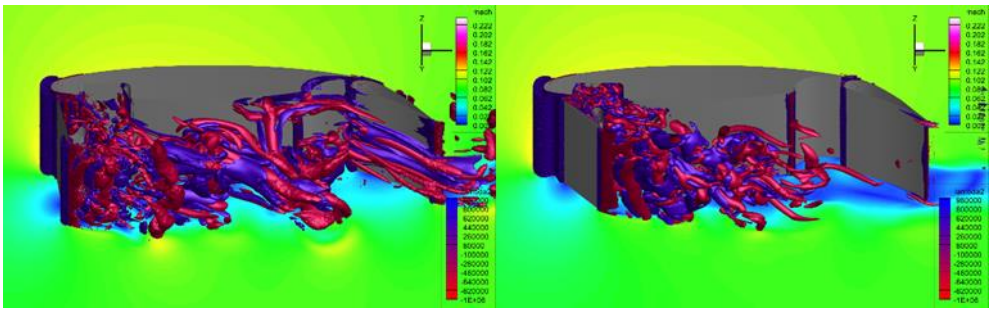

Figure 57: Flow field around DLR-F15 with full-span flap (ONERA-L1)

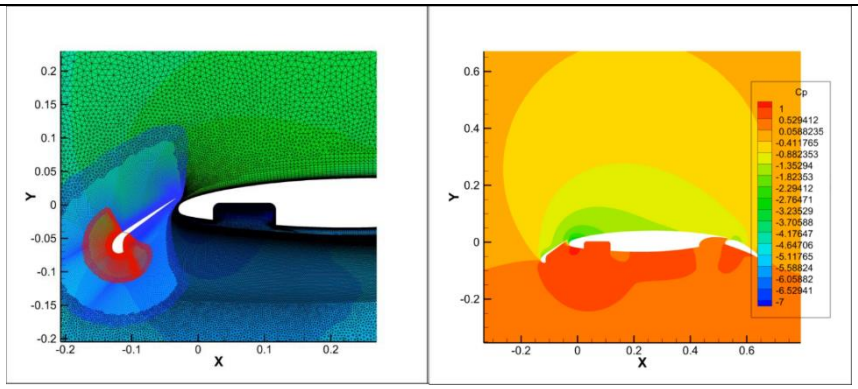

Figure 58: Chimera activities on Kruger deployment (ONERA-L1)

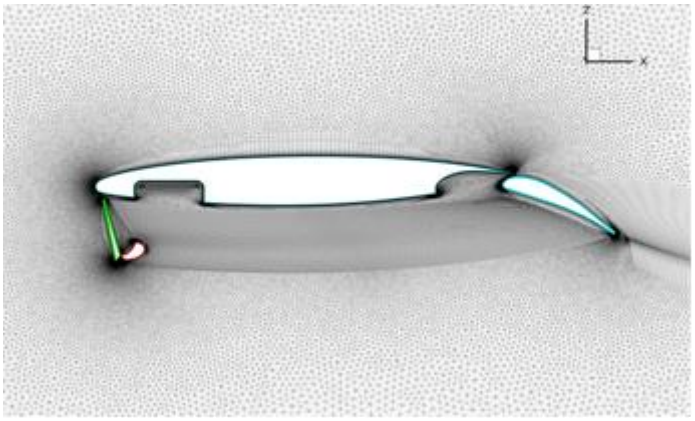

Figure 59: Kruger panel set to 75°

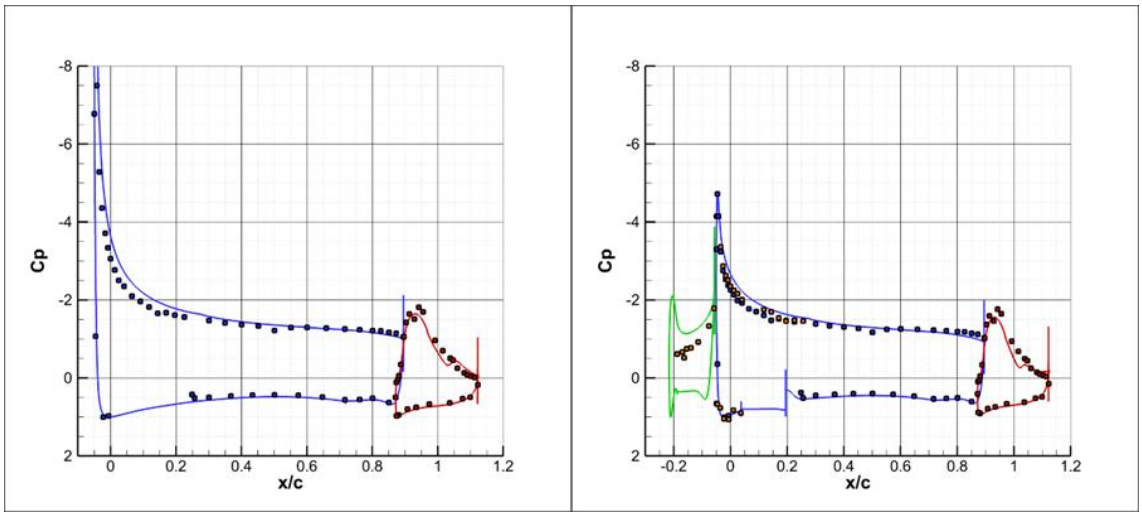

Figure 60: Comparison of Cp distributions. CFD (solid lines) and experiment (dots). Fully retracted Krueger flap (left), fully extended (right). AoA = 6°.

Contribution of Partner 4 – ONERA

The ONERA activities were focused on L1 test assessment by means of URANS simulation based on 2D Chimera (structured) approach. Evaluations of the use of chimera technique with Elsa software to deal with the 2-element Kruger airfoil deployment were carried out, and grid generation of the shapes/configurations tested during L1 test were performed as well. The CFD simulation were concentrated on comparisons and assessment of flow solver vs experiments. ONERA contributed in evaluating mainly the chimera overset grid approach, and improving its CFD tools. ONERA focused its effort on 2D unsteady simulations of the Krueger slat motion under deployment or retraction phases, which will be representative of the main characteristics of the flow for a restrained restitution

time. The flow simulations were carried out on the flow conditions of the Task 3.3 experiments performed in ONERA-L1 wind tunnels. In Task 4.1 ONERA simulated the Krueger movement during deployment and retraction phase by means of a 2D chimera approach. Two deployment times were considered, 4 s. and 1 s., for a tunnel speed of 45 m/s. The CFD analyses results show that:

- Flow solutions during the transient movement are more stable for the 4 sec. case.
- Loss of lift observed on the main wing component mainly.
- Panel element has a large drag variation.
- Stabilization of the efforts on the different elements about 1 sec. after the end of the deployment. However, some turbulent structures are still present on the airfoils lower size even after 10 sec.
- When the Krueger starts or stop its movement, some pressure waves are computed in the flow. These waves have a larger effect during the retraction phase (when the movement is in the main flow direction) than during the deployment.
- Flow on the flap is affected both by these pressure waves and the turbulent structures emerging from the Krueger "wake".
- Some numerical problems to compute the "fully retracted" case at the end of the retraction phase

More detailed information about ONERA activities can be found in Deliverable D41-7.

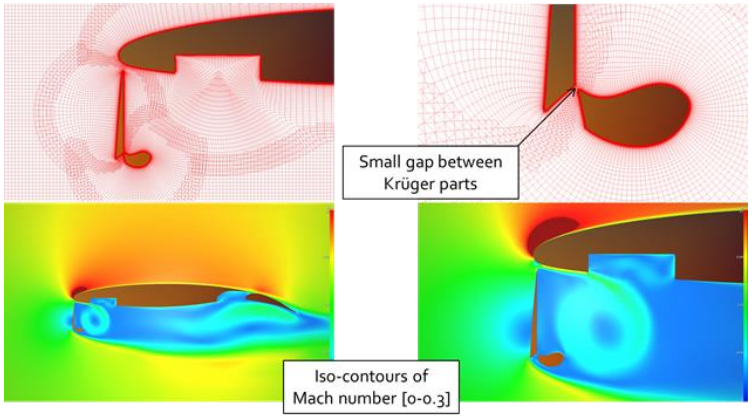

Figure 61: Use of chimera technique Kruger deployment (ONERA-L1) half deflected

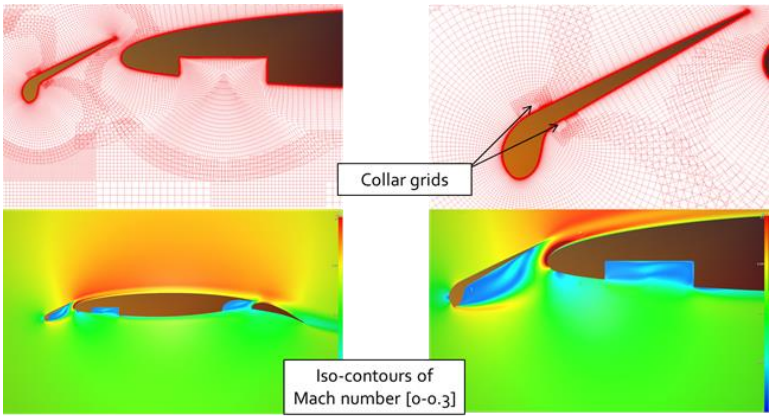

Figure 62: Use of chimera technique Kruger deployment (ONERA-L1) fully deflected

Contribution of Partner 5 – INTA

INTA activities are related to CFD computations for the ONERA-L1 case. The initially planned DNW-NWB calculations were skipped in order to focus the entire effort on ONERA-L1 configuration to improve results and perform deeper analyses. All the calculations were performed and the results obtained with a lattice Boltzmann method (LBM), which uses a scale-resolving simulation to model the turbulence effects. In particular, an LBM-based Wall-Modelled Large Eddy Simulation approach (LBM-WMLES) has been used to perform the calculations focusing on the ONERA L1 test campaign carried out within Task 3.3. Since the computational demand of the LBM-WMLES approach is high, the study has been limited to a reduced number of simulations. The aim of the study was to cover a reasonable set of cases to assess the performance of the LBM approach and its ability to predict the relevant flow features present during the deployment/retraction phases. Specifically, the analysis has been limited to assess the dynamic effects produced in the fast deployment of the Krueger device by comparing dynamic and static (fixed) calculations for one of the tested velocities. Additionally, a comparison of static simulations for two W/T velocities has been carried out to assess the influence of the W/T velocity on the simulation results. The dynamic and static numerical simulations performed in Task 4.1 using the lattice Boltzmann Method were able to assess the ability of this methodology to capture the complex physics produced when the Krueger device is deployed and retracted. In particular, the scale-resolving turbulence model based on WMLES with non-equilibrium wall functions shown good results in modelling turbulent effects. In order to have reasonable computational times for dynamic simulations a specific tuning mesh resolution in different regions of the configuration was used. Numerical simulations predict a hysteresis phenomenon during the Krueger deployment and retraction phases due to the different timing of the impact of the Krueger device wake on the stall of the flap. Dynamical effects are highlighted when static and dynamic simulations are compared, showing large discrepancies at several Krueger angles. Nevertheless, both types of simulations agree quantitatively in the prediction of the maximum amount of lift lost during the deployment/retraction cycle, which is around 50% of the lift of the fully retracted configuration. This prediction will be confronted with experimental results and simulations from other partners in Task 4.2. More detailed information about INTA activities can be found in Deliverable D41-5.

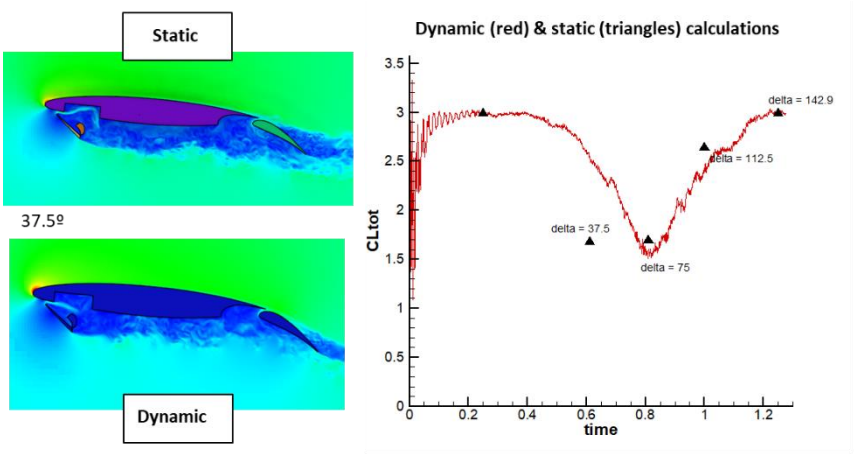

Figure 63: Comparison between static and dynamic computations (ONERA-L1)

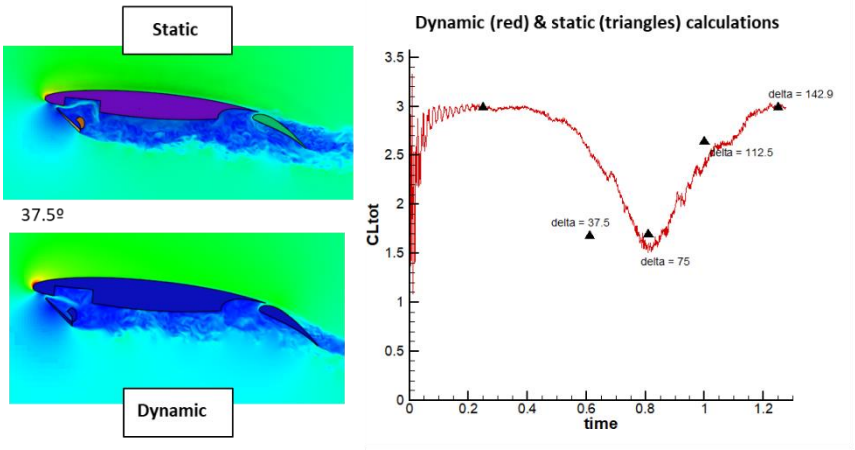

Figure 64: Comparison between static and dynamic computations (ONERA-L1)

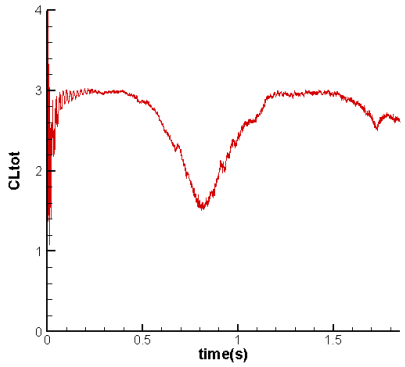

Figure 65: Retraction phase ONERA-L1)

Contribution of Partner 6 – NLR

The NLR contribute to Task 4.1 consists in exploratory steady and time-dependent flow simulations for the ONERA L1, DNW-NWB and DNW-LLF wind-tunnel models.

The technical progress concerns grid generation activities and test computations using the Chimera method for the 2D and 2.5D configurations. The development work carried out by NLR on simulation methodologies for unsteady flows and rigid body motion within the UHURA project renders the modelling approach based on sliding grids as obsolete. the application range of the novel Chimera method based on overlapping grids is extended to 3D high-lift configurations that feature a deploying part-span multi-element Krueger device. The objective of NLR Task 4.1 activities is to prepare the CFD models for the three test articles and perform exploratory simulations in order to verify the numerical results for selected nominal test conditions.

The experience obtained with respect to the generation of Chimera grids and time-accurate simulations for the full span Kruger is exploited for the part-span Krueger configurations. Flow modelling activities have been performed for three wind-tunnel models: ONERA L1, DNW-NWB and DNW-LLF in order to assess the effects of wing sweep and deployment speed on the time-dependent aerodynamic characteristics of the high-lift configuration as well as the changing loads of the Krueger device. The Chimera grids are constructed by concatenating multi-block structured meshes for the high-lift wing and the moving entities, i.e. the Kruger panel and the Bullnose. The considered configurations include the retracted Krueger where the Bullnose is folding into the wing cavity. The related geometry features small gaps of a few millimetre in chord-wise and span-wise direction of the wing. The Chimera implementation is capable to address these challenging applications by constructing an efficient set of interface/interpolation cells for the moving grids.

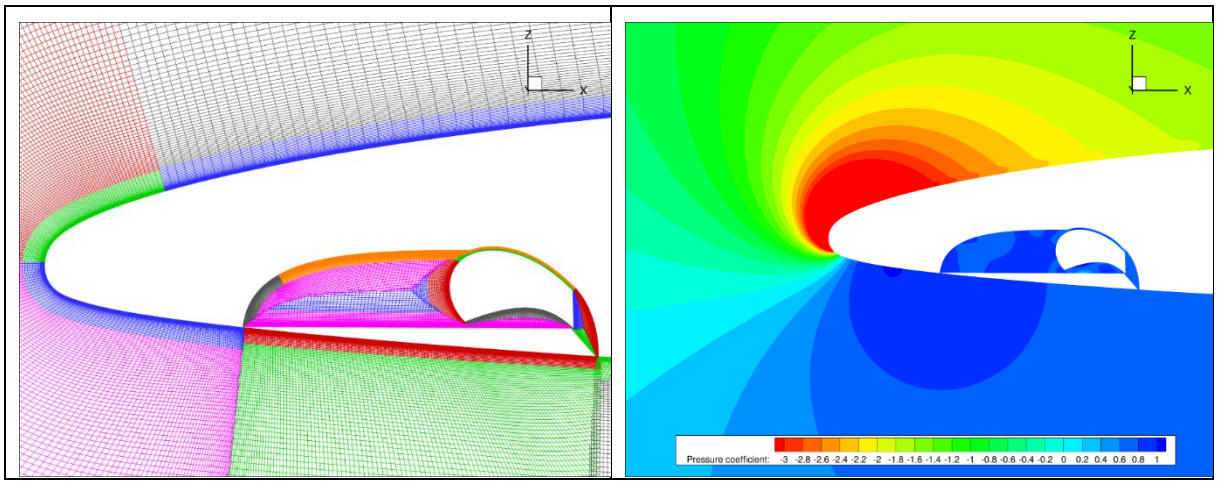

Figure 66: chimera setup based on block-structured meshes for ONERA-L1 setup

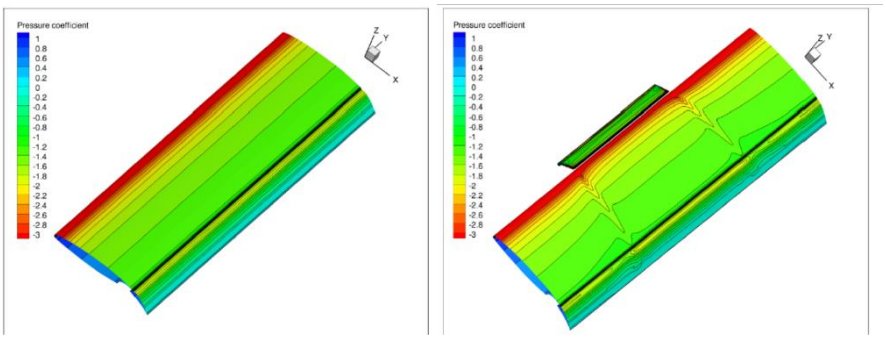

Figure 67: ONERA-L1 configuration (V_N = 45 m/s; α = 6°)

The experience gained during the construction of overlapping grids for the UHURA applications (12 in total) has contributed to a more robust algorithm for the assignment of interpolation cells. Regarding rigid body motion, the specification of the kinematics has been extended to an arbitrary motion. This extension was required to prepare for the adoption of the measured time-history for the motion of a motorized Krueger device in a wind tunnel facility for validation purposes. Both static and dynamic deployment cases have been considered. Here, the static cases include retracted, full-deflected and partly-deflected Krueger configurations whereas the dynamic cases consider a deploying two-component Krueger device. The lift curves for the ONERA L1 and DNW-NWB models are evaluated using steady (RANS) simulations. The sectional pressure coefficient distributions are exploited to arrive at flow conditions for the swept wing configurations using wing sweep theory. Flow similarity on the test articles is targeted for the identification of wing sweep effects.

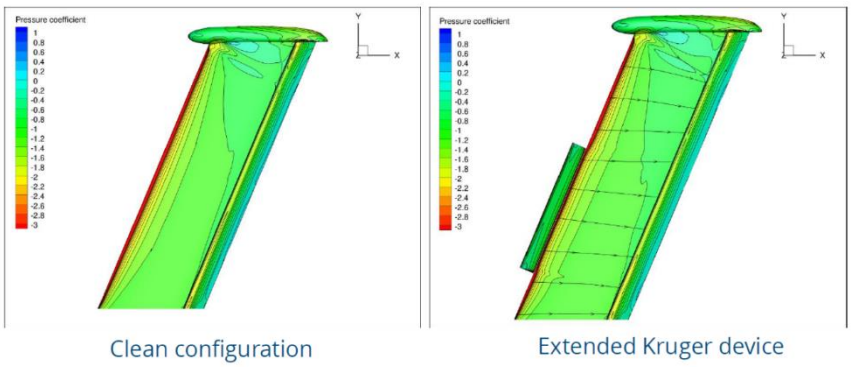

Figure 68: DNW-NWB configuration (V_N = 45 m/s; α = 8°)

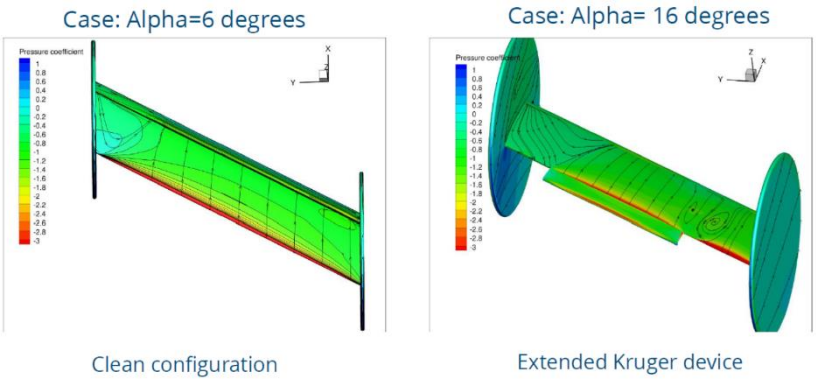

Figure 69: DNW-LLF configuration (V_N = 45 m/s)

The aerodynamic characteristics (high-lift polars) for the fully deployed Krueger device have been computed using steady (RANS) simulations. Subsequently, unsteady simulations (URANS) are performed for the full-span and part-span configuration of a deploying two-element Krueger device using multi-block structured grids and a Chimera approach for the moving body kinematics. Here, the aerodynamic forces are evaluated for the individual elements of the Krueger device for an initial load assessment and future comparison with wind tunnel measurement data.

The flow simulations consider steady-state and time-dependent flow problems for wind tunnel test conditions. The simulation results for the static deployment cases have initially been utilized for verification purposes of time-accurate results. The computed flow for a clean wing was exploited to remedy the detrimental effect of gap flow leakage on leading-edge stall for the retracted Krueger configuration. The same is true for the full deflected cases to verify the flow field of the deploying Krueger device at final deployment angles. The outcome of these verification activities is that the CFD models qualify for final validation simulations based on the actual test conditions. The analysis of the Krueger deployment characteristics from a flight physics and loads perspectives show the interaction of the main-wing and the moving Krueger device in front of the wing which results in a temporary loss of lift. The latter defines the transient lift characteristics of the high-lift configuration. The changing loads on the Kruger device components show a reversal of the load direction during deployment and identify the full deflected case as the sizing case. The investigation of the Krueger deployment characteristics with respect to deployment speed and wing sweep shows that the sweep angle is the leading parameter to reduce the lift transients. The deployment speed of the Krueger has an impact on the lift transient for an unswept wing only. Here, an increase of the angular velocity leads to a reduction of the time-dependent lift losses.

The verification simulations of static and dynamic deployment cases defined for the ONERA L1, NWB and LLF WT models are completed. Analysis of sectional pressure distributions form a flow physics point of view for the retracted, partly-deflected, fully-deflected Krueger configurations have been performed and analysis of the transient forces for the deploying part-span Krueger devices have been carried out. The available numerical investigations for the identification of wing sweep and Kruger device deployment have been documented in the Deliverable D41-6 (NLR) "Report on temporal aspects of the flow dynamics and characterization of the aero-loads during Krueger deployment".

Based on the selection of wind tunnel test conditions in Task 4.2, additional simulations are conducted for ONERA L1, DNW-NWB and DNW-LLF test configurations at V_N = 45 m/s using the measured deployment characteristics of the Krueger device. Here, the comparison of numerical and experimental pressure distributions is presented for static deployment cases related to the NWB model. The c_p-distributions show an excellent agreement which indicates that the interaction of the Krueger device and the main-wing is well captured along with the implications for the aerodynamic performance of the high-lift configuration and that the prediction of the loads on the Krueger components is validated.

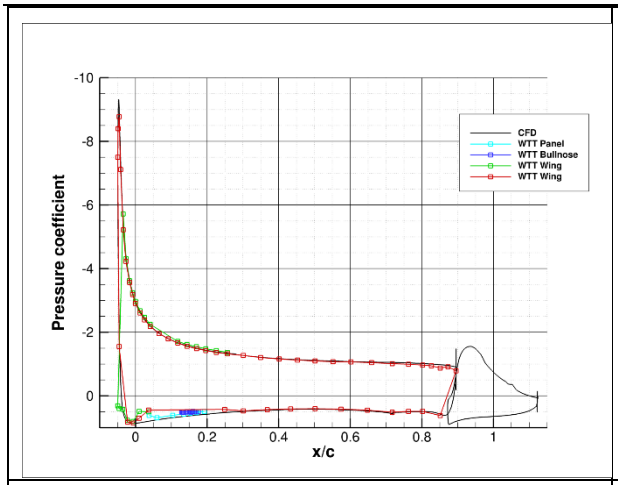

Retracted Krueger

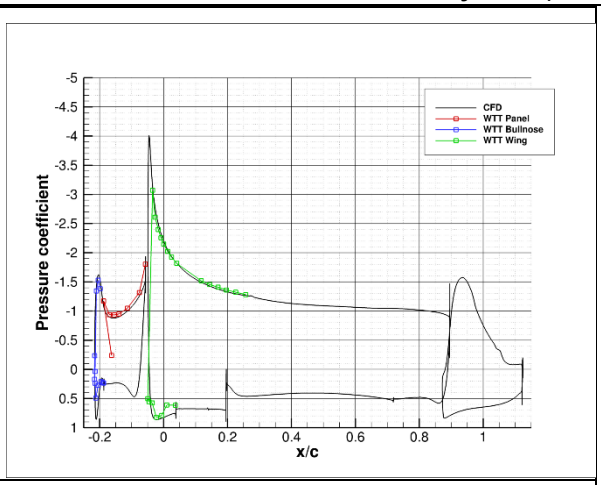

Fully deployed Krueger

Figure 70: Comparison of predicted and measured pressure distributions (DNW-NWB, V_N = 45 m/s)

Contribution of Partner 8 – KTH

The KTH activities in Task 4.1 aim to study the transient turbulent flows over high-lift wings with a foldable Krüger device during a complete deployment and retraction cycle according to the setups in ONERA-L1 and DNW-LLF wind tunnels by advanced CFD methods. During the Krüger deployment and retraction, there is a large time scale difference between dynamics of the device movement and the rapid turbulence fluctuations. This indicates that accurately capturing the flow physics for both time scales would be expensive by conventional LES methods. Also, hybrid RANS-LES methods were expected to be cumbersome in computational effort. With the required resolution $c/\Delta x$ = 200 and the convective CFL number, $CFL_c = \Delta t U''/\Delta x$ = 0.2, the number of required time steps are in the order of 70.000 for one single deployment of 1s. Before the study within WP2 for optimizing the setup, we estimated the number of sub-iterations to 50 per time step, and the clock time of 2s per iteration resulting in almost 3 months of wall time. With the optimization and improvements from WP2 as well as better parallel scaling than expected (running on a different cluster) the wall time for 1s physical time was reduced to a couple of days running on not more than 500 cores. Hence, we could run several full deployment/retraction cycles. In addition, URANS calculations have been computed and comparisons with wind-tunnel data was made. Both with wind-tunnel walls present and with a far-field external domain. Moreover, the statistically 2D setup was verified by full 3D computations with the wind-tunnel walls at fixed positions using RANS.

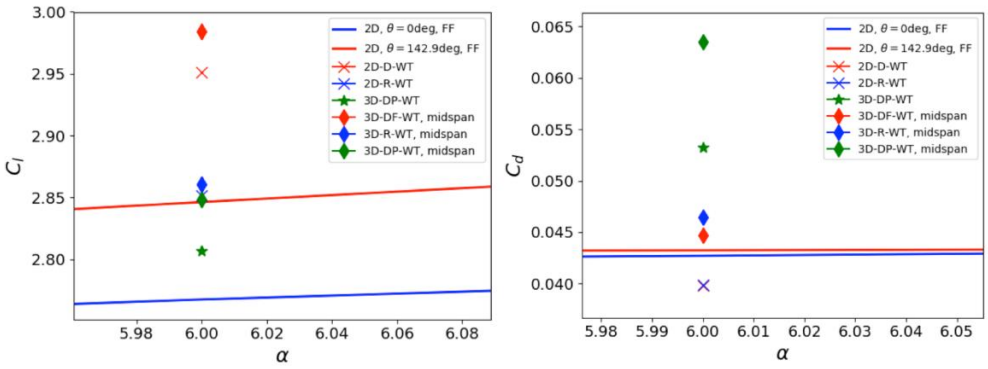

Figure 71: Comparison 2D vs 3D static-steady RANS with and without WT-walls effect (ONERA-L1)

From the 3D study of different static settings within the wind tunnel is possible to conclude that there are significant 3D effects for the cases where the Krüger device is covering only the central third part, the part-span deployment cases. However, the 3D effects are small and limited and the 2D approximation is justified and comparisons can be made even though a small offset can be expected. Probably of the most important conclusion from this study is that URANS seems to be as accurate as

more complex and computationally expensive hybrid RANS-LES computations. The reason for this might be that the massive separation downstream of the Krüger device is mainly driven by the moving geometries and not so much through flow instabilities and turbulence production mechanisms. URANS can be enabled for full scale real 3D geometries of relevance for the aircraft industries. In fact, the optimized procedure for the dynamic hybrid RANS-LES would make it possible to run the full cycle for the complete 3D geometry as well including wind-tunnel walls with similar resolution. The mesh size would be in the order of a few 100 millions, number of time steps around 200.000 which will take a few weeks on 5-10 thousands of CPU cores. The main difficulty in predicting this flow seems to be related to the flow over the T.E. flap, which separates and reattaches during the deployment and retraction cycle. The loss of lift at the flap will strongly influence the circulation, with some time delay, and cause loss of suction over the main wing and Krüger flap as well. It seems like the underpredicted lift by CFD is associated with massive separation over the T.E. flap.

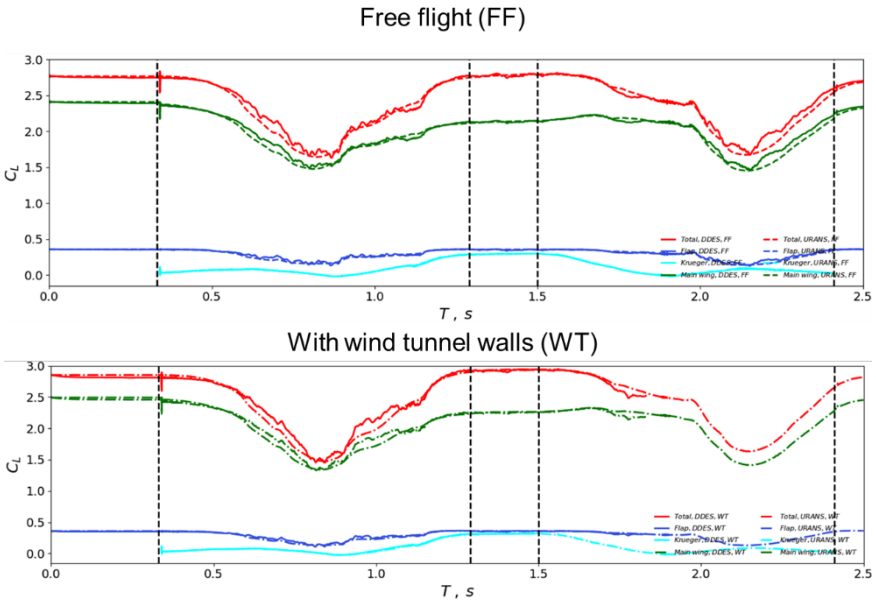

Figure 72: Comparison URANS vs DDES with and without WT-walls effect (ONERA-L1)

The flow over the T.E. flap is dynamically forced by the large-scale turbulence from the separated region under the wing entraining through the flap gap and being mixed with the wake from the main wing. The unsteady turbulent forcing of the flow over the flap will most likely delay massive flow separation in reality. However, the hybrid RANS-LES computations are not sufficiently resolved in the flap gap and on the upper side of the flap resulting in that the flow over the flap basically being in RANS mode. Moreover, hybrid models lack the necessary mechanisms for capturing the mixing of an incoming RANS wake from the main wing with the turbulence entraining through the flap gap. Hence, both URANS and hybrid RANS-LES approaches will have problems in capturing this effect correctly. Unfortunately, no measurements were taken over the T.E. flap to verify this hypothesis. Moreover, flow separation over the T.E. flap seems to be responsible for much of the lift deficit seen in these simulations. One should consider to use a less aggressive flap setting for a smoother deployment and retraction process and to increase the flap angle after deployment before reaching the landing conditions. More detailed information about KTH activities can be found in Deliverable D41-8.

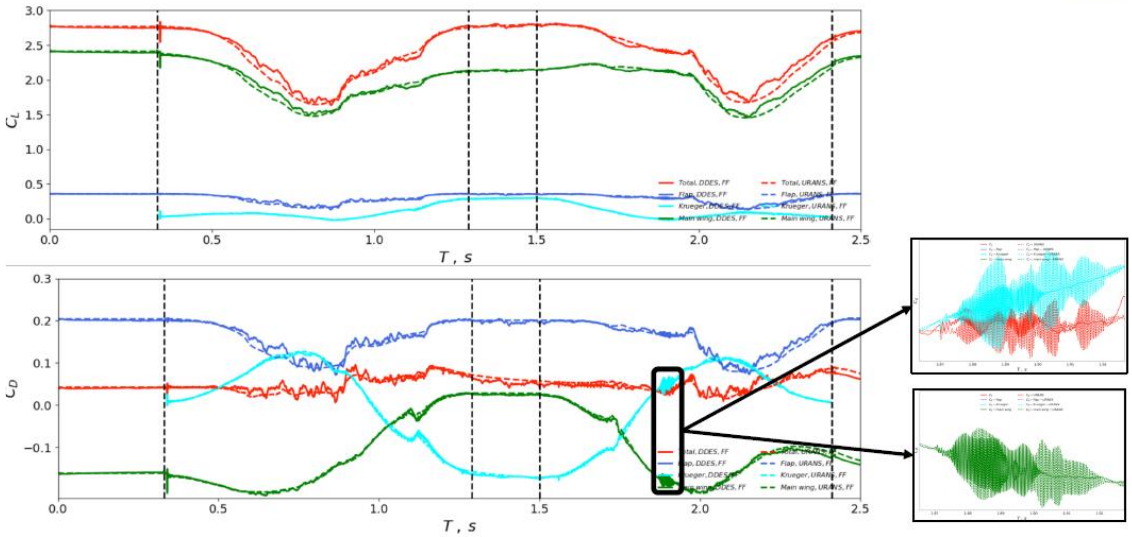

Figure 73: URANS vs DDES Free-flight conditions

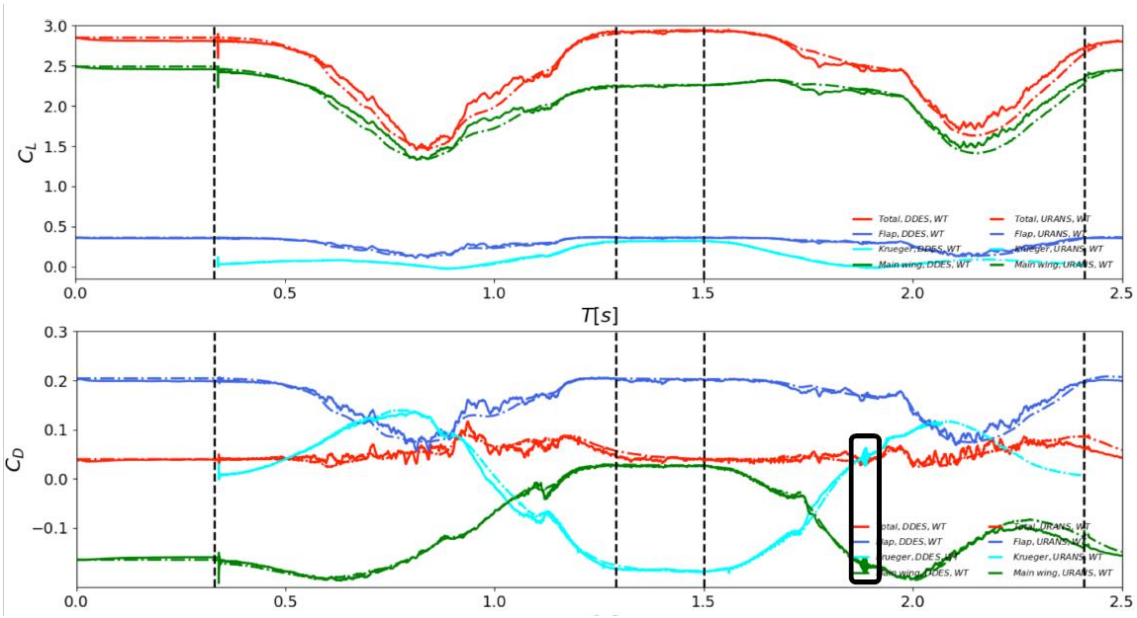

Figure 74: URANS vs DDES WT conditions

Contribution of Partner 9 – IBK

The IBK activities in Task 4.1 are focused on FSI simulations used to provide aero-loads prediction. The FSI-simulations are carried out to provide aero-loads prediction. The FSI method employs the partitioned approach where the existing CFD and CSM codes are coupled via an FSI-interface tool. In this work, the CIRA's CFD-Solver SIMBA with its immersed boundary method is coupled with the CSM solver NASTRAN via the developed FSI-interface "Fe-tool". There are two coupling strategies, the static two-way coupling, employing the Nastran static solver SOL101 and the dynamic two-way coupling, employing the NASTRAN transient solver SOL129. The interface works constantly propagating the 2D-CFD load to the span in CSM model, after structural simulation, the CSM mid-section is chosen for 2D-deformation and transferred to CFD. By using this interface, both static two-way coupling and dynamic two-way coupling were exercised.

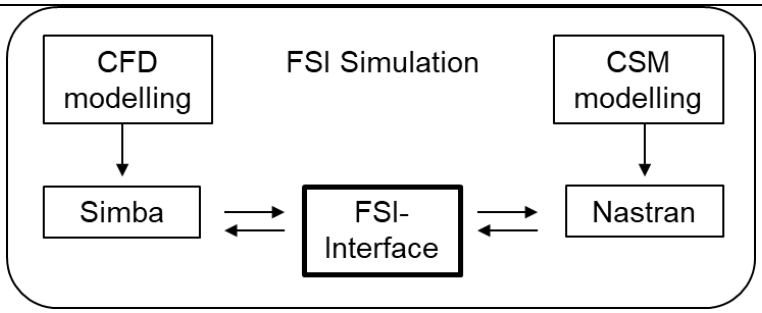

Figure 75: FSI interface flow-chart

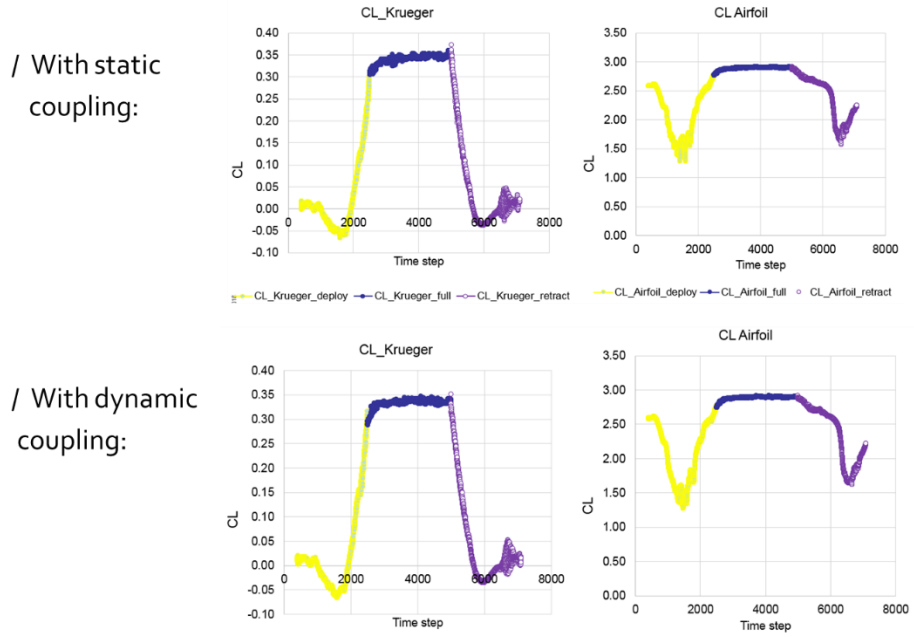

Figure 76: FSI-result Aeroloads (ONERA-L1)

Some cases, which reproduce wind tunnel test conditions for ONERA-L1 model, are investigated. These include the Krueger movement process involving deployment, holding and retraction, the fixed Krueger setting at 75° and the polar sweep at max. deployed Krueger. For the Krueger movement process, both FSI simulation strategies with static and dynamic two-way couplings are exercised. The results from both coupling strategies are comparable in general. However, the static coupling delivers more conservative deformation. The results from moving Krueger suggest that the structural flexibility changes the mean lift loads at most at its max. deployment position where the deformation is correspondingly the largest. It is however to remind that the loads oscillation amplitude can be significant. The simulation on the fixed Krueger setting at 75° has shown that the vortex development past the Krueger triggers high amplitude of loads oscillation. Finally, the polar sweep simulations show that the effect of structural flexibility is more pronounced for lift coefficient, especially at high AoA, where the lift coefficient values are slightly higher. However, the mean drag and pitching moment values are only less affected by the flexibility. More detailed information about KTH activities can be found in Deliverable D41-3.

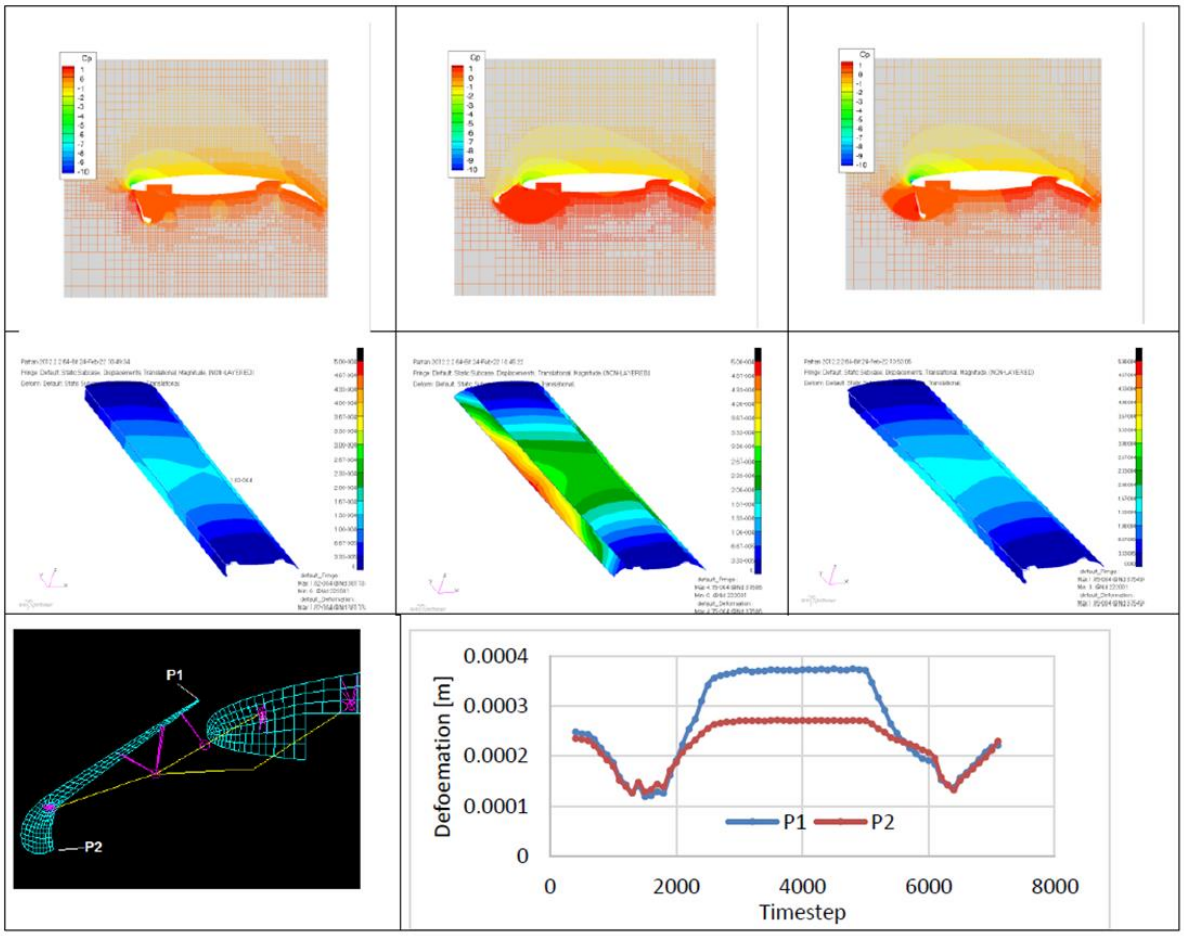

Figure 77: Simba instantaneous field pressure solution and mesh [top] and its Nastran static (SOL101) deformation solution, at time step – from left – 1200 (deflecting), 3700 (holding), 6300 (retracting) [middle] and deformation history at points P1 and P2 [bottom]

Contribution of Partner 11 – DASSAV

The Dassault target activity in Task 4.1 is to carry out CFD simulations on DNW-LLF test case by using a 2.5D static-unsteady approach based on Delayed Detached Eddy Simulation. The in-house developed code AETHER (AEro-THERmodynamics) was used to this scope. In particular, one of the main goals of Dassault in Task 4.1 is to assess the capability of this software to evaluate the critical loads. The interest was focused on a innovative methodology to create adapted meshes suitable for hybrid RANS-LES computation. The work on ONERA-L1 test cases was used to develop this novel mesh refinement strategy.

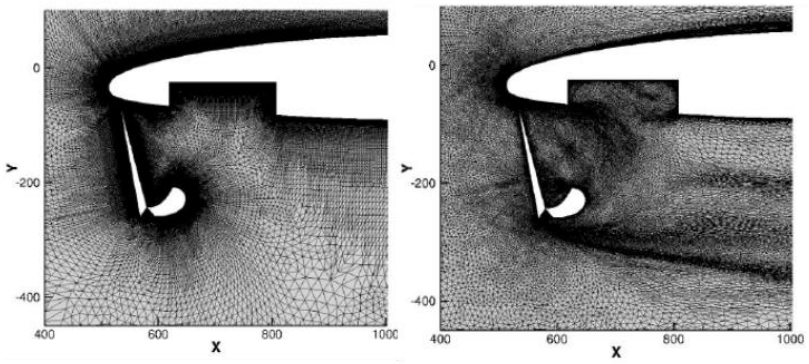

Figure 78: Mesh refinement example (ONERA-L1)

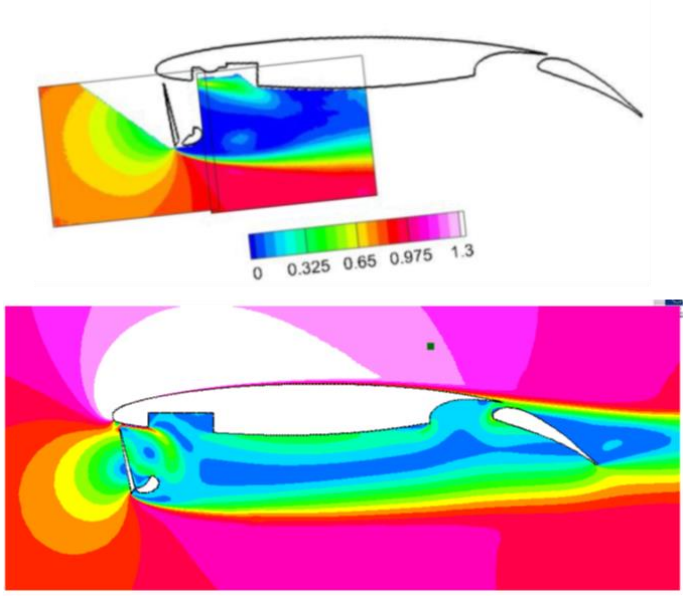

Figure 79: (ONERA-L1): Preliminary comparison PIV vs CFD (ONERA-L1)

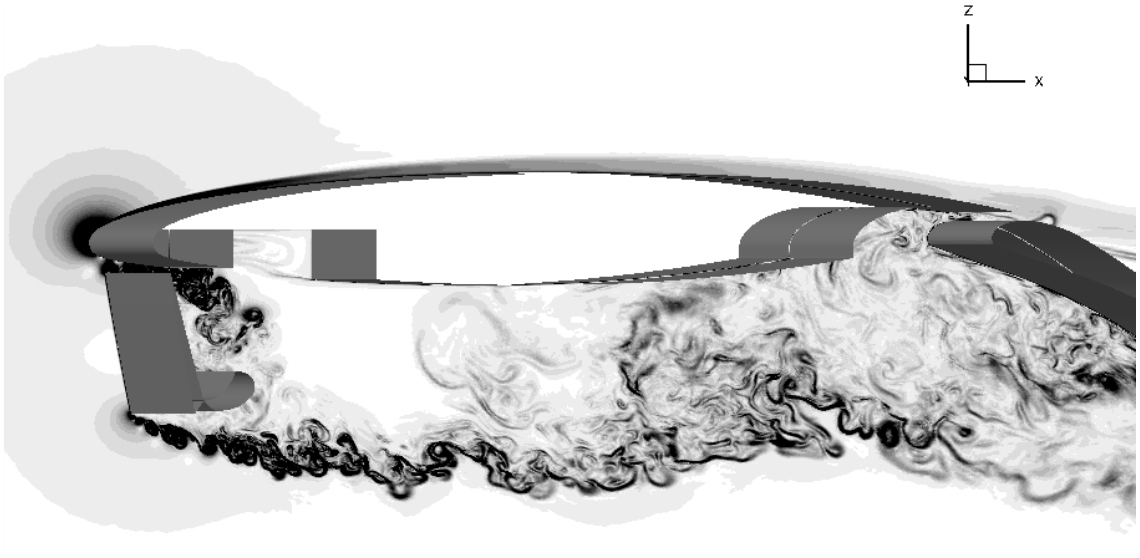

Figure 80: Lateral view of the swept wing and numerical Schlieren

In order to evaluate the code prediction capabilities on a Kruger geometry, a first comparison on the retracted configuration was performed by means of a 2D RANS computation. This comparison was in part satisfactory and shed a light on the importance of WTT correction, as a reminder the CFD is done at an AoA of 5.2° and the WTT at an AoA of 15.7°. Then, a new methodology to produce adapted meshes for unsteady computations has been put in place. A whole cycle of adaptation, able to produce the meshes manually, has been presented and the possibility to automate it has been concluded. This automated process would lead to some interesting possibility in terms of reduction of human inputs during the production of meshes for complex unsteady flow predictions. This has yet to be implemented and tested on several configurations to gain in maturity. There are also open questions on the way to modify the metrics to consider the turbulence data information that comes from the RANS computations. It was also shown that without an adjoint based technique based on some objective function the adaptation targets all features of the flow and not the ones we consider relevant. Therefore, there is still need for user to provide targeted zones of interest for which he would give a targeted number of points. Concerning the WTT data comparison, the results have shown that with the 2D with sweep hypothesis, the load on the Kruger panel are overpredicted by a factor 2. This is mainly due to the prediction of the flow downstream the Kruger panel. The reasons for the over

prediction can come for the 2D with sweep hypothesis, considering the Kruger kinematics and the WTT correction. The differences could be more finely understood by comparing with the PIV data and computing the full 3D configuration with Kruger kinematics. More detailed information about INTA activities can be found in Deliverable D41-4.

2.4.2 Task 4.2 – Validation and assessment – data comparison of numerics and experiment

Lead: VZLU

Task 4.2 objectives

- establish a roadmap for the comparison of wind tunnel test data and numerical results of simulations
- Data collection, analysis and comparison from the wind tunnel experiments and CFD
- Finalization of deliverables and reports

Progress achieved/results

The data gathered during coordination meetings, available documentation and other discussions regarding mainly the experimental campaigns was summed, put into the context of CFD work. Information on future wind tunnel data has been gathered from coordination meetings in WP3 regarding the experimental campaigns and test article instrumentation in available design reports. Future comparison of surface pressures, flow field data (PIV) and loads data are described in deliverable D42-1 "Roadmap for the comparison of wind tunnel test data and numerical results". The document has been reviewed and submitted.

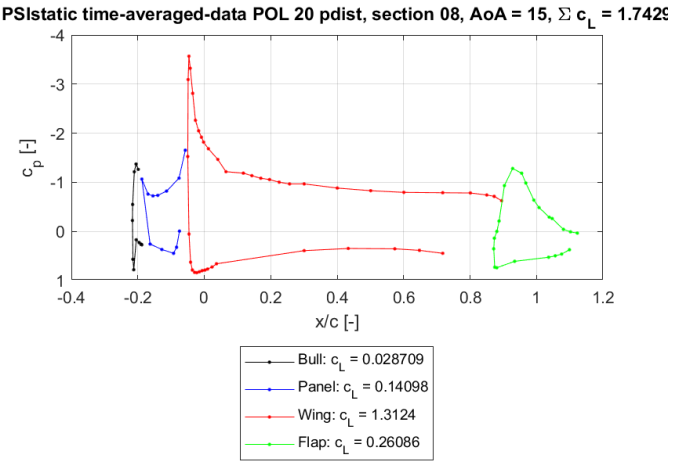

Figure 81: Force integration of the time-averaged data from a static wind tunnel measurement (DNW-LLF).

The activity in the first period remains in low levels. Ongoing discussions and presence within WP3 and Task 4.1 meetings are aimed to clarify any remaining ambiguity and to provide guidelines for future work. As a first action, DLR provided phase and time averaged pressure data of the DNW-NWB and DNW-LLF wind tunnel tests for inspection of suitability for comparisons. The further analysis of the data, obtained by various measurement techniques, is aimed at the possibility of integration of aerodynamic force coefficients, because the forces are not measured directly during the experiments.

The Task 4.2 follows closely the activities of Task 4.1 and of Task 3.3. The progress is directly linked to the progress in these activities. The finalization of the activities was shifted towards the end of the project as the final CFD results from Task 4.1 were delivered and the wind tunnel data from Task 3.3 were available. Individual partners active in this Task used mainly their CFD data for the

comparison with the experimental measurement, to address various aspects of dynamic Krueger flap deflection.

Contribution of Partner 1 – DLR

DLR contributed by the analysis of the wind tunnel data, which was post-processed and delivered to the IBK server. During the last phase of the project, the validation of the simulation method was targeted. After a first simulation with the ideal motion profile, significant difference was observed. For this reason, the CFD setup and the experimental data was revisited. A significant impact of the mechanics on the motion profile in the DNW-NWB case, where the flap is driven from one side only was observed (see Figure 82).

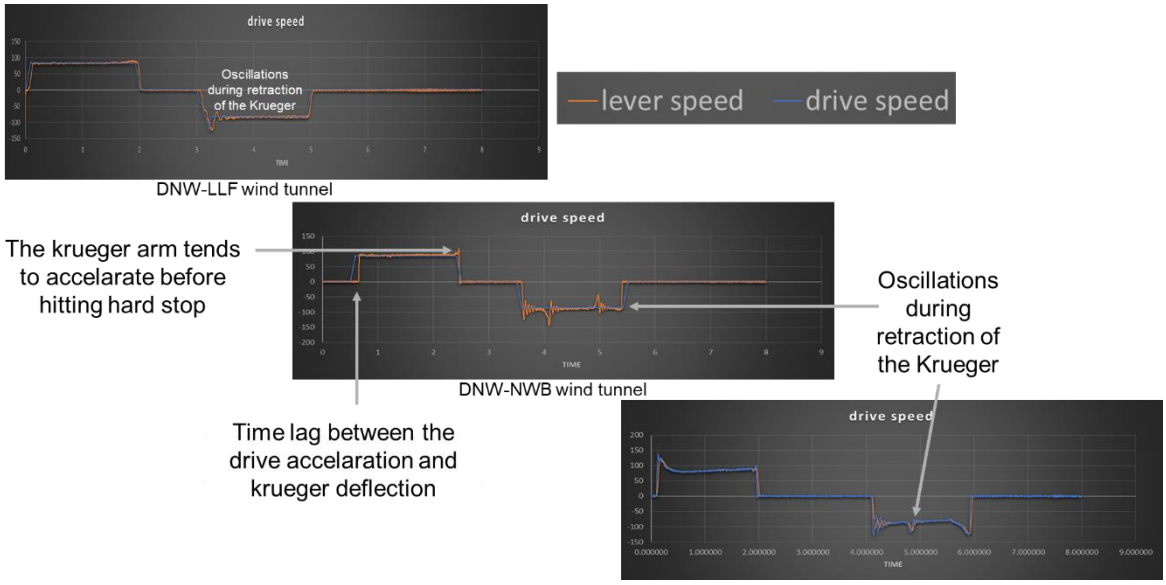

Figure 82: Comparison of ideal motion profiles and recorded kinematics motion at drive shaft encoder.

After the simulations used the measured deployment path and an improved CFD setup, a new comparison showed an excellent agreement in the pressure distributions all along the deployment path, exemplarily shown in figure below.

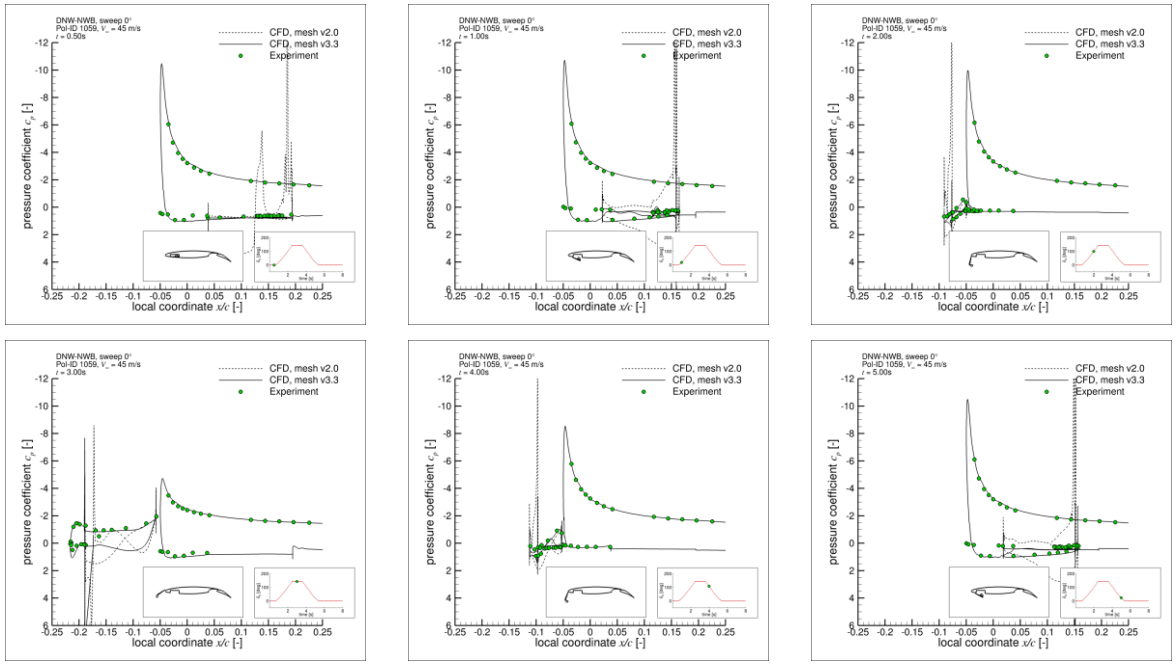

Figure 83: Comparison of CFD and experimental pressure distributions at different states during the dynamic motion path. Wind speed V_N = 45 m/s; deflection time t_d = 1 s, hold time t_h = 1 s.

The contribution was summarized in D42-2 (Report on influence of wind tunnel setups on characteristic flow features for validation). DLR also contributed with its CFD data to the common comparison activity.

Contribution of Partner 3 – VZLU

VZLU contributed to the preparation and analysis of the wind tunnel data, communicating with Task 3.3 for clarification of possible misunderstandings and errors. The data from the CFD were collected and prepared for the common comparison documented in D42-3 *(Validation and assessment of the unsteady flow and load characteristics for a deploying Krueger device)*. The wind tunnel data were sorted out according to the characteristic flow conditions and Krueger motion cases and made available through the IBK server for future use by the partners (ONERA-L1, DNW-NWB, DNW-LLF cases). The data sets CFD data from WP4.1 were collected and analysed (DLR, CIRA, VZLU, ONERA, INTA, KTH).

The effect of wind tunnel setup was analysed for static and dynamic cases. It was found that the differences, namely between ONERA-L1 experiment, which represents a 2D flow, and other cases were significant. The wall-to-wall installation of ONERA-L1 experiment causes significant separation downstream of the Krueger flap for partially retracted positions, which also affects the suction side of the wing. Such an effect is greatly reduced even for DNW-NWB 0° wing sweep configuration, and even less pronounced for the swept wing cases (DNW-NWB, DNW-LLF), refer to Figure 84.

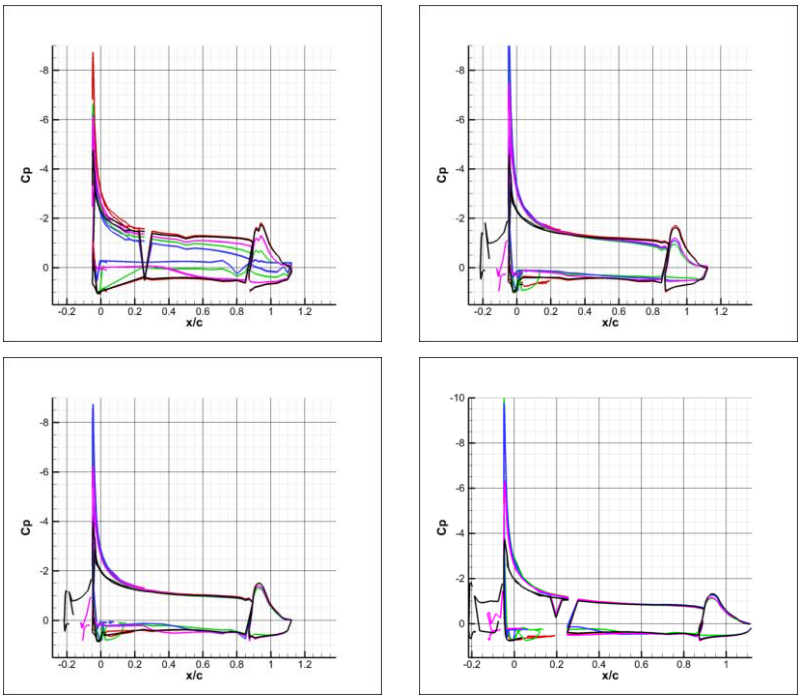

Figure 84: Comparison of experimental data for four different WT setups: ONERA-L1, DNW-NWB 0° sweep, DNW-NWB 23° sweep, DNW-LLF (from left to right, top to bottom). Colours represent different position of the Krueger flap

The study of the dynamic measurements relies on the unsteady pressure measurement by means of MEMS. We can see that the dynamic effects are large on the leading edge of the wing, there is a significant difference between extension and retraction phase. On the other hand, it is nearly negligible on the Krueger flap, cf. Figure 85 for partial C_L integration based on the c_p MEMS data of the ONERA-L1 case. Similar behaviour was observed for other cases, however, with reduced amplitude.

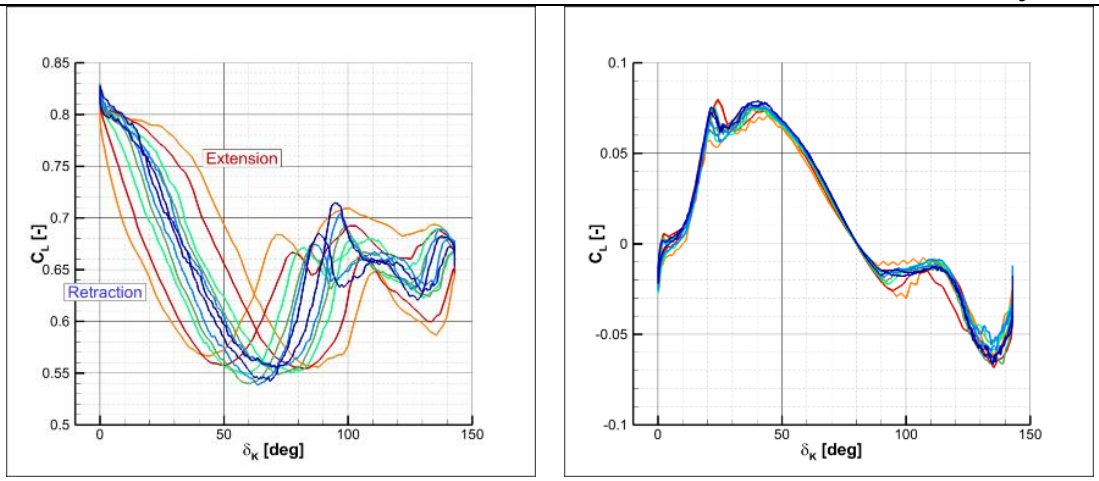

Figure 85: CL evolution during extension and retraction. Colours distinguish the cases (orange: 1 s, 30 m/s; red: 1 s, 45 m/s; light green: 2 s, 30 m/s; green: 2 s, 45 m/s; light blue: 4 s, 30 m/s; dark blue: 4 s, 30 m/s). Leading edge integration (left), Krueger panel (right).

The common comparison of CFD and validation with respect to the wind tunnel data was performed for all configurations, with most partners contributing to ONERA-L1 and DNW-LLF cases. In general, we observe good match between CFD and wind tunnel and among the CFD partners for static (Figure 86) and dynamic cases. CFD partners covered a wide range of methodologies for grid motion (chimera, mesh deformation, immersed boundaries) and for the flow modelling (uRANS, hybrid RANS-LES, LBM). It is, however, not possible to pick the winner. Any methodology, if carefully applied, seems to give reasonable results.

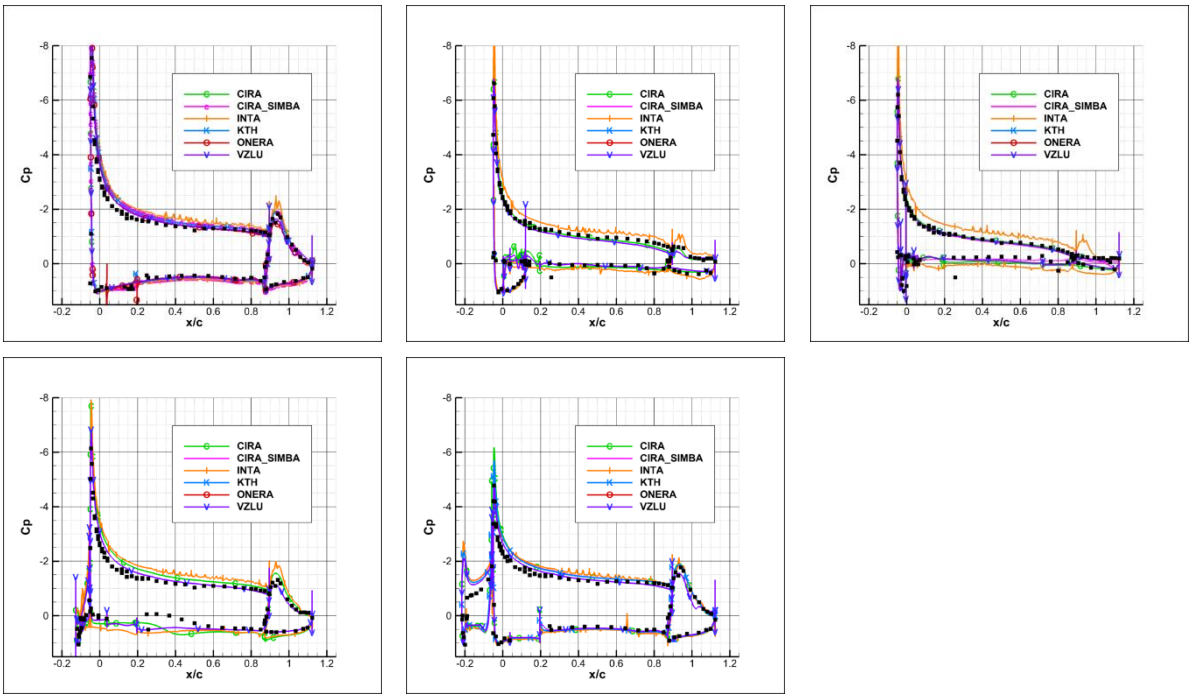

Figure 86: ONERA-L1 case comparison of Cp for static case (different Krueger flap positions).

Similar situation was observed also for dynamic simulations, where we can only compare to the MEMS data covering wing leading edge and the Krueger flap, and the DNW-LLF case, refer to Figure 87.

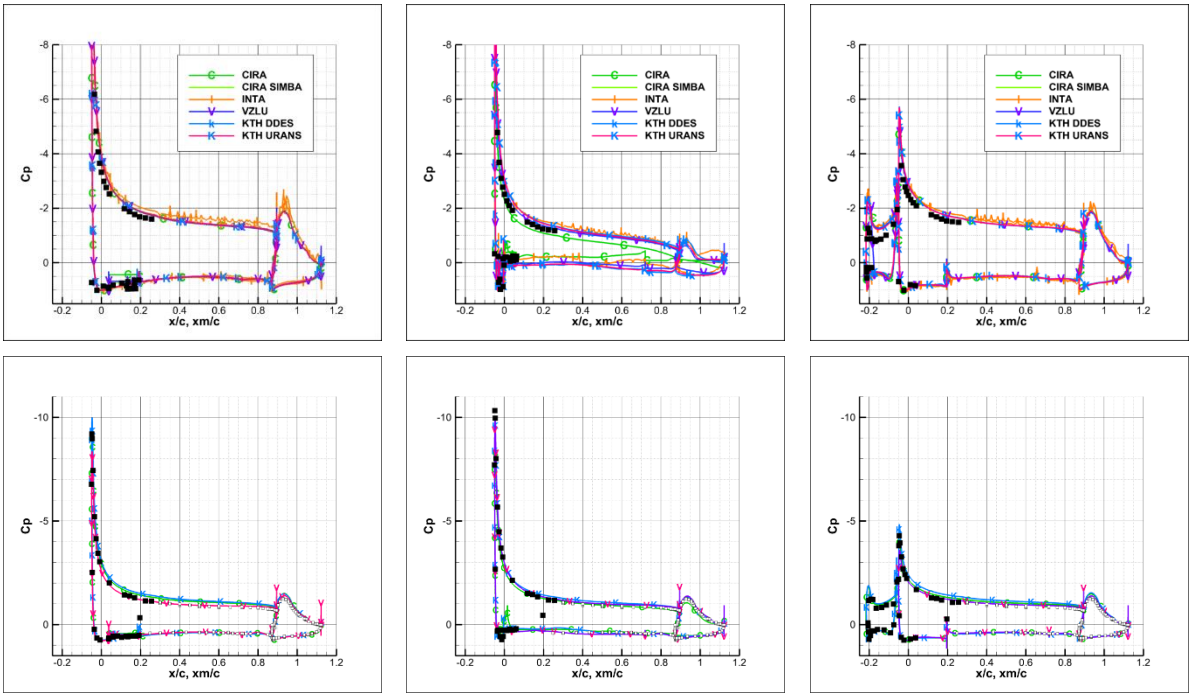

Figure 87: ONERA-L1 dynamic case comparison (top) and DNW-LLF dynamic case (bottom). Fully closed Krueger flap (left), barn-door position (middle), fully open (right).

Contribution of Partner 4 – ONERA

ONERA focused on the study of the ONERA-L1 experiment, their results are summarized in D42-8 *(Analysis of flow field characteristics in the L1 test campaign. Comparison between experiments and numerical results).* The effort was focused on 2D unsteady simulations of the Krueger slat motion under deployment or retraction phases. Static simulations were run for a Krueger flap sweep, simulating not only the characteristic positions, but following the available wind tunnel data and to study in deeper detail the evolution of the flow field. The dynamic simulations were investigated for 1 s and 4 s Krueger flap deflection times.

Contribution of Partner 5 – INTA

INTA used the data from their activity regarding LBM model, as summarized in D42-6 *(Validation of LBM* approach for a deploying Krueger device). It has been found that, in general terms, the simulations capture reasonably well the evolution of the pressure distribution in dynamic deployment/retraction cycle, see Figure 88. The pressure suction on the wing's upper side is slightly over-predicted in comparison with the experiments, but overall, the trend is reasonably well captured. The simulations predict well the important dynamic effects that appear in the full deployment/retraction cycle for the full-span configuration model in the ONERA L1 W/T experiments.

ONERA-L1 PIV experiments have been compared with time averaged velocities and turbulent kinetic energy from the simulations, refer to Figure 89. The agreement is quite good for the critical perpendicular Krueger flap position. The simulation predicts reasonably well the averaged wake and the turbulent kinetic energy peaks present in the shear layer. It can be concluded that the LBM approach shows great potential for the simulation of this kind of unsteady high lift simulations although there is still room for improvement in LBM physical models (turbulence) and numerical aspects.

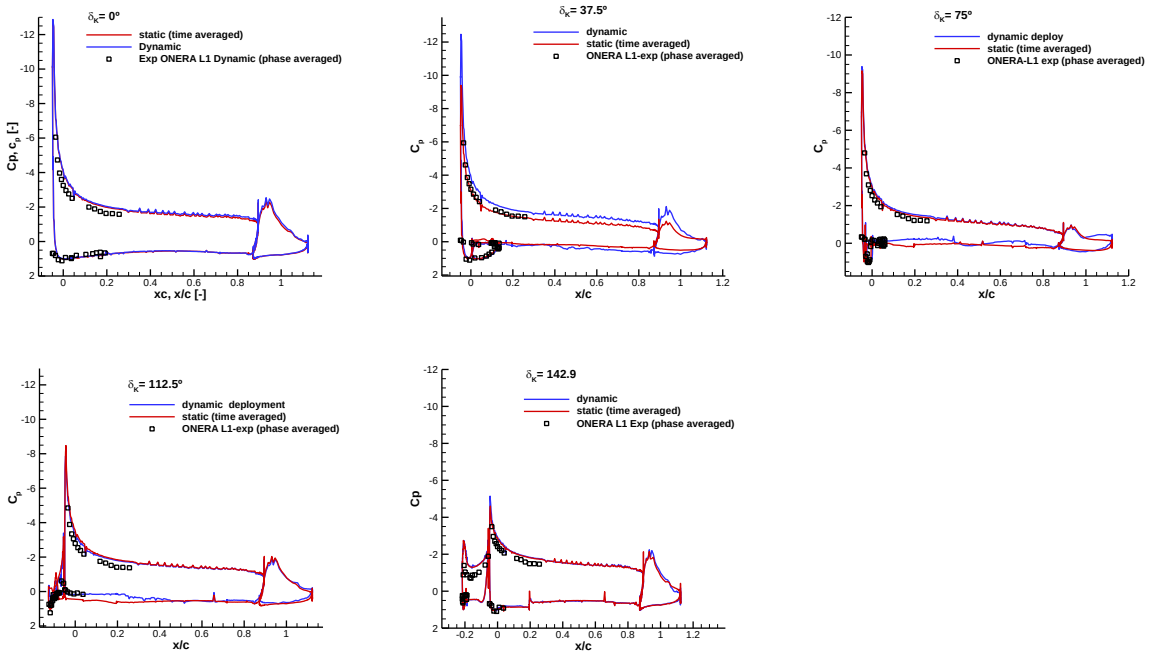

Figure 88: Comparison of LBM results and experimental pressure distributions at different positions in deployment phase. V = 30 m/s; deflection time 1 s.

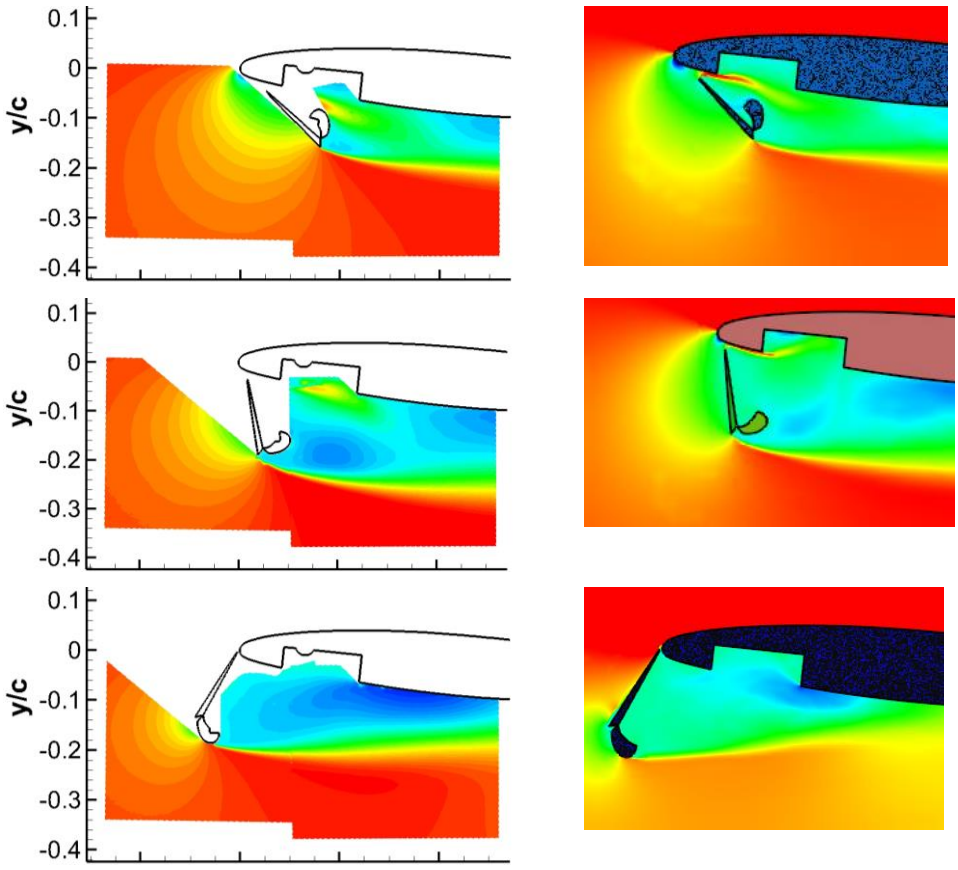

Figure 89: Comparison of PIV (left) and LBM results (right), mean velocity.

Contribution of Partner 6 – NLR

The objectives for the NLR contribution are summarized as: analysis of available wind tunnel test results, selection of suitable test conditions for final validation simulations and assessment of the prediction capability of the Chimera method for static and dynamic Kruger device deployment in a comparison of experimental and numerical results.

The wind tunnel test results of the DNW-NWB and DNW-LLF have been analysed with respect to the main-parameters of the experimental investigation: the Krueger deployment speed and the wing sweep angle as a representative of Krueger installation. Supplemental static and dynamic simulations have been performed for WT test conditions in which the time history of the motion for the motorized Krueger has been replicated. The results of the activities mentioned above are documented in deliverable D42-5. The Cp data from measurement were compared with the CFD results, see Figure 90, which shows as an example a dynamic simulation related to the DNW-NWB case in swept configuration. The final comparison shows a good agreement for the static defection cases of the DNW-NWB model and the dynamic deflection cases on the LLF model resulting in a validated prediction of the transient aerodynamic characteristics of the high-lift configuration in combination with wing sweep and the changing loads on the Krueger components.

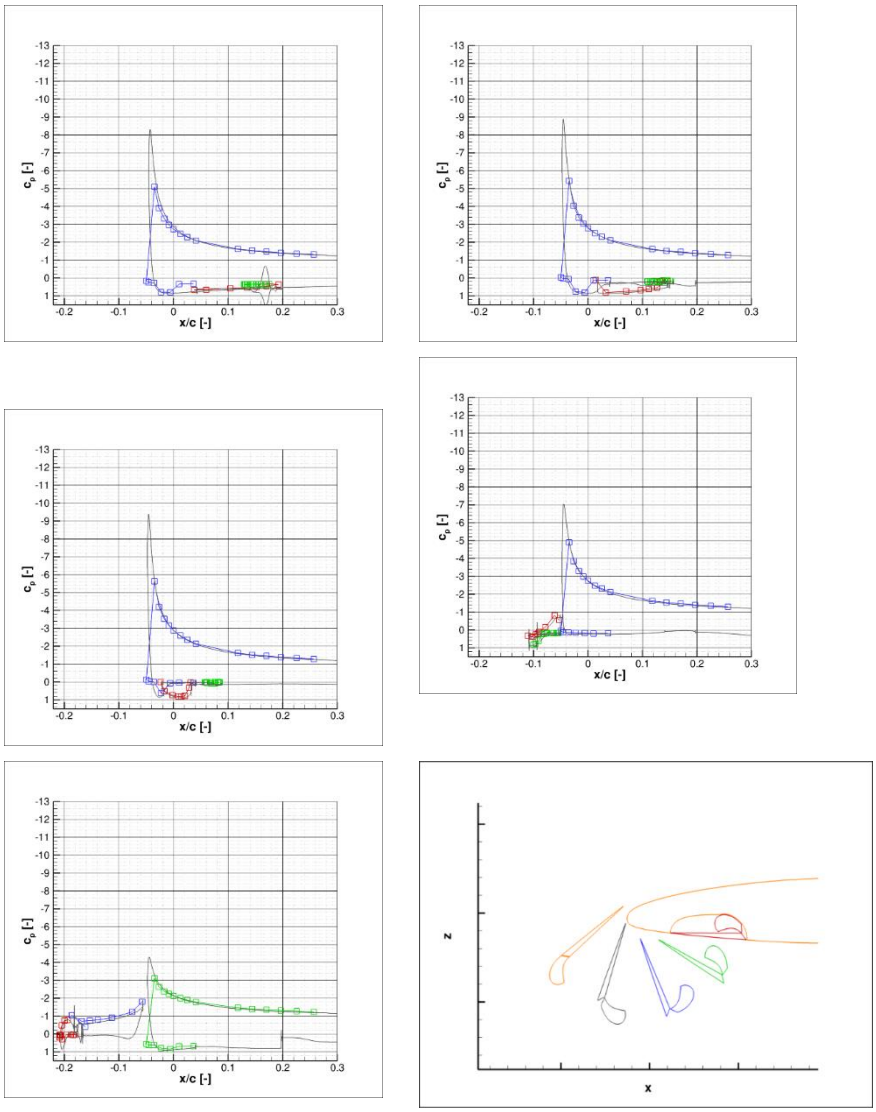

Figure 90: DNW-NWB (polar 2052) comparison with chimera based CFD results by NLR.

The validation activity for the static deployment cases shows a very good correlation of the measured and predicted surface pressure distribution for the retracted, full extended and failure deployment case. The static loads on the Krueger device were accurately predicted.

Contribution of Partner 8 – KTH

KTH contributed with their analysis of their CFD simulations using a hybrid RANS-LES model, coupled with fluid-structure interaction (FSI). The results are summed up in *D42-4 (Analysis of the unsteady turbulent flow field characteristics at critical deployment stages).*

The two-way FSI was simulated by a fully coupled and energy conservative numerical scheme. The turbulent flow filed was simulated by a hybrid RANS-LES method and the structural problem is simplified with a number of structural eigenmodes from an eigenvalue analysis of the complete structural model of the wind-tunnel model, see Figure 91.

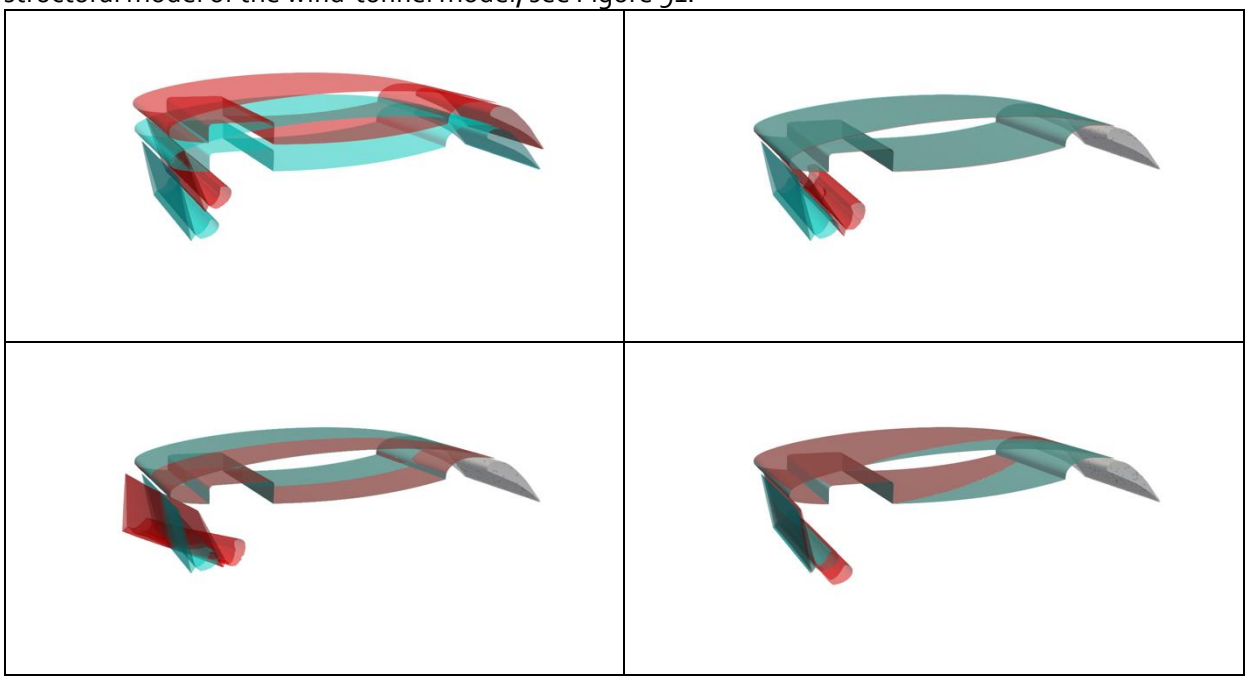

Figure 91: The first four structural eigenmodes in red with the stiff geometry in blue.

The amplitude of the predicted vibrations of the Krüger device was compared with the measurements. The maximum displacement in LE and TE point of the Krueger flap is around 0.5mm. The acceleration compares well with the measured values, see Figure 92.

The analysis of KTH shows that the turbulence is well resolved in the region downstream of the Krüger device and no difference in the turbulent flow field between the stiff and flexible structure could be seen. The simulation shows that the model is not unstable concerning FSI.

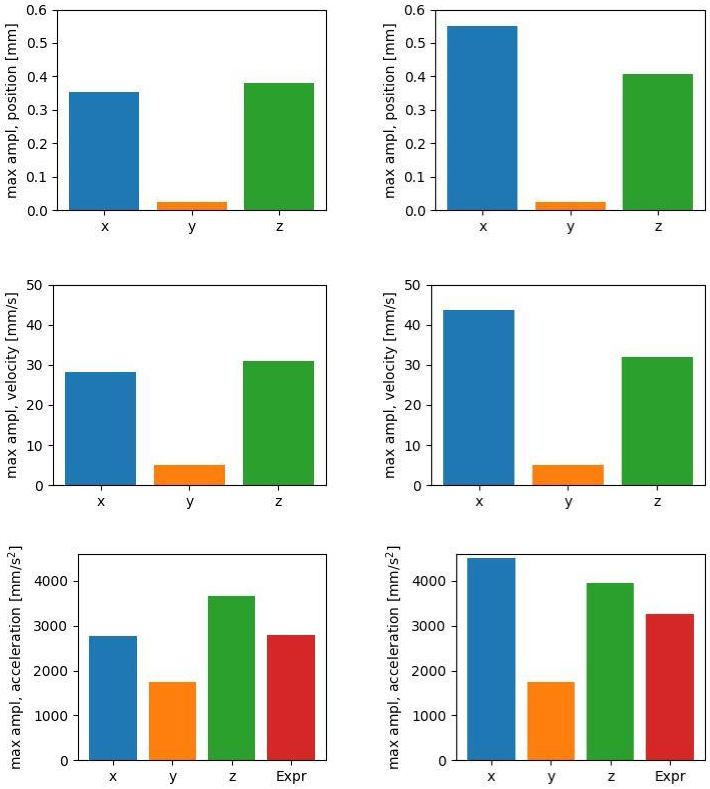

Figure 92: Max amplitude of the movement of L.E (left) and T.E. (right) points for position, velocity, and acceleration.

Contribution of Partner 9 – IBK

IBK made a progress towards the D42-7 (Report on the comparison between calculated loads and deformations of the Krueger flap and WT Measurements). The analysis of the WT data was performed, and the wind tunnel test deformations were extracted from DNW wind tunnel test campaigns. The comparisons of loads and deformation between wind tunnel test results and computations was performed.

2.4.3 Task 4.3 – Assessment and exploitation

Lead: AID

Task 4.3 objectives

- Asses impact of Krueger flap motion on handling quality (Subtask 4.3.1)
- Structural design of Krueger panel and bullnose on theoretical full-scale A/C constellation with emphasize on weight optimization (Subtask 4.3.2)
- assess the impact of UHURA findings on overall aircraft design level (Subtask 4.3.3)
- exploiting the gained knowledge on dynamic CFD simulation to other possibly fast-moving aircraft components (Subtask 4.3.3).

Progress achieved/results)

Subtask 4.3.1 Handling Qualities

Contribution of Partner 6 – NLR

The objective is to assess the flight dynamic response of an A320 aircraft representation to dynamic Kruger deployment. The impact of the span-wise implementation is considered with respect to the aircraft response. For this purpose, the deployment characteristics of a two-component Kruger device for a swept wing, as determined in CFD and WT tests in Task 4.2, is exploited in flight

dynamics simulations for an A320 model. The effect of a full-span and segmented implementation is investigated with respect to lift loss, vertical acceleration (n_z) etc as a precursor to handling qualities assessment.

The results of the investigation are being compiled in the Deliverable D43-1

Subtask 4.3.2 Weight benefits

Contribution of Partner 9 – IBK

Provided with Krueger kinematic design by ASCO, the Krueger and fixed wing leading-edge design for a representative full-scale A/C constellation is assessed. The loads envelope for the structural analyses are agreed between DLR and ASCO and derived from the wind tunnel test results of the DLR-F15 Large model (DNW-LLF). The Kruger design assessment aims to search for any weight reduction potentials. A basic 2.5D Krueger configuration with 2 kinematic supports are exercised, with a representative wing span of 2.4 m and chord length of 3.6. Fixed LE-design and Kruger surface are optimised with different designs. In general, the stress patterns are acceptable. However, at some connection points there are some peaks which are locally beyond the allowable limits. Weight assessment has shown that with composites material the Krueger and LE-wing design can be comparable to the slat design.

The configuration is then extended by doubling the wing span and kinematic supports (4.8m span with 4 kinematics). A failure case with one kinematics down is exercised in this configuration to see the structural effect. It is shown that the failure case is critical since the stress is beyond the allowable limits. Further investigation and design efforts are still required to solve the stress problems.

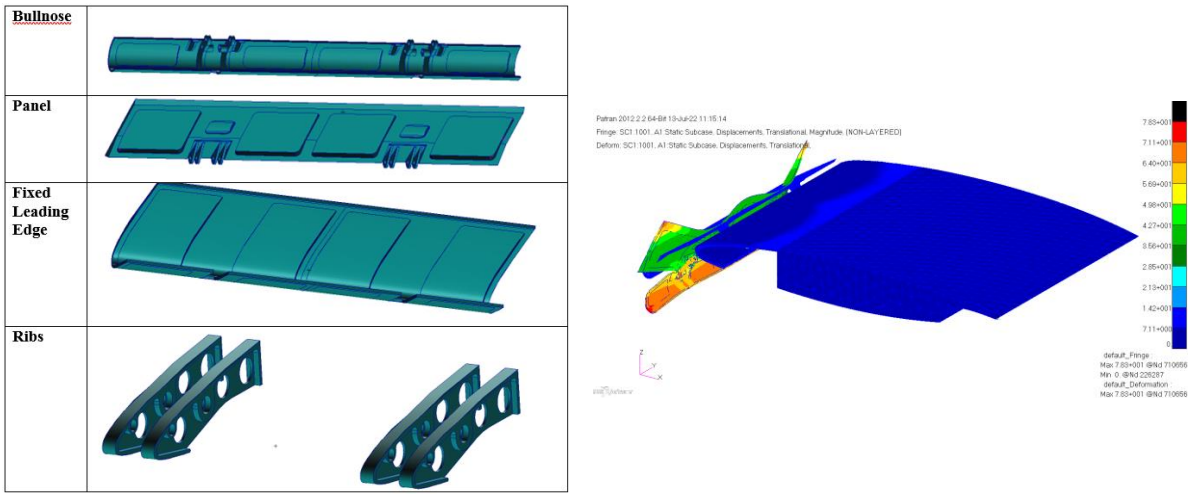

Figure 93: Krueger/LE-design (left) and stress analysis result for the basic conf. (2 kinematics supports)

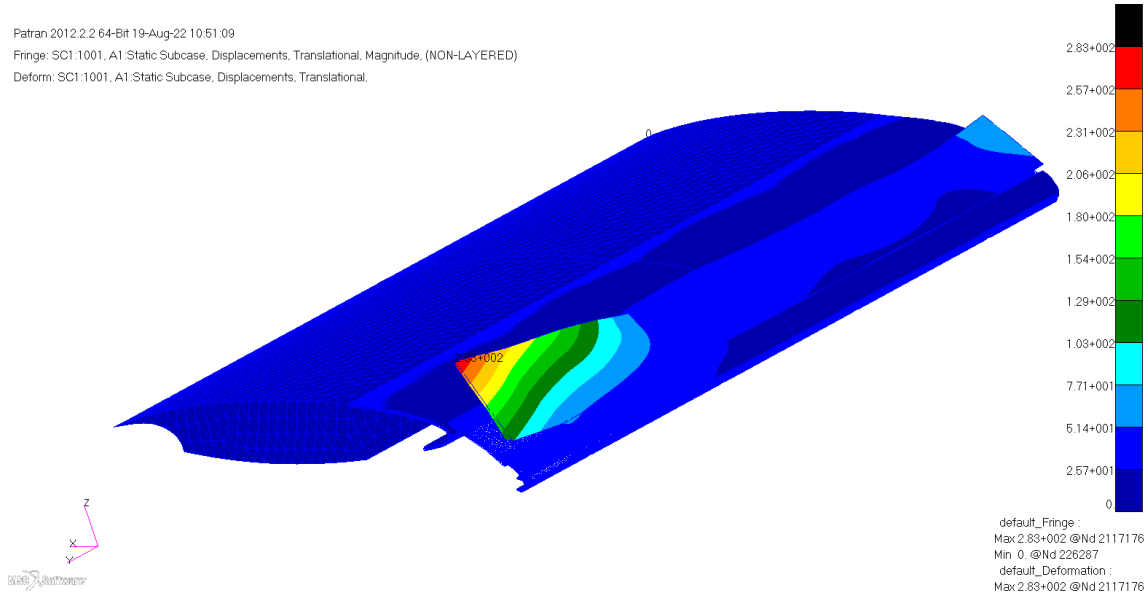

Figure 94: Failure case (one kinematics down) on the configuration with 4 kinematics supports

Subtask 4.3.3 Overall Aircraft Design (OAD) aspects (AID, DAV)

Contribution of Partner 10 – AID:

The project UHURA has focused for the first time on simulating and measuring the aerodynamic effects during the unsteady deployment and retraction process. In the reporting period Subtask 4.3.3 has been investigated how the obtained results affect the high lift system layout and what impact on overall aircraft level it has.

The fields touched on were:

1. **Aerodynamic component loads**, which appear during the deployment and retraction of a Krüger, must be known as early as possible, including potential reversal of aero loads.
2. A folding bull nose Krüger requires **complex kinematics** with a high number of moving structural parts. This may lead to high weight and cost, increased maintenance effort or reduced dispatch reliability, increased number of potential failure cases.
3. Open Krüger cavity and fragmented support structure opposed to the flow act as **aeroacoustics noise** sources. This may lead to unacceptable high noise levels during take-off and in particular landing phase. The high noise level may endanger the noise certification of the aircraft, can lead to low acceptance communities and airlines (higher landing fees).
4. High aspect ratio Krüger elements (Bull Nose, Panel) are more **flexible** and prone to deformation and such object to reinforcements, which may lead to higher **weight** and cost.
5. Flow separation on the wing upper and lower side appears during Krüger deployment and retraction procedure, which may lead to unacceptable **handling qualities** and degraded passenger comfort.
6. The resulting need for sequential/overlapping Krüger device deployment results in a more **complex drive system** with distributed motors.

The most significant impact on overall aircraft level can be expected from aerodynamic component loads, which drive the sizing of movable's structure and kinematic supports, as well as from handling qualities due to the temporary flow separation in the wake of the rotating Krüger.

It was found that the maximum aerodynamic component loads appear in deployed position at maximum angle of attack and not during the Krüger rotation. Hysteresis effects are small and can be neglected. A reversal happens for lateral force during rotation, which is not seen as critical for the design of the structure, kinematics and drive system.

Static measurements of component loads at various Krüger deflection angles match the continues measurements well. From a component loads perspective, no measurements with continues rotation are required in the future. Even the static measurements of intermediate deflections may be saved as it was demonstrated that steady and unsteady CFD simulation of the rotation match the experiment well and can be used as a data source in the future, however still with significant computational effort.

It can be concluded that aerodynamic component loads during Krüger rotation are not limiting, which is a very valuable information on overall aircraft level.

The second field with large impact on overall aircraft level is handling qualities. It was shown that during the rotation of the Krüger, the flow below the wing is significantly disturbed, which leads also to temporary weak flow or flow separation on upper side of wing and flap. The resulting changes in lift can affect the aircraft stability. It was shown by NLR's flight dynamic simulations, which were fed with delta lift from validated CFD simulations, that the effect on vertical acceleration and flight trajectory can be reduced by not deploying all Krüger panels simultaneously, but sequentially. Overlapping between the Krueger flaps reduces the effect further and reduces the time to deploy and retract, which can be an option to optimise flight procedures. With the three different UHURA wind tunnel test it was shown that the increase of wing sweep reduces the impact of drive speed on lift loss, which leads to a reduction of power demand for Krüger drive systems on swept wings as no strong need for fast deployments is required.

The need for sequential and overlapping deployment leads to a complete change of the high lift drive system architecture: instead of a central drive motor, distributed drives are required. Each Krüger panel has its own electrical motor, which means a potential increase of weight, cost and complexity. For instance, the number of sensors to monitor the Krüger positions will increase, which can reduce the dispatch reliability of the aircraft. The distributed drives allow the rotation of different Krüger panels individually, e.g. in groups or with overlapping. As each motor can be controlled individually, the deployment scheme can be tuned and optimised during the aircraft development, even during the flight test phase, which is a high value risk mitigation on overall aircraft level.

The results have been summarized in D43-3 "Impact of unsteady Krüger motion on overall aircraft level".

Contribution of Partner 11 – DASSAV

Subtask 4.3.3 was dedicated to the feasibility of transposing unsteady flow simulation technology based on DDES methodology to other unsteady load cases than the Krueger flap. It was applied to the unsteady loads during the aircraft landing phase related to the interaction between the thrust reversers and both rear fuselage and horizontal tail plane and it was validated using available private industrial ground test data.

The developed meshing strategy was applied to create an equivalent high-order mesh of Falcon 2000EX with deployed thrust reverser plates. Three new unsteady methodologies were investigated on this aircraft configuration: order 1 and order 2 new ZDES 2020 model and the Variational Multi-Scale method.

The results obtained with the 3 methods were in relatively good agreement with the spectra of the acoustic ground test measurements. Order 2 methods were characterised by an increase of the acoustic loads close to the nozzle exit and on the windward side of the engine mast.

Unfortunately, variational Multi-scale method did not allow, as expected, increasing the cut-off frequency of the simulated spectra. The use of even more refined meshes would help to reach that goal and also to reveal more clearly all the potential of high-order methods.
The results have been summarized in D43-4 "Feasibilty analysis of transposing unsteady flow simulation technology".

2.5 WP 5: Management

Task	Title	Starting at	Completion	Status
5.1	**Management**	**M1**	**M48**	**completed**
5.2	**Dissemination**	**M16**	**M48**	**completed**
5.3	**Databank & maintenance**	**M1**	**M48**	**completed**

Lead: DLR

The objective of this work package is the continuous management and progress monitoring of the project including preparations of major meetings. Especially in the ramp up of the project the installation of database for communication and data exchange was a major aim.

The project was started on time and a kick-off meeting was held in October 2018 where already first steps were reported, mainly on the provision of background information and the setup of the database. The database server has been installed and access information has been provided to all partners.

The 1st Progress Meeting was held in April 2019 at KTH, Stockholm, Sweden. The 2nd Progress Meeting was held in September 2019 at INTA, Madrid, Spain.

The Midterm Review Meeting has been held virtually on April 2nd. Minor delays are encountered in few work packages. Status of issues is closely tracked to minimize the impact on the overall project. Database is up and working for data exchange.

The 3rd project progress meeting was held virtually on October 6th, 2020. The 4th project progress meeting was held virtually on March 25th, 2021.

In order to accommodate the delays in the experimental work package due to COVID-19 crisis, an amendment to the GA has been settled prolongating the project run-time by 12 months (Amendment AMD-769088-17). This is mainly to ensure the postponed wind tunnel tests. In this scope, budget transfer has been established to cope the additional costs of the second entries both at ONERA and DNW. Further, the work packages 1 & 2 have been balanced and underspending has been shifted to active tasks in WP 3, 4 & 5.

The project is running smoothly. Significant delays due to the COVID 19 pandemic are recognized, especially in the experimental work package. Any impacts of these delays are tried to be kept at a minimum by very close monitoring.

The 2nd Review Meeting was held virtually on September 20th, 2021. The 5th Project Progress Meeting was held virtually April 22nd, 2022. A closing event for the project in terms of a common Final Workshop & Review Meeting was held on Sept. 5th & 6th, 2022. It has been arranged as a hybrid meeting with on-site presence at Airbus, Bremen, Germany.

The database is up running and maintained and heavily used for data exchange. Especially in the reporting period, the experimental database has been made fully available to all partners this way.

Table 4 WP5 Milestones, deliverables, time schedule & spending

Deliverables in WP5		*Partner(s)*	*Month due*	*Month completed*
D53-1	Databank server with online access capabilities	IBK	M2	M4
D53-2	Guideline for the access, security and data transfer for the UHURA data base server	IBK	M5	M4
D51-1	1st Progress Report	DLR	M6⇨M8	M8
D51-2	2nd Progress Report	DLR	M12⇨M13	M15
D52-1	Mid-term dissemination summary	DLR	M19	M19
D51-3	Midterm Review Meeting	DLR	M18⇨M20	M19
D51-4	Midterm Assessment Report	DLR	M18⇨M19	M20
D51-5	3rd Progress Report	DLR	M24⇨M25	M26
D51-6	4th Progress Report	DLR	M30⇨M31	M31
D51-7	2nd Review Meeting	DLR	M37	M37
D51-8	5th Progress Report	DLR	M37	M38
D52-2	2nd Dissemination Report	DLR	M36	M42
D51-9	6th Progress Report	DLR	M42	M44
D51-10	Final Project Report	DLR	M36⇨M48	M50
D52-2	Summary on dissemination activities during project run time	DLR	M36⇨M48	M48
D53-3	Summary of the UHURA databank entries	IBK	M36⇨M48	M50

Milestones in WP5		*Partner*	*Month due*	*Month achieved*
	Midterm Review	All	M18	M20
	2nd Review	All	M36⇨M37	M37
	Final Review	All	M48	M49

2.5.1 Task 5.1 – Management

Lead: DLR

Task 5.1 objectives

- Perform Quarterly Status Reporting
- arrange and hold Project Progress Meeting (PPM) s every 6 months
- compile and provide Project Progress Report every 6 months
- compile and provide Review Reporting according to reporting periods (M18, M36m M48)
- arrange and hold Project Review Meetings (PRM) according to reporting periods (M18, M36, M48)
- Update of UHURA Handbook
- Submission of Deliverables

Progress achieved/results

The management of the UHURA project has run smoothly during the first reporting period of the project. No cost or serious time problems have been reported.

The Kick-off meeting took place on October-16th/17th, 2018 at ASCO, Zaventem, Belgium. The first Progress Meeting (PPM1) and General Assembly has been held on April 4th/5th., 2019 at KTH, Stockholm, Sweden, the second Progress Meeting (PPM2) and General Assembly on Sept 18th/19th, 2019 at INTA, Madrid, Spain. For all meetings it is intended to always combine General Assembly and Progress Meetings in order to bring all partners together for a technical review and discussion.

Contribution of Partner 1 – DLR

The Kick-Off meeting was prepared and held on October 16th/17th at ASCO premises.

Quarterly Status Reporting was initiated and collected every three months.

Updates of the UHURA handbook have been issued including the status reports obtained by Quarterly Status Reporting.

The 1st Progress Meeting (PPM1) has been held on April 4th/5th at KTH, Stockholm.

The 1st Progress Report (D51-1) has been completed and submitted.

The 2nd Progress Meeting (PPM2) is has been held on Sep 18th/19th at INTA, Madrid.

The 2nd Progress Report (D51-2) has been completed and submitted.

The 1st Progress Review Meeting (PRM1) has been held virtually on April 2nd, 2020. Minutes have been provided as D51-3.

The Midterm Review Report (D51-4) has been completed and submitted.

The 3rd Progress Meeting (PPM3) is scheduled to be held virtually on Oct 6th.

The 3rd Progress Report has been initiated.

The 4th Progress Meeting (PPM4) has been held virtually on March 25th.

The 4th Progress Report (D51-6) has been completed and submitted.

The 2nd Progress Review Meeting (PRM2) has been prepared and has been held virtually virtually on September 20th, 2021.. Minutes have been provided as D51-7.

The 5th Progress Report (D51-8) has been completed and submitted.

The 5th Progress Meeting (PPM5) has been held virtually on April 22nd, 2022.

The 6th Progress Report (D51-9) has been completed and submitted.

The Final Review Meeting is organized in conjunction with a Final workshop for September 5th & 6th at Airbus, Bremen, Germany.

The Final Project Report is this report

70 deliverables in total have been submitted in the meantime to the SyGma site.

Details on project meetings are tabulated in section 4.4.Table 10 shows the planned and scheduled project meetings up to now. Table 11 lists additional meetings of dedicated Tasks and Work packages to more closely establish the cooperation.

2.5.2 Task 5.2 – Dissemination

Lead: DLR

Task 5.2 objectives

- Monitor dissemination activities of the project
- coordinate common dissemination activities at European conferences

Progress achieved/results

In Table 5 the events of project dissemination are listed. In the scope of the International Aeronautics Exhibition ILA '20 it is planned to provide a slide show to be shown at the INEA exhibition. A major part of dissemination of the UHURA project is the deployment of the scientific results to the community, majorly by contributions to scientific conferences and articles in peer reviewed journals. Table 6 lists the currently published contributions to conferences and scientific journals.

As part of a general dissemination activity, a special session on the UHURA project with focus on achievements of the almost closed WP2 is organized in the course of the 10th EASN International Conference on "Innovation in Aviation & Space to the Satisfaction of the European Citizens" to take place virtually on September 2nd-4th, 2020. Aside an overview presentation on the project as a whole, five specific presentations on the achievements made in WP2 are prepared. Two further contributions have been provided to the ECCOMAS 2020 conference in the scope of a Special Technology Session STS07 with respect to "Progress in Simulation and Validation of High-Lift System Aerodynamics". For the ECCOMAS 2022 a full session on the project has been provided in the scope of a Special Technology Session STS03, and finally, the project outcome is communicated at the 12th EASN International Conference.

A public website has been made available online at address http://uhura-project.eu. It contains basic information on the project and will be enriched by project achievements, especially links to publications, in the progress of the project.

Contribution of Partner 1 – DLR

The exhibition of UHURA together with the AFLoNext Ground Based Demonstrator has been proposed to the organizing committee of the AeroDays 2019 conference. Unfortunately, due to complexity of the setup it was only able to show the demonstrator during specific visits to INCAS where the GBD is stored.

In the frame of the ECCOMAS 2020 conference, a Special Technology Session (STS 07) has been setup, which contains some scientific overview presentation on UHURA achievements. The ECCOMAS 2020 conference has finally been held as a virtual conference in January 2021. The previously mentioned Special Technology has been provided, including two specific contributions on the UHURA project.

For the ECCOMAS 2022 conference a Special Technology Session is organized to disseminate the results of the UHURA project. In total five presentations are scheduled for the presentation on numerical results of the project.

For the 12th EASN International Conference a special session on the complete project is agreed with the organizers. It is intended to give 5 presentation, one for each work package.

Table 5 events to disseminate UHURA's results and achievements

Event	Type	Expected date	Audience	Aim
10th Aerospace Technology Congress	conference	October 2019	scientific	highlight UHURA meshing strategies
3DExperience Conference Design, Modeling & Simulation	conference	March 2020	scientific	preliminary assessment of LBM methods for the UHURA application
ILA 2020	aeronautics fair	May 2020	wider audience interested in aeronautics	showcase video on UHURA activities

Event	Type	Expected date	Audience	Aim
10th EASN virtual International Conference	conference	September 2nd - 4th, 2020	scientific	special session to disseminate the project intermediate results
AEROSPATIAL 2020	conference	October 15th, 2020	scientific	overview presentation on UHURA project
ECCOMAS 2020	conference	January 2021	scientific	special technology session on high-lift aerodynamics simulations
ECOMAS CM3	workshop	Nov 22nd, 2021	scientific	overview presentation on UHURA project
ECCOMAS 2022	conference	June 5th – 9th, 2022	scientific	special technology session to disseminate the project final results
EUCASS 2022	conference	June 27th – July 1st, 2022	scientific	contribution to communicate the project to the worldwide community
UHURA Final Workshop	workshop conference	September 5th, 2022	representatives of stakeholders, industry and funding bodies	provide information on UHURA's achievements to an audience of prospected users, especially industrial entities not directly involved in the project.
12th EASN International Conference	conference	October 18th – 21st, 2022	scientific	special session to disseminate the project final results

Table 6: List of documents and papers published

No.	Author(s)	Title	Where/when published
1	Wallin S, Hanifi A, Bagheri F	Meshing and CFD strategies for large scale turboprop WT model integrating morphing high-lift devices"	10th Aerospace Technology Congress, October 8-9, 2019, Stockholm, Sweden
2	Ponsin J	Experiences of using LBM Xflow in the EU H2020 Project UHURA	3DExperience Conference Design, Modeling & Simulation, March 11-12, 2020, Barcelona, Spain
3	J. Wild	Unsteady High-Lift Aerodynamics – Unsteady RANS Validation An Overview on the UHURA Project	10th EASN International Conference, Sep 2, 2020, virtual
4	H. Maseland, J. Wild, H. van der Ven	Progress in Meshing for Dynamic High-Lift CFD	10th EASN International Conference, Sep 2, 2020, virtual
5	A. Prachar, R. Heinrich, A. Raichle, J.C. Kok, F. Moens, T. Renaud	Progress towards numerical simulation of the dynamic Krueger motion with Chimera methods	10th EASN International Conference, Sep 2, 2020, virtual
6	S. Chen, F. Bagheri, S. Wallin	Hybrid RANS-LES simulation of a deflecting Krüger device	10th EASN International Conference, Sep 2, 2020, virtual
7	F. Capizzano, T. Sucipto	A dynamic Immersed Boundary method for moving bodies and FSI applications	10th EASN International Conference, Sep 2, 2020, virtual

8	J Ponsin, C. Lozano	Progress towards simulation of Krueger devices motion with Lattice Boltzmann Methods	10th EASN International Conference, Sep 2, 2020, virtual
9	J. Wild	Unsteady High-Lift Aerodynamics – Unsteady RANS Validation An Overview on the UHURA Project	AEROSPATIAL 2020, Oct 15, 2020, virtual
10	Wallin S, Cappizano F, Prachar A, Ponsin J	Unsteady CFD Results for Deflecting High-Lift Systems	8th European Congress on Computational Methods in Applied Science and Engineering (ECCOMAS 2020), January, 11 – 15, 2021
11	Wild J, Schmidt M, Vervliet A	A 2D Validation Experiment for Dynamic High-Lift System Aerodynamics	8th European Congress on Computational Methods in Applied Science and Engineering (ECCOMAS 2020), January, 11 – 15, 2021
12	F. Capizzano, T. Sucipto	A dynamic Immersed Boundary method for moving bodies and FSI applications	IOP Conf. Ser.: Mater. Sci. Eng. 1024 012049 doi:10.1088/1757-899X/1024/1/012049
13	J Ponsin, C. Lozano	Progress towards simulation of Krueger devices motion with Lattice Boltzmann Methods	IOP Conf. Ser.: Mater. Sci. Eng. 1024 012050 doi:10.1088/1757-899X/1024/1/012050
14	F. Capizzano, T. Sucipto	Studying the deployment of high-lift devices by using dynamic immersed boundaries	Aircraft Engineering and Aerospace Technology, Vol. 94 No. 1, pp. 99-111 DOI 10.1108/AEAT-12-2020-0325
15	Wild J, Ponsin J	Unsteady High-Lift Aerodynamics - Unsteady RANS Validation Progress of the UHURA Project	ECCOMAS CM3 conference November 22nd 2021, Barcelona, Spain
16	Wild J, Schmidt M, Vervliet A, Tanguy G	A 2D Validation Experiment for Dynamic High-Lift System Aerodynamics	To be published in: "Advances in Computational Methods and Technologies in Aeronautics and Industry" (Editors: D. Knoerzer, J. Periaux and T. Tuovinen)
17	Wild J, Strüber H, Moens F, van Rooijen B, Maseland H	A Validation Program for Dynamic High-Lift System Aerodynamics	9th European Congress on Computational Methods in Applied Science and Engineering (ECCOMAS 2022), 5 – 9 June 2022, Oslo, Norway
18	Iulioano E, Quagliarella D, Wild J	Krueger High-Lift System Design Optimization	9th European Congress on Computational Methods in Applied Science and Engineering (ECCOMAS 2022), 5 – 9 June 2022, Oslo, Norway
19	Hasabnis a, Maseland H, Moens F, Prachař A, Wild J	Lessons Learnt from Chimera Method Application to a Deploying Krueger Device	9th European Congress on Computational Methods in Applied Science and Engineering (ECCOMAS 2022), 5 – 9 June 2022, Oslo, Norway
20	Wallin s, Montecchia M, Eliasson P, Prachař A	Scale-resolved simulations of the deployment and retraction of a Krueger high-lift device	9th European Congress on Computational Methods in Applied Science and Engineering (ECCOMAS 2022), 5 – 9 June 2022, Oslo, Norway
21	Ponsin J, Lozano C	Lattice Boltzmann simulation of a deploying Krueger device	9th European Congress on Computational Methods in Applied Science and Engineering (ECCOMAS 2022) 5 – 9 June 2022, Oslo, Norway
22	Tanguy G, Monnier JC,	Experimental aerodynamic investigation of a Krueger flap device using Particle Image Velocimetry	9th European Conference for Aeronautics and Space Sciences (EUCASS 2022), 27 June–1 July 2022, Lille, France

	Verbeke C, Jochen Wild		
23	Hasabnis A, Wild J, Strüber H, Moens F, van Rooijen B Maseland H	The UHURA project at a glance – motivation and objectives	12th EASN International Conference, Oct 18 - 20, 2022, Barcelona, Spain
24	Strüber H Wild J, Vervliet A, Moens F	Krueger Design and Motion Requirements	12th EASN International Conference, Oct 18 - 20, 2022, Barcelona, Spain
25	Moens F, Wallin S Maseland H	CFD methods for unsteady high-lift simulation	12th EASN International Conference, Oct 18 - 20, 2022, Barcelona, Spain
26	Tanguy G, van Rooijen B Schröder A Wild J	Validation Experiments	12th EASN International Conference, Oct 18 - 20, 2022, Barcelona, Spain
27	Maseland H, Andreutti G, Prachař A, Strüebr H	CFD method validation & Lessons Learnt	12th EASN International Conference, Oct 18 - 20, 2022, Barcelona, Spain

Contribution of Partner 7 – ASCO

ASCO performs internal dissemination to early implement the project's content into its business strategy.

Contribution of Partner 9 – IBK

IBK implemented and published the public project web-site. The UHURA project website is online since M20 at http://www.uhura-project.eu or http://uhura-project.eu. IBK implemented updates on the UHURA website, the most recent after the DNW-LLF wind tunnel test campaign in May 2022.

2.5.3 Task 5.3 – Database

Lead: IBK – S. Adden

Task 5.3 objectives

- Provision of the UHURA database server on which all technical input data, reports, deliverables, minutes of technical and management meetings, technical results and publications are stored and exchanged between partners. Access to the server are granted and restricted only to the UHURA participants only.
- Maintenance of database server and providing technical support.
- Maintenance of UHURA-project Website

Progress achieved/results before reporting period (M1-M36)

The database server had been established and already in service. It provides a common platform for data exchange between all UHURA-partners. Guidelines for accessing the server has been issued and all partners can now access the server. Two deliverables had been issued, namely:

- D53-1 Database server with online access capabilities
- D53-2 Guideline for the access, security and data transfer for the UHURA database server.

Database server is maintained online around the clock, enabling partners to access the server for data uploading and downloading

Technical support is provided to place the data on the right place and also to help partners in accessing data. Additional support for setting and hosting virtual-meetings are also provided.

. Table 7 lists the actual statistics of the database entries

Table 7: statistics on database entries

Folder	*Size*	*no. of files*
Deliverables:	247 MB	73
Meetings:	1.56 MB	171
Publications:	6 MB	4
pub (exchange files):	15.29 GB	146
WP1:	26 MB	38
WP2:	463 MB	33
WP3:	27.75GB	123
WP4:	7.61 GB	138
WP5:	955 MB	121

Contribution of Partner 9 – IBK

IBK is the only participant within the Task 5.3. All the task objectives mentioned above are performed by IBK

3 Impact

The UHURA project addresses the mode specific challenges in the area of „Aviation". UHURA as a Research and Innovation Action (RIA) concentrates on focused research on advanced high-lift aerodynamics targeting two broad lines of activities that is specified by the Horizon 2020 Programme

- Resource efficient transport that respects the environment and
- Global leadership for the European transport industry

governed by the Transport Challenge "Smart, green and integrated transport".

3.1 Impact on society by addressing environmental footprint of aviation

UHURA aims to qualify the Krueger flap device as the leading edge high-lift system enabling laminar wing technology which, contributes to a reduction of aircraft drag of approximately 10% and consequently a reduction of fuel consumption and emissions. The project results of UHURA have increased the understanding of several important fields. This will help to better manage on aircraft level the introduction of Krueger devices on a future aircraft design.

A Krueger flap has been designed for the DLR-F15-LLE airfoil. The requirements of aircraft industry have thoroughly been considered. By this, the current design and related experiences closely match the needs of industry and reflect the current expectations on potential improvements. Finally, the detailed information expected to be obtained from the coming wind tunnel test will provide further insight on the impact of integrating the high-lift design into the laminar wing. Thus, the project will at the end provide answers to important questions of integrating laminar wing technology into future aircraft designs. Due to the improved simulation capabilities introduced in the frame of UHURA, a simplification of the high-lift system is envisaged that significantly contributes to increased system reliability and safety, reduced Recurring Costs (RC) in production and assembly as well as COC benefits through reduced maintenance efforts, overhaul and repair.

It was demonstrated that the maximum aerodynamic component loads appear in fully deployed position at high angle of attack and not during Krüger rotation. This is a highly valuable information, because it helps to reduce the risk on loads level change during development, which can be very costly.

The second field with large impact on overall aircraft level is handling qualities. It was found that the Krüger rotation disturbs the flow around the wing significantly. However, it was shown by NLR with flight dynamics simulation, that the impact on the aircraft stability and control is rather limited and can be further reduced by deploying the Krüger sequentially and not all in one. This result increases the confidence that the handling qualities during Krüger rotation can be mastered to allow a safe and comfortable flight.

The obvious need for sequential deployment leads to an unavoidable change in Krüger drive system architecture, away from a central drive architecture to a distributed drive lay out. This will have a significant impact on aircraft level, as each Krüger will be actuated and controlled individually, which gives a high degree of freedom to tune the sequence of retraction and deployment, even in flight test (groups, timely overlap). This is a great opportunity of risk mitigation on aircraft level. On the other hand, lots of new possible failure cases will originate from distributed drive system, which have to be reliably detected and mastered.

The work of ASCO and IBK has shown that a Krüger system can be built at a comparable weight level like conventional slats. Fulfilling a failsafe design requirement may lead to double weight figures.

3.2 Impact on society by strengthening European aviation industry as key employer

UHURA will contribute towards maintaining the leadership of the European aeronautics industry. UHURA will develop computing solutions for key industrial problems to facilitate the introduction of innovative products and services. In order to validate numerical simulation approaches, two existing wind tunnel models are currently modified. Numerical simulation methods have been adopted to be able to simulate the unsteady aerodynamics of high-lift devices and the experimental setup for performing dedicated experiments to create validation data has been designed and mostly manufactured. By this, the tools for a full validation and quantification of the unknown unsteady aerodynamics are available for the second phase of the project. The experimental data base that will be created during the UHURA project is expected to serve as a broad validation data base for the future.

The exploitation of unsteady high-lift aerodynamic modelling including CFD-CSM coupling and its validation thanks to enhanced wind tunnel testing techniques addressed by the UHURA project aims

- to eliminate the uncertainty imposed by the impact of unsteady flow during deflection/retraction within the high-lift design with consequences on aircraft loads and therefore structural weight;
- to provide validated numerical flow analysis and CFD-CSM coupled simulation enabling consideration of critical load cases during deflection/retraction of the high-lift system at high accuracy;
- to transfer the knowledge and capabilities gained in this project to other types of moving surfaces at an aircraft, e.g. control surfaces, spoilers, speed brakes, landing gear doors, or thrust reversal, to contribute to a reduction in weight and costs of those devices too, due to a more prediction of unsteady loads and corresponding improved sizing of such components;
- by this to contribute to a significant reduction in the design cycle time due to more accurate and more early specific design even for non-primary flight conditions.

UHURA partners have shown that the aerodynamic effects of unsteady Krüger deployment and retraction process can be accurately simulated with today's meshing and CFD tools. The validation with high quality experimental data, allows in the future to efficiently simulate unsteady flow.

The close integration of major European aircraft manufacturers into the project guarantees the future application of the experience gained in the project within the design procedures. By rolling out simulation capabilities refined and validated in the project enables those to fully exploit the gained experience into the processes needed to implement Krueger devices on new aircraft types. Dassault Aviation has demonstrated that the capabilities developed in UHURA can be also applied to other unsteady flow phenomena, like deploying thrust reversers.

4 Project management

4.1 Monitoring of Work progress

Table 8 provides an overview on the revised and amended time schedule of the UHURA project

Table 8: GANTT chart of the UHURA project – planned and actual (Amendment AMD-769088-17)

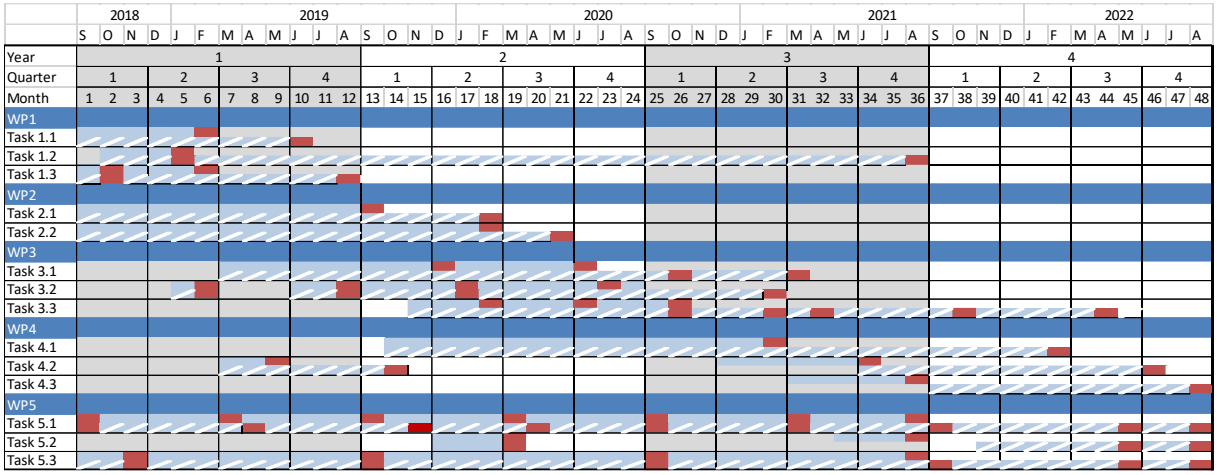

4.2 Risk assessment and mitigation

Risk assessment and mitigation is supported by a quarterly report procedure. Tasks indicate arising issues in terms of budget, schedule or content and propose a measure to minimize the impact on the overall project. Table 9 provides an overview on the quarterly reporting done so far indicating few minor time problems (yellow) as already reported above. Explanations on the (yellow) feedback received are provided in the critical items list shown in **Fehler! Verweisquelle konnte nicht gefunden werden.**.

Table 9 Quarterly status summary of UHURA tasks

Task	Leader	Q1 M1-3 Sep-Nov '18	Q2 M4-6 Dec'18-Feb'19	Q3 M7-9 Mar-May'19	Q4 M10-12 Jun-Aug'19	Q5 M13-15 Sep-Nov'19	Q6 M16-18 Dec'19-Feb'20	Q7 M19-21 Mar-May'20	Q8 M22-24 Jun-Aug'20	Q9 M25-27 Sep-Nov'20	Q10 M28-30 Dec'20-Feb'21	Q11 M31-33 Mar-May'21	Q12 M34-36 Jun-Aug'21	Q13 M37-39 Sep-Nov'21	Q14 M40-42 Dec'21-Feb'22	Q15 M43-45 Mar-May'22	Q16 M46-48 Jun-Aug'22
1.1	Wild, J.		S	C													
1.2	Vervliet, A.				T				S	S	S	S		S	C		
1.3	Strüber, H.		T	SC													
2.1	Maseland,H.		S	S	T	T	C										
2.2	Wallin. S.				T	T	T		S	S	S	C					
3.1	Wild, J.				T	T	T	S	S	S	S	C					
3.2	Schröder, A.											S	S	C			
3.3	v. Rooijen, B.							S	S	S	S				S	S	
4.1	Andreutti, G							S	S	S	S	S					

Task	Leader	Q1	Q2	Q3	Q4	Q5	Q6	Q7	Q8	Q9	Q10	Q11	Q12	Q13	Q14	Q15	Q16
		M1-3	M4-6	M7-9	M10-12	M13-15	M16-18	M19-21	M22-24	M25-27	M28-30	M31-33	M34-36	M37-39	M40-42	M43-45	M46-48
		Sep-Nov '18	Dec'18-Feb'19	Mar-May'19	Jun-Aug'19	Sep-Nov'19	Dec'19-Feb'20	Mar-May'20	Jun-Aug'20	Sep-Nov'20	Dec'20-Feb'21	Mar-May'21	Jun-Aug'21	Sep-Nov'21	Dec'21-Feb'22	Mar-May'22	Jun-Aug'22
4.2	Prachar, A.			T	T	T											
4.3	Strüber, H.																
5.1	Wild, J.																
5.2	Wild, J.																
5.3	Adden, S.																

color code

- not started
- no problems
- minor problems
- **major problems**
- finalized

T - **Technical** Problem

B - **Budget** problem

S - **Schedule** problem

C - Task **completed**

4.3 Use of Resources

Figure 95 shows the budget planned for the overall project in relation to the actual costs of the project About 94% of the estimated budget has been spent. The cost category "Travel" is significantly less used due to the COVID-19 pandemics and thus banned travel. Half of the project period, from March 202 to May 2022, project meetings and conferences were conducted fully virtual. Just the latest events – The ECCOMAS 2022 congress, the 12th EASN International Conference and the project's Final Review Meeting & Workshop – were held in person again.

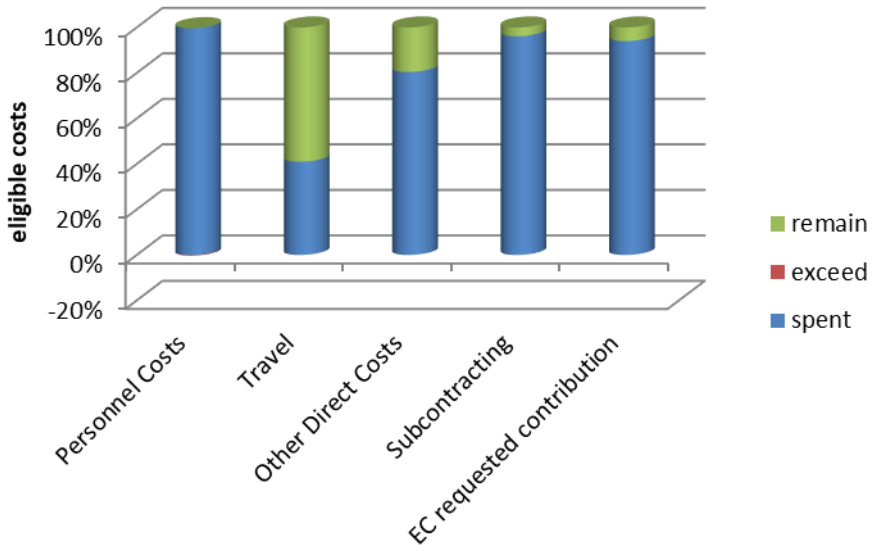

Figure 95: overview on spent budget divided into cost categories Figure 96 lists the planned work effort for the full project runtime and used personal effort divided into the work packages. It shows that the actual personal effort is 7% higher than planned. Some more effort has been put in the major work packages of simulation and experiment, the latter addressed to the split up of the wind tunnel tests in ONERA-L1 and DNW-LLF. This is counteracted by a more straight-forward design task in WP1 and a lean project management in WP5. Anyhow, due to different costs of technical and scientific staff, the overall personnel costs are in line with the project planning.

As a general conclusion, the project is in a good shape in terms of budget. The use of resources and budget is in relation with the work content and the results obtained.

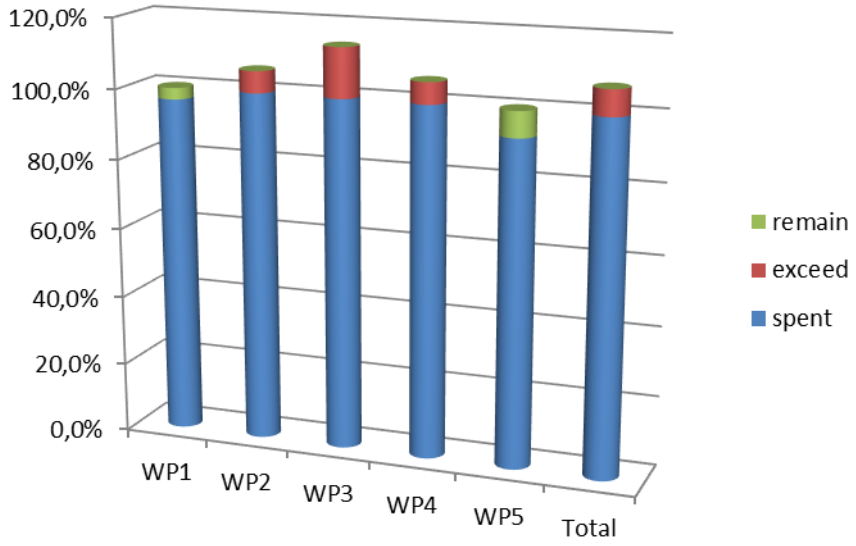

Figure 96: comparison of used personal effort resources and planned work for overall project runtime divided into work packages

4.4 *List of project meetings, dates and venues and reporting*

Table 10 shows the planned and scheduled project meetings up to now. Table 11 lists additional meetings of dedicated Tasks and Work packages to more closely establish the cooperation.

Table 10 List of project meetings, dates and venues;

Month of UHURA	Progress Meetings; General Assembly	Progress Reporting
M1 **Kick-off**	Oct 16th/17th, 2018 – ASCO (Zaventem)	-
M7	PPM1 Apr 4th/5th, 2019; KTH (Stockholm)	1st Project Progress Report (D51-1) May-2019
M13	PPM2 Sep 18th/19th, 2019, INTA (Madrid)	2nd Project Progress Report (D51-2) Oct-2019
M19	PRM1 Apr 2nd, 2020, virtual	Midterm Assessment Report (D51-4) Apr-2020
M25	PPM3 Sep 25th, 2020, virtual	3rd Project Progress Report (D51-5) Oct-2020
M31	PPM4 Mar 25th, 2021, virtual	4th Project Progress Report (D51-6) May-2021
M37	PRM2	5th Project Progress Report (D51-8)

Month of UHURA	Progress Meetings; General Assembly	Progress Reporting
	Sep 20th, 2021, virtual	Oct 2021
M43	PPM5 Apr 22nd, 2022, virtual	6th Project Progress Report (D51-9) Apr 2022
M48	PRM3 Sep 5th/6th, 2022, AID (Bremen)	Final Progress Report (D51-10) Oct-2022

Table 11 additional WP/task technical meetings schedule

WP	Topic of Meeting	Lead	Date	Host / Location
1	WP 1 progress	AID	18/01/2019	Telecon
1	WP 1 progress	AID	21/02/2019	Telecon
1	WP 1 progress	AID	08/03/2019	Telecon
3.3	Task 3.3 Kick Off meeting	ONERA	28/01/2019	ONERA (Lille)
3.3	Task 3.3 – Progress (Model/Equipment etc ..)	ONERA	21/03/2019	Telecon
WP3	Regular Meeting WP3: Validation-Experiments	DNW	30/04/2020 – 16/09/2020	regularly bi-weekly
3.1	Task 3.1 Kick-Off meeting	DLR	07/05/2019	NLR (Amsterdam)
3.1	Task 3.1 progress	DLR	as of 22/05/2019	regularly bi-weekly
3.1	PDR of the DLR-F15 model	DLR	17/09/2019	INTA (Madrid)
3.1	F15LS Kinematics integration	ASCO	18/06/2020 – 31/08/2020	regularly bi-weekly
3.1	CDR of the DLR-F15 model	DLR	04/12/2019	NLR (Amsterdam)
3.1	PDR of the DLR-F15LS model	DLR	02/07/2020	virtual
4.1	Task 4.1 Kick-Off	CIRA	08/07/2020	virtual
3.1	CDR of the DLR-F15LS model	DLR	03/09/2020	virtual
3	Regular Meeting WP3: Validation-Experiments	DNW	as of 26/11/2020	Virtual, regularly bi-weekly
4.1	Task 4.1 progress meeting	CIRA	24/02/2021	virtual
4.1	Task 4.1 progress meeting	CIRA	24/06/2021	virtual
4.3	T4.3.2 ASCO weight report	AID	17/08/2021	virtual
4.3	T4.3 progress, PRM2 prep	AID	17/09/2021	virtual
4.3	T4.3.2 harmonize IBK/ASCO workshare	AID	21/09/2021	virtual

WP	Topic of Meeting	Lead	Date	Host / Location
4.3	T4.3.2 loads and failure cases	AID	12/10/2021	virtual
4.3	T4.3.2 progress	AID	15/11/2021	virtual
4.3	T4.3.2 progress	AID	30/03/2022	virtual
4.3	T4.3 progress & PPM5 prep	AID	20/04/2022	virtual
4.3	T4.3.1 progress	AID	11/05/2022	virtual
4.3	T4.3 progress	AID	28/06/2022	virtual
4.3	T4.3 progress	AID	22/08/2022	virtual
4.3	T4.3 WS & Final review prep	AID	02/09/2022	virtual